Institut für Chemie

Arbeitskreis Angewandte Polymerchemie

Development of Functional Hydrogels for Sensor Applications

Dissertation

zur Erlangung des akademischen Grades

“doctor rerum naturalium” (Dr. rer. nat.)

in der Wissenschaftsdisziplin Polymerchemie

eingereicht an der

Mathematisch-Naturwissenschaftlichen Fakultät

der Universität Potsdam

von

M.Sc. Sandor Dippel

Potsdam, den 30. November 2016

Published online at the
Institutional Repository of the University of Potsdam:
URN urn:nbn:de:kobv:517-opus4-398252
http://nbn-resolving.de/urn:nbn:de:kobv:517-opus4-398252

Acknowledgements

Zu allererst möchte ich Herrn Prof. Laschewsky herzlich dafür danken in seiner Arbeitsgruppe über dieses interessanten Thema promovieren zu können, für alle spannenden Diskussionen und seine weitreichende Unterstützung.

Vielen Dank auch an Herrn Dr. Wischerhoff für die Betreuung im Alltag und Anstöße für neue Ideen.

Dank der Kooperation zwischen der Universität Potsdam und dem Fraunhofer Institut für Angewandte Polymerforschung(IAP) konnte ich die Räumlichkeiten und technischen Möglichkeiten des IAP mitbenutzen, dafür danke ich stellvertretend dem Institutsleiter Herrn Prof. Böker danken.

Meine Arbeit war nur möglich durch die engagierte Kooperation und Austausch im Rahmen des Taschentuchlabor-Projekts mit Dr. Memczak, Dr. Michel, Dr. Stöcklein, Dr. Tang, Dr. Hettrich, Dr. Inal, Dr. Rötch, R . Bernin, Dr. Kölsch und Dr. Hildebrand – vielen Dank!

Ein großes Dankeschön auch an das FB 4 Team für die warme Aufnahme und die gute Atmosphäre bei der Arbeit. „Meinen“ Studenten Faty Makthoum, Nicole Sickert, Dr. Kamil Kaminski und Raphael Suminski vielen Dank für die Zusammenarbeit und das Interesse – durch euch konnte auch ich viel lernen!

Ein besonders liebes Dankeschön an die Doktorandentruppe – Jens, Martin, Jean-Phillipe, Robert, Viet, Jonas, Laura, Frank, Anne & Anna aber natürlich auch Geri, Clara und Sandra – die Zeit mit euch war großartig.

Ganz zuletzt meiner Mutter und meiner Schwester einen herzlichen Dank für die Unterstützung über all die Jahre, ebenso meiner lieben Claudia – ohne di was ned halb so schee!

Selbständigkeitserklärung

Hiermit erkläre ich an Eides statt, dass ich die vorliegende Arbeit selbstständig verfasst und nur unter Verwendung der angegebenen Quellen und Hilfsmittel angefertigt habe. Weder diese noch eine andere Arbeit wurde von mir an einer anderen Universität oder Hochschule zum Zwecke der Einleitung eines Promotionsverfahrens vorgelegt.

Olching , den 29. November 2016 Sandor Dippel

Abstract

In this work, a sensor system based on thermoresponsive materials is developed by utilizing a modular approach. By synthesizing three different key monomers containing either a carboxyl, alkene or alkyne end group connected with a spacer to the methacrylic polymerizable unit, a flexible copolymerization strategy has been set up with oligo ethylene glycol methacrylates. This allows to tune the lower critical solution temperature (LCST) of the polymers in aqueous media. The molar masses are variable thanks to the excurse taken in polymerization in ionic liquids thus stretching molar masses from 25 to over 1000 kDa. The systems that were shown shown to be effective in aqueous solution could be immobilized on surfaces by copolymerizing photo crosslinkable units. The immobilized systems were formulated to give different layer thicknesses, swelling ratios and mesh sizes depending on the demand of the coupling reaction.

The coupling of detector units or model molecules is approached via reactions of the click chemistry pool, and the reactions are evaluated on their efficiency under those aspects, too. These coupling reactions are followed by surface plasmon resonance spectroscopy (SPR) to judge efficiency. With these tools at hand, Salmonella saccharides could be selectively detected by SPR. Influenza viruses were detected in solution by turbidimetry in solution as well as by a copolymerized solvatochromic dye to track binding via the changes of the polymers' fluorescence by said binding event. This effect could also be achieved by utilizing the thermoresponsive behavior. Another demonstrator consists of the detection system bound to a quartz surface, thus allowing the virus detection on a solid carrier.

The experiments show the great potential of combining the concepts of thermoresponsive materials and click chemistry to develop technically simple sensors for large biomolecules and viruses.

Zusammenfassung

Diese Arbeit befasst sich mit der Entwicklung von Sensorsystemen für biologische Analyten wie Bakterien und Viren. Die Sensoren beruhen auf thermoresponsiven Polymeren und die Entwicklung wird Schritt für Schritt ausgehend von der Monomersynthese dargelegt. Die Grundidee ist es alle Einzelschritte so modular wie möglich zu halten. Die Kopplungseinheiten für die späteren Erkennungsgruppen bestehen aus Carboxyl, Alken und Alkinfunktionalitäten, die zuerst mit einem Ethylenglycolspacer mit variabler Länge verknüpft werden und dann mit der polymerisierbaren Methylmethacrylatgruppe versehen werden. Diese koppelbaren Monomere werden mit Di- oder (Oligoethylenglycol)methacrylaten copolymerisiert. Je nach Verhältnis ist so auch die untere kritische Entmischungstemperatur (LCST) einstellbar. Mit der Erweiterung der Polymerisationstechnik um ionische Flüssigkeiten als Lösemittel lassen sich Molmassen von 25 bis über 1000 kDa einstellen. Um die Polymere funktionell zu erweitern, lassen sich auch benzophenonhaltige Monomere zur Vernetzung oder Immobilisierung copolymerisieren. Naphthalsäureimidhaltige Monomere wiederum dienen als Signaleinheit, da sie durch Verändern der Polarität ihrer Umgebung solvatochrom reagieren. Durch Aufschleudern und UV-Vernetzen lassen sich Gelschichten mit guter Schichtdickenkontrolle herstellen. Dabei sind die Substrate nur auf den jeweiligen Zweck beschränkt. Dank des Baukastenprinzips kann auch die Maschenweite oder der Quellgrad der Gele eingestellt werden.

Die Polymere oder Hydrogele werden mit Hilfe von effizienten Reaktionen swe aogenannten „Click Chemie“ umgesetzt und die Reaktionen werden durchleuchtet, ob sie diesen Ansprüchen gerecht werden. Je nach Möglichkeit wird das Anknüpfen mittels Oberflächenplasmonenresonanzspektroskopie(SPR) verfolgt, so wie zum Beispiel die Kopplung eines Phagen-Oberflächenproteins und das selektive Binden eines Membransaccharids des Salmonellen Bakteriums. Influenza Viren werden selektiv mit Hilfe eines Erkennungspeptids gebunden und mit Hilfe von Trübungsspektroskopie bzw. dem thermoresponsiven Verhalten des Trägerpolymers nachgewiesen. Ein weiterer dargelegter Ansatz ist das Nachweisen von geringen Virenkonzentrationen mit Hilfe eines Hydrogels oder von Polymeren in Lösung, die jeweils mit einem solvatochromen Farbstoff ausgestattet sind, der auf die Umgebungsänderung durch den Virus reagiert.

Die Experimente zeigen das große Potential von geschickt kombinierten thermoresponsiven Materialien, die mittels Funktionalisierung durch Click-Chemie zu technisch einfachen Nachweissystemen für Biomoleküle und sogar ganze Zellen entwickelt werden können

Contents

Contents

Abbrevations

LCST	Lower critical solution temperature
SPR	Surface plasmon resonance
AIBN	Azobisisobutyronitrile
ATRP	Atom-transfer radical-polymerization
DCM	Dichloromethane
DMF	Dimethylformamide
EDC	1-Ethyl-3-(3-dimethylaminopropyl)carbodiimide
EMIM PF_6	1-Ethyl-3-methylimidazolium Hexafluorophosphate
HEPES	2-[4-(2-hydroxyethyl)piperazin-1-yl]ethanesulfonic acid
IL	Ionic liquid
LOD	Limit of detection
MEO_2MA	Methoxy diethyleneglycole methacrylate
NHS	N-Hydroxy succinimide
NIPMAM	N-Isopropyl-methacrylamide
OEGMA	Oligo-ethylenglycol methacrylate
PHEMA	Poly-(hydroxyethylmethacrylate)
PMMA	Poly-(methylmethacrylate)
PNIPMAM	Poly-N-Isopropylacrylamide
RAFT	Reversible addition−fragmentation chain-transfer (polymerization)
SR	Swelling ratio
TEA	Triethanolamine
TEG	Tetraethylenglycol
THF	Tetrahydrofurane
TLC	Thin layer chromatography
UCST	Upper critical solution temperature

1. Introduction

Smart materials are a more and more commonly used term to describe polymers or polymer based materials that show a stimuli responsive behavior. By applying a stimulus to the system, a change is induced in the material. A stimulus can be light (1, 2), ionic strength(3, 4), pH(5-7) or temperature(8-14). The responsive behavior can consist of a phase change (15) or a change in optical properties(16) as an example. There is a clear distinction to a reaction, as no material is exchanged, added or lost. These changes can be reversible but they need not have to be.

Stimuli responsive materials can be found in nature, alginate is pH responsive(17) and gelatin is thermoresponsive(18) to name two simple examples. Science is picking up concepts and ideas from such materials in order to understand them better and transfer them to applications. The motivation behind this is manifold. Especially biomedical applications are on the rise. This ranges from tissue engineering (19), drug delivery and release systems(20, 21), biomimetics(22) or coatings for cell ad- or desorption(23). The detection of biological analytes is also a point of interest (24, 25).

A common denominator for those systems is that they should be water based as in vitro and in vivo environments are targeted, and naturally, they are water based, too. While in vivo applications tissue engineering has to struggle with toxicity and rejection reaction, in vitro systems and especially any sensor application faces the challenge of the complexity of fluids from biological sources. These samples are highly complex in their mixture, be it by pH, salts or interfering cells or molecules. To counter this these interferences cause signal noise or cause the detection to fail (26). This is why these unspecific interactions have to be eliminated by choosing the right materials, commonly referred to as anti-fouling properties(27, 28).

From an application design perspective, utilizing surfaces as carrier for sensor application is a good idea. By selecting them properly, multiple analysis methods are opened up and even detection of different parameters on the same material are possible. The ease of handling especially comes into play if samples can be sputtered on surfaces or micropipettes can be used for micro well based system and so on. This is important simply because low amounts of material available is a common issue for biomedical applications.

The development of new responsive materials and the design of analytical systems on surfaces is still a challenge, as is the proper integration of recognition and signaling systems. The interaction between these parts has to be better understood and analyzed to make steps towards better biosensors.

2. Objectives and Outline

In this work an exemplary pathway for the development of a surface bound sensor for biomolecules is outlined beginning with the synthesis of the monomer units, the polymerization technique and the immobilization on surfaces to the detection of virus cells. The detection concept is to bind recognition units like peptides or proteins to the functional polymers or polymer modified surfaces. The reaction of these modified polymer systems to an addition of the analyte substances like bacteria fragments or said viruses are monitored via different analytical methods. Changes in the phase transition temperature of the modified polymer system reacting to the analyte are used for signal generation, if applicable.

This work is sectioned into three major parts, divided by the chemistry used to bind potential recognition units to a thermoresponsive polymer backbone. In chapter 4, the focus lies on identifying the requirements from a synthetic point of view, such as the special requirements on material purity and the polymer composition. Especially the composition is identified as a major parameter for the performance of the materials, and designing them for binding partners will be discussed. The physical properties of the resulting polymers and hydrogels will be characterized. In the end, two different methods for virus detection will be used as demonstrators to show the viability of using a thermoresponsive material as a starting point for sensor systems. One pathway relies solely on the shift in cloud point and the resulting turbidity, whereas the other pathway utilizes the phase transition to influence the emission spectra of a fluorescent dye. Carboxylic groups are used as coupling units for the more advanced systems. This approach was chosen due to the availability of biologically relevant recognition units and especially their analytes. The chemistry for said attachment of the recognition unit to the polymeric background relies on activated ester chemistry between the carboxylic group and the amine terminal end of amino acids from peptides and proteins. As the systems are water based, amines were preferred to hydroxylic group to make the reaction more efficient and specific. This conjugation techniques are embedded in the “click chemistry” terminology coined by Barry Sharpless (29).

In Chapters 4 and 5 the idea of utilizing click chemistry is followed up with alkene and alkyne binding groups. Both are able to undergo a radical thiol addition, which will be

tested for model substrates. They have the advantage of not being influenced by water and are very specific in their reaction. Alkynes also undergo a cycloaddition with azides which will be discussed in terms of catalysis and the limits of the “click chemistry” descriptor. These three different approaches of binding a receptor unit are set up orthogonal to each other, meaning that each one could react independently of the other and thus additions can be made sequentially. This gives a flexibility to integrate more sensor units for the analyte, additional signaling units or for immobilization on surfaces and crosslinking.

In order to characterize the system, the main analytical tools used are turbidity measurements, surface plasmon resonance spectroscopy, ellipsometry and fluorescence. This work has a very broad scope of goals to follow through and topics to span, so the focus is set more on the step by step development of the different sensor systems and not the very last detail of effects. This is partially due to time and material availability constraints of such a work, but is also chosen in order to show how to walk the line to a surface bound, smart polymer dependent biosensor from start to finish.

3. Concepts of this Work

3.1. Theoretical Background

In this chapter, the general concepts that will be used throughout the different parts of this work will be explained. While in no way as exhaustive as a matching text book dedicated to the subject, a broad overview is presented.

3.2. Free Radical Polymerization

Radical polymerization describes a reaction mechanism of polymer growth that follows a chain growth profile (over a step growth one) of one or more types of monomer units with an active center on the end of the chain. The polymerization has three main steps, the initiation of the reactive site - basically the radical generation-, then the growth or propagation step, and finally the termination. In addition, chain-transfer is a possibility, too – this event causes the reactive center to be transferred to another chain. This does not stop the polymerization per se, but instead transfers the growing radical to another site; this e.g. is one of the main causes for branching.

The two methods of radical initiation that are most commonly used are thermal and via UV irradiation. Thermal initiators commonly derive from azo or peroxide compounds, such as azoisobutyronitrile (AIBN) or dicumylperoxide. Photoinitators exist in a broader variety like the benzoin class shown below (Figure 1)

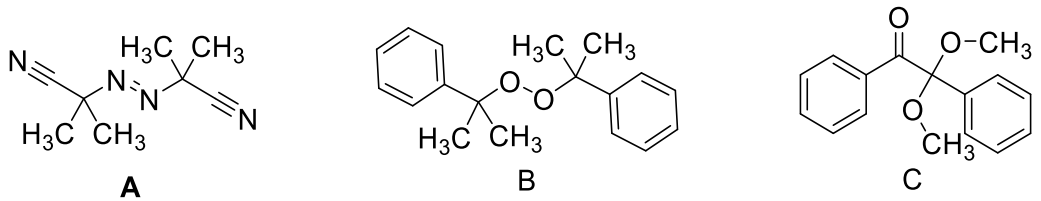

***Figure 1: A** Azoisobutyronitrile (AIBN); **B** Dicumylperoxide; **C** Dimethoxy-phenylacetophenone*

Monomers for radical polymerization are very numerous, as a rule of thumb vinylic, allylic double bonds can be candidates for polymerization. Polymerization by ring

opening of strained rings is also a (rare) possibility. This work focusses entirely on methacrylic monomers (*Figure 2*)

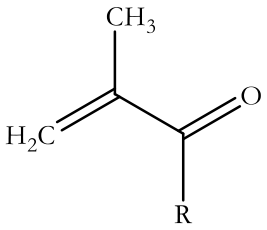

Figure 2: Methacrylic Monomer Core Structure

This type of monomer is commercially available in many different variations and functionalities that make them easy to use as synthesis starting materials like methacrylic acid or methacryloyl chloride, or for direct use as co monomer such a methoxy diethyleneglycole methacrylate (MEO_2MA) or its derivatives with longer glycol chains. Importantly, the methyl group provides some hydrophobicity as well as increased stability against hydrolysis of the esters commonly employed.

While the polymerizations in this work do not make use of overly complex chemicals to direct their chain growth and shape, the conditions are set to achieve long macromolecular chains and unbranched structures as goals. In free radical polymerization the reaction temperature makes a big difference. It defines how fast a thermal initiator generates radicals, defined by its half-life $t_{1/2,}$ and thus how many active chains are growing at a given time. Higher temperatures cause more growing chains, typically producing shorter polymers. Also, as the reactivity of the species increases, their selectivity drops, which can cause unwanted cross-linking and other defects. The drawback of choosing lower temperatures is longer reaction times to achieve the same conversion(30). The solvent also plays a certain role, for instance hydrogen bonding solvents may slow down the reaction rate as they can stabilize the radicals(31, 32). A quite obvious factor are the used concentrations of initiator and monomers. While low initiator concentrations lead to less chains globally, one cannot go too low either as one can “lose” radicals and reactive sites by side reactions and thus lower the yields and turnover of monomers. Thus, a balance has to be found. Monomer concentration in solution also impacts the chain growth – the higher the more reactive partners are available at a given time, increasing turnover but also the chances for unwanted/unselective reactions, while at low concentrations selectivity is improved but reactions take longer to get to completion and risk intramolecular

reactions.(33, 34). A final remark on the polymerization itself is the question of monomer distribution. This work is based entirely on copolymerizations of different monomers. Their close to random distribution is essential for this work as a block-like polymerization is unwanted for functionality. Functional groups such as coupling groups, should be distributed evenly across the chain to have the same impact everywhere. The “filler” and co-crosslinking monomers should behave the same to avoid clusters with e.g. a different, local LCST behavior and so on. This is also one of the main reason that only methacrylics were chosen, as for the esters at least, the copolymerization behavior is generally close to ideal azeotropic, thus avoiding compositional drifts(32).

3.3. Thermoresponsive Polymers

3.3.1. Thermoresponsive Behavior

Thermoresponsive behavior of polymer solutions is one of the major themes of this work. The idea is to induce an a priori thermal phase transition of a polymer isothermally upon specific binding events. This concept is followed through for solutions of polymers as well as hydrogels on surfaces.

The lower critical solution temperature describes the minimum temperature in a phase diagram, above which the solvent(water in this work) and the polymer are no longer completely miscible.(Figure 3) The miscible and the phase separated regions are segregated by the binodal and spinodal lines.

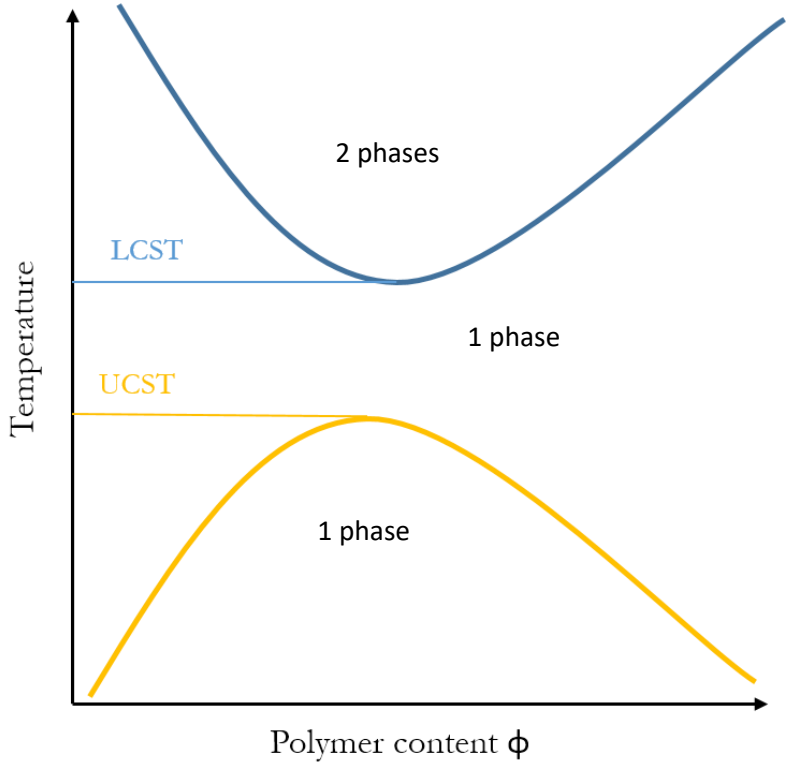

Figure 3: *Schematic phase diagram showing LCST and UCST behavior of polymers in solvents*

At the point of reaching the transition curve, the previously homogeneous system separates into a two phases, one phase being rich in polymer and the second phase being rich in solvent. Typically, studies analyze the phase transition in a certain concentration range more than focusing on finding the exact LCST value; this work is not different in this aspect. In fact, most of the time the focus will be on the cloud point of the polymer, which is a characteristic point at which the separation of the two phases is measured, meaning a turbidity of a sample can be quantified (not necessarily by the eye). This point might be on the phase transition line for some polymers but it can also be shifted.

The second curve in Figure 3 shows the inverted phenomena, the occurrence of an Upper Critical Solution Temperature (UCST) and the formation of a two phase system upon cooling. Both of these solubility phenomenons are influenced by the pH value and salt concentration of the solvent (if aqueous), as well as the solvent composition itself.

How can this behavior be explained from a thermodynamic point of view? The key driving force is entropy as seen in *Equation 1* below.

$$\Delta G_{mix} = \Delta H_{mix} - T\Delta S_{mix} \qquad \textit{Equation 1}$$

In order to allow mixing, the free enthalpy ΔG_{mix}has to be negative. Concerning the mixing enthalpy ΔH_{mix}, the hydrogen bonds between the solvent (water) and the polymer units, which are energetically favorable, render ΔH_{mix} negative. The overall mixing entropy ΔS_{mix} however is negative due to the well-organized hydration shell built around the hydrophobic parts of the polymer upon solvation. The higher the temperature gets, the bigger is the effect of this entropic factor on ΔG_{mix}. Thus, as soon as the entropy gained by "freeing" the hydration shell outweighs the energy gained by polymer-water-hydrogen bonds, the demixing is taking place.

3.3.2. Thermoresponsive Polymers and Materials

Thermoresponsive polymers share some structural requirements. There has to be a structural balance between hydrophilic and hydrophobic parts. The hydrophobic parts for most terms consist of hydrocarbon fragments. The hydrophilic parts are typically amides, alcohols, ethers, esters or other groups that act as hydrogen bond donors or acceptors. Exact predictions on how these groups interact to induce a lower or upper critical solution temperature are hard to make especially in copolymers or modified polymers, where the nature of repeat units can shift LCSTs of the parent homopolymer considerably(10, 11). A homopolymer in a defined solvent gives a typical value though. Polymer classes as peptides, polyacrylamides, polymethacrylamides, polyviny ethers, polyphosphonates or the already mentioned (meth) acrylic esters with oligo ethyleneglycol side chains are just examples of the most common ones (12, 13, 35, 36). One of the most thoroughly discussed polymer in recent literature is poly-N-isopropylacrylamide (PNIPAM) (36-48), with a LCST of 32 °C, which is shown in the figure below (Figure 4)

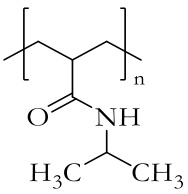

Figure 4: *Poly-N-isopropyl acrylamide constitutional repeat unit*

More recently, another type of polymer has come into focus, namely differently modified and copolymerized oligoethyleneglycol acrylates and methacrylates (OEGAs and OEGMAs)(12, 39, 49-51). Here, the idea of using (commercially) accessible materials is taken to change the LCST of the final polymer by changing the ratio of co-monomers with different chain lengths. This way, a very wide range of lower critical solution temperatures can be realized without changing the chemical system fundamentally (39, 52-54).

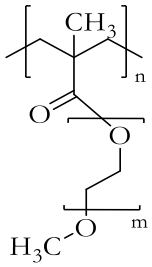

Figure 5: *Monomethyl (oligo ethyleneglycol) methacrylate repeat unit*

The monomer type for the polymer shown in Figure 5 is readily available with side chain lengths of m = 1 to 30. For aqueous systems, lengths of 2 to 9 ethyleneglycol units are the most interesting as their homopolymers have a LCST between 23 °C and 95°C(55). Due to the lack of charged groups or hydrophobic groups prone to interact with proteins, ethylene glycol based materials are sought after for their anti fouling properties. This behavior is extended by the flexibility of the chains themselves which contributes highly to the system itself and binding events would be energetically unfavorable. This means that no or very little unspecific interaction with proteins or bio material is taking place, making these types of polymers popular in bio-medical applications as well as in drug delivery systems(56-65).

3.3.3. Analysis of Thermoresponsive Polymers

Depending on the general structure of the polymer, different types of analytical options are possible. Taking into account that aqueous systems are in focus, temperature ranges are realistically between 1°C and roughly 80-90°C depending on the time the procedure takes for evaporation and concentration changes as the application of pressure on the system by using a closed vessel is to be avoided. Thermoresponsive in this work also means that the effect of an exterior stimulus is happening within a certain, reasonable time frame. So while minutes are certainly within the scope and one to two hours might be viable, too, longer response times are not practical and therefore avoided.

For polymers in solution, this work utilizes turbidimetry as method of choice to follow phase transitions induced by temperature changes and binding events. The principle is rather simple: a light source, for example a UV/Vis spectrometer equipped with a heated sample cell is set to a fitting wavelength of the cuvette used and the solvent of choice. The absorbance is measured as a heat gradient is applied or another external stimuli such as analyte addition is applied. The absorbance will change as soon as the previously dissolved polymers are agglomerating together, increasing the scattering of the light, and thus the absorbance. This phenomenon is visible by the eye, too, by seeing a clear solution going turbid. The time for this transformation can differ from polymer from polymer, and varies with the solvent as well (66, 67). Therefore care has to be taken to allow the system enough response time. If the phase change is spread out over a broader temperature window instead of inducing a sharp transition, and a pronounced hysteresis might appear as well in heating/cooling cycles.

3.4. Hydrogels on Surfaces

3.4.1. Hydrogels

By the broadest definition a network swollen with water or an aqueous solvent mix that shows a yield point can be considered a hydrogel. So a Jell-O would fall under this definition as well as a contact lens made of Poly-(hydroxyethylmethacrylate)

(PHEMA). Hydrogels can be relatively hard and resilient or soft and jelly like. While consisting mostly out of water, they behave like a compact elastic solid. Responsible for this behavior is the continuous, solid phase – a network of molecules that is crosslinked. Crosslinking can be either physical, chemical in or via electrostatic interactions(68).

Hydrogels are used in many applications. Lately focus has been on biomedical ones as wound treatment, drug delivery or tissue engineering(69). The materials in use are manifold from purely synthetic materials as PMMA to bioinspired ones as saccharides, peptides(69-71) or collagen (72).

Expanding the possibilities further, thermoresponsive hydrogels can change their swelling ratio upon a temperature stimulus. The swelling ratio (SR) is defined by Equation 2. Φ is the volume fraction of the polymer, m describes the mass of the hydrogel in the swollen or unswollen state.

$$SR = \frac{\Phi_{dry\ polymer}}{\Phi_{wet\ polymer}} \approx \frac{m_{swollen\ hydrogel}}{m_{dry\ hydrogel}} \qquad \text{Equation 2}$$

This equation will be further utilized in chapter 4.3. In order to describe the hydrogel in more detail, one can look at the process of swelling a gel. The first step is to solubilize the hydrophilic compounds of the polymer network and building up a hydration shell. In the next step, the osmotic pressure causes more water to diffuse into the system. This only happens until a certain point where the pressure equals the retraction force of the polymer network(73). This balance limits the elongation a polymer chain in the gel at a given temperature and solvent. The limit is defined by the junction points of the polymer chains– with chemically bound hydrogels as used in this work, this would be a covalent bond formed between originally different polymer chains. Expanded into three dimensions, this is the mesh size of the hydrogel. The Flory-Rehner-Theory that connects swelling ratio with the amount of monomer units between crosslinking points (N_C) can now be used

$$SR \propto N_C^{\frac{5}{3}} \qquad \text{Equation 3}$$

to connect the physical properties with the chemical structure in Equation 3 (74, 75). Predicting the exact behavior of a thermoresponsive hydrogel is still difficult though. By putting the system above the LCST transition of the polymer, the retracting force adds up with the force from the phase shifts desolution which is powered by the entropy gained as shown in Equation 1. Both oppose the osmotic force driving the water back into the gel matrix. In the systems shown in this work, no bonds are broken, so the process is reversible: upon cooling an LCST type hydrogel, it will swell with water again.

3.4.2. Surface Immobilization of Hydrogels

Surface immobilization is a step used in this work to make hydrogels easier to handle physically, and also to have a platform to manipulate and analyze them conveniently during reactions and binding experiments. A hydrogel immobilized on a surface can be washed with different buffers or reactive media without complicated clean up methods. Depending on the goal, different surfaces were used in this work; choices mostly related to the analytics performed during or after the experiment. The scope ranges from silicon wafers, gold, polyethylene, poly (methacrylic acid), glass to quartz glass.

The two main concepts of attaching hydrogels on surfaces are the grafting-from and grafting-to approaches.

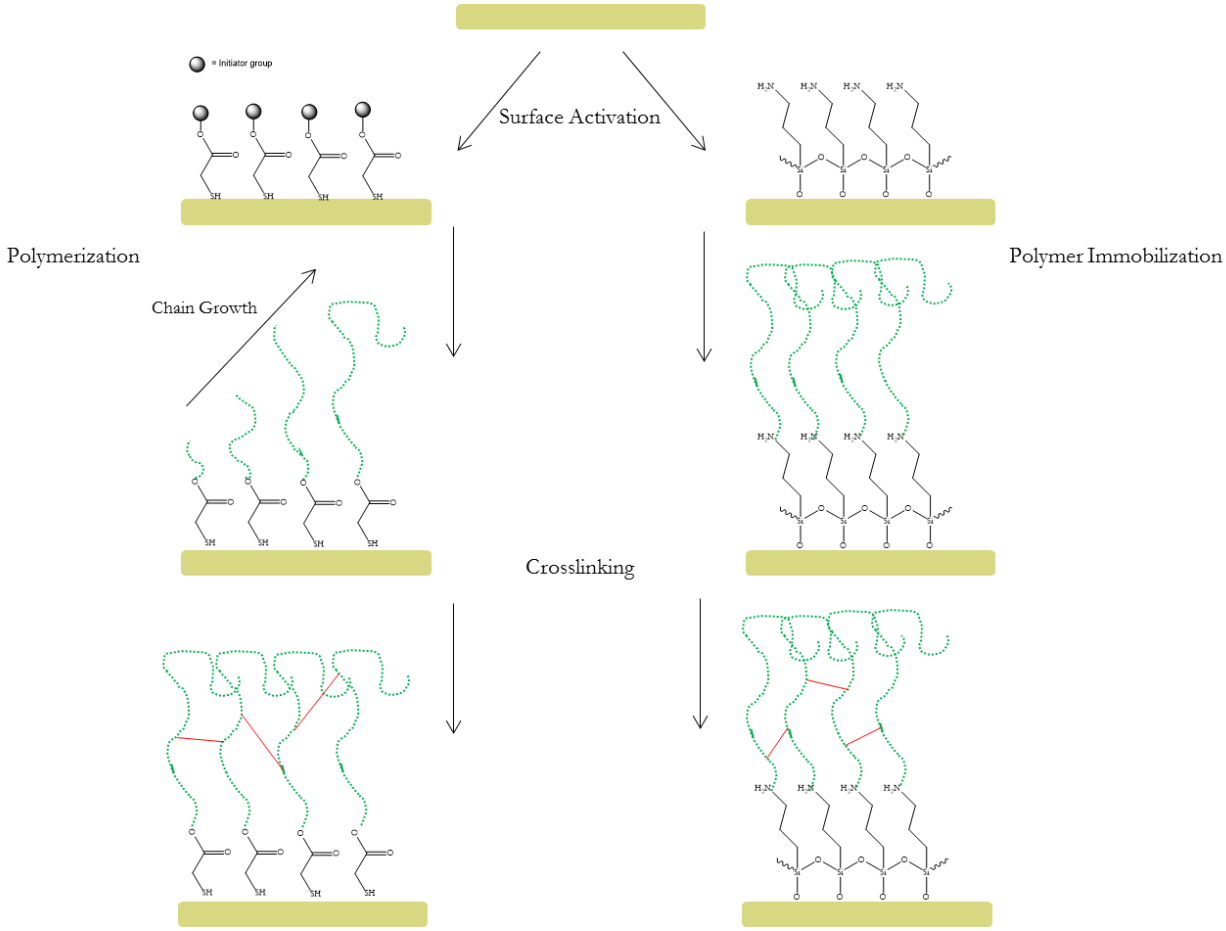

Figure 6: *Grafting-from and grafting-to approaches in surface modification*

In Figure 6, these concepts are exemplified. The left side shows the grafting-from process, the right presents the grafting-to case. The surface is prepared for the modification. Gold surfaces are often modified by thiols (optionally with secondary functionalities)(76, 77), materials such glass or pure silicon can be silanized with a multitude of functionalized silanes (78, 79). Then, depending on the polymerization technique used, the polymer is grown directly from the surface. Staying with the example, a peptide could be grown from it by step polymerization (80), alternate possibilities include free radical polymerization or RAFT methods (81). The advantage of this pathway is that the chains can be more dense on the surface in comparison with the grafting-to strategy (77). Crosslinking the polymer chains has to be done separately, either by using reactive groups within the polymer or by using a separate crosslinker.

The grafting-to approach uses premade polymers instead, that can either be immobilized by reacting an end group in a targeted fashion, as often done with peptide chains via amide bonds (82). Alternatively, it can be done in a more randomized way

utilizing radicals generated on the polymer chain, e.g. by benzophenone groups (83, 84) that get activated by UV-light. In the latter example, the crosslinking occurs at the same time as the surface fixation. Also, the density of the polymer chains would be lower due to the steric repulsion caused by dangling polymer chains in their vicinity.

The grafting-from approach is less used in scientific studies as the resulting surface layer tends to be thinner and, more importantly, the analysis of the resulting polymer is inherently limited by being surface bound. An advantage for the grafting-to method is the general flexibility, being able to mix and match different types of polymers depending on the task at hand. For instance, one could combine different polymerization techniques and use the same surface to graft onto in order to gain composite materials. For this work, polymer chain length is a key parameter, if the hydrogels should become flexible towards the kind of recognition units or bonding sites they can accommodate. As explained before, the mesh size is directly related to polymer chain length. The need for large mesh sizes becomes even more pronounced when dealing with analytes that are as large as viruses(5-300 nm (85)) and bacteria(up to 0,75 mm (86)). From a practical perspective, only having to pretreated surfaces to incorporate sites that can couple with a given polymer, is simpler than fixing a multitude of different initiator group-containing molecules on different surfaces.

3.4.3. Thin Film Analysis by Ellipsometry

Ellipsometry is a method to analyze thin films by measuring the change of polarization of incident light in relation to the reflected light upon hitting said film. These measurements give primarily information about dielectric properties, as the complex refractive index and permittivity. These measurements can be translated into more material properties such as layer thickness, surface roughness and composition of the film. For hydrogels, it is a convenient method to determine the swelling ratio of immobilized films, and the mesh size of the gel as well as swelling or deswelling upon temperature stimuli. It is also possible to follow chemical modifications of end groups and the impact of analyte binding events, too.

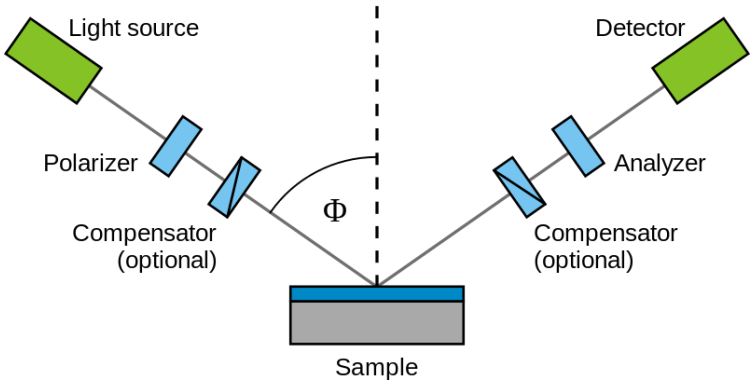

Figure 7: *Setup of an ellipsometry measurement(87).*

Figure 7 shows the schematic setup of the experiment. The laser light beam gets polarized linearly or circularly. It might be sent through a compensator quarter wave plate, or optical glass as in submersed measurements, before it hits the sample. The beam is reflected and refracted and scattered at the sample film. The reflected light leaves in the angle Φ, and might hit a quarter wave plate again. It passes through a second polarizer, the analyzer, before reaching the detector. The analyzer is the only moving part in this setup and changes its angular position perpendicular to the beam, the detector picks up the intensity of the light that is left behind the analyzer.

The incident beam and the reflected beam define a plane by their direction. The light beam itself can be separated into the component parallel to this plane, called p-polarized. The component perpendicular to this plane is called s-polarized. Both have an amplitude component Ψ and a phase difference Δ. If linearly polarized light hits the surface, it is refracted and defracted. The defracted part is reflected at the end of the layer it is moving through – in this case the hydrogel (it can be defracted again, depending on the system). The reflected beam would get to the surface to be reflected internally or diffracted outside the sample and so on. The light moving from the sample to the detector has changed polarization through this process to an ellipsoid polarization, meaning that the p and s components have different amplitudes and phases now. This relation is expressed in the ratio ρ in Equation 4

$$\rho = \frac{r_p}{r_s} = \tan(\Psi)e^{i\Delta}$$

Equation 4

If the angle of incidence Φ is chosen close to the Brewster angle, this difference reaches its maximum, and thus only the s-polarized portion is reflected to the detector. By rotating the analyzer the minimum and maximum intensities can be found for their specific phase angle. In accordance to Fresnel equations, the function shown above is also a function of the wavelength λ of the light, which is well known due to being a laser but also the refractive index of the surrounding medium (water or air), the hydrogel film and the carrying substrate as well as the corresponding layer thicknesses. Using computer governed iterative calculations, solutions for the model analysis are found in accordance with the Fresnel equations. As some factors are known, the system can be simplified, using the known refractive index of air and an infinite layer thickens on the one side of the film, and on the bottom of it a well controllable substrate such as silicon wafers, which leave the film as the open variables. As thickness analysis is the main target for this work, one can use iterations- A dry film consists mostly of organic materials whose refractive index one can measure. If wet and swollen appropriately, a ratio of the refractive index of water and the organic material can be used, though using the value of water is not too far off for highly swollen materials. With these steps and iterations, layer thicknesses are accessible. Even more complex layer structures can be calculated, even when immersing the sample in water or solvent.

3.4.4. Surface Plasmon Resonance Spectroscopy of Hydrogels

Surface Plasmon spectroscopy (SPR) is another method to analyze surfaces. It is specialized to determine the adsorption of material on top of a thin metal layer and is basically another way do gauge refractive indices of materials and film thicknesses(88). In this work, the Kretschmann configuration was used so this will be the focus of the chapter, too. The setup is a laser beam used to generate p-polarized light that gets diffracted into a triangular glass prism on one prism leg and hits the bottom that is coated with a thin layer of gold. On this layer, the beam gets reflected to the other prism leg of the prisms triangle and then into a detector. The incident angle of the laser beam can be changed. On the backside of the gold layer the sample is located, typically in a heatable flow cell. In this setup, the beam is guided through a medium with a higher refractive index (the prism) than the underlying layer (the gold

layer) with a lower refractive index with an angle of incidence above the total reflection, so no light is diffracted into the gold layer. Still, an evanescent field is generated by the beam in the gold layer. The field gets dampened within the layers interfaces without losing energy. If there is a layer of energy absorbing material on the gold film, e.g. a hydrogel film, the intensity of the reflected light is lowered. By changing the angle of incidence, this intensity can be brought to a minimum, this angle is called the angle of resonance. Measuring at this angle causes the photons of the beam resonate with the electrons of the gold layer. This means that the electron density is oscillating, this coupling effect is called a Plasmon. The oscillation in turn generates an electromagnetic field that is declining exponentially but still reaching the sample. If the sample properties change, as with an absorption or binding event, the refractive index (and the thickness) of the layer changes, thus influencing the electromagnetic field. This in turn changes the angle of resonance in order to obtain the resonant plasmon wave. For the practical application, this means that the angle of resonance and the change of it is proportional to the change in the refractive index and the layer thickness of the sample. If the angle is kept fixed, the intensity of the reflected beam is following proportionally. A fixed angle is used to study kinetics of adsorption or desorption, if it can be assumed that the layer structure is not changing drastically.

3.5. Click Chemistry for Post-Polymerization Modifications

“Click chemistry” has become a widely used label to describe many different reactions. Originally click chemistry was a selection of reactions by Sharpless et al. as well as a guide which other or new reactions would also fit into this group by definition(29). He sets up the following requirements: A “click” reaction has to be:

- Modular and wide in scope
- High yielding
- Giving only inoffensive byproducts that are easily removable without chromatography
- Regio- or possibly stereospecific
- Using simple reaction conditions, ideally being water and oxygen tolerant
- Using readily available reagents and reactants
- Solvent -free or preferably working with water or other nontoxic solvents that are easily removed

Even though the reactions he proposed were not new, the idea of click chemistry is to use modular building blocks in clever combinations. Sharpless favored carbon-heteroatom-bonds over carbon-carbon bonds with a few exceptions. In any case, energetically spring loaded reactions are his mainstay motivator for the click nomenclature. Some prominent examples include 1,3- dipolar cycloadditions of azides and alkynes, Diels-Alder cyclizations, nucleophilic ring openings of epoxides or aziridines, selected reactions of the carbonyl groups like (thio)urea and amide formation as well as additions to favorable double bonds, epoxide ring openings and even more so Michael additions.

These concepts from Sharpless original paper, while coming from a more pharmaceutical point of view, were quickly adopted to polymer chemistry. Reviews try to categorize and focus on specific parts of the concept (56, 89-96). While the lively discussion and ongoing discoveries broaden the “click” horizon, one may question if every reaction labeled as “click” fulfills all or at least most of the criteria defined by Sharpless (97). Through the different chapters of this work, typical click reactions will

be presented in detail as tools for modifying polymers and hydrogels. The major advantage of choosing click reactions as a guidance comes from practical considerations. Water, buffered systems, or water miscible mild solvents are necessary for sensible peptides and cells – while possibly more or less significant traces of unremoved solvent could cause problems. Solvent removal by dialysis is one of the most convenient methods for polymers, while simple washing is sufficient for surface bound hydrogels. While little is cared for stereospecific reactions, high yields in the post polymerization reactions are mandatory simply because the coupling partners are hard to come by and the spring loadedness of the reactions is the selection criterion for this work. This of course implies that the starting products and reagents are not easily obtainable, especially as soon as the conjugates become peptides. The question if a certain reaction or experiment is conform to the “click concept” will be issued and critically discussed.

3.6. Thermoresponsive Materials as Biosensors

Thermoresponsive materials have been used for biosensors before, with different approaches. They often have in common that they use recognition sites to bind biomolecules, forming a bioconjugate. Examples of different concepts are hydrogel coated particles able to collect inflammatory cells by attaching to proteins and then getting concentrated by heat switching(98), or enzymes blocked by a thermoresponsive modified “plug” type analyte, which is removed. This activates the enzyme by collapsing the polymer and thus removing it from the binding site (99). Dostalek et al. show that with a combination of a modified poly-NIPAM hydrogel on a surface plasmon spectrometer (SPR) modified with a fluorescence spectrometer and a fast heatable/coolable setup. By expanding and collapsing the hydrogel he can make binding sites available, resulting in a strong fluorescence signal, or collapse the gel, omitting binding and a signal increase(100). Blocking binding sites by utilizing LCST polymers and their phase transition has also been shown as a viable approach for a size selective sensor by Hofman (101). A different approach was followed by the group of Vee-Sin Lee. They used a thermoresponsive hydrogel modified with a recognition

unit to form networks of colloidal crystals in combination with the analyte – producing a visible optical change by this network build up. The thermoresponsive aspect can be used to tune the optical properties further (102).

The sensors envisioned in this work follow some of these concepts. It is hydrogel based and targets a narrow set of analytes. The gel portion may be used as a carrier but the signal is ideally boosted by signal amplification or signal cascading, which would translate in a change of the physical properties of the hydrogel, either collapsing or swelling. This amplification is needed in order to lower the limit of detection (LOD). Ideally, the limit of detection should to be in the lower µg/ml area, between 1 -100 µg/ml. Examples from medical studies can be found at around 95 µg/ml with salmonella as analyte for other rapid testing methods (103). These rely on analyte pre-concentration, so in order to be viable for a test without purification, an order of magnitude lower would be highly favorable.

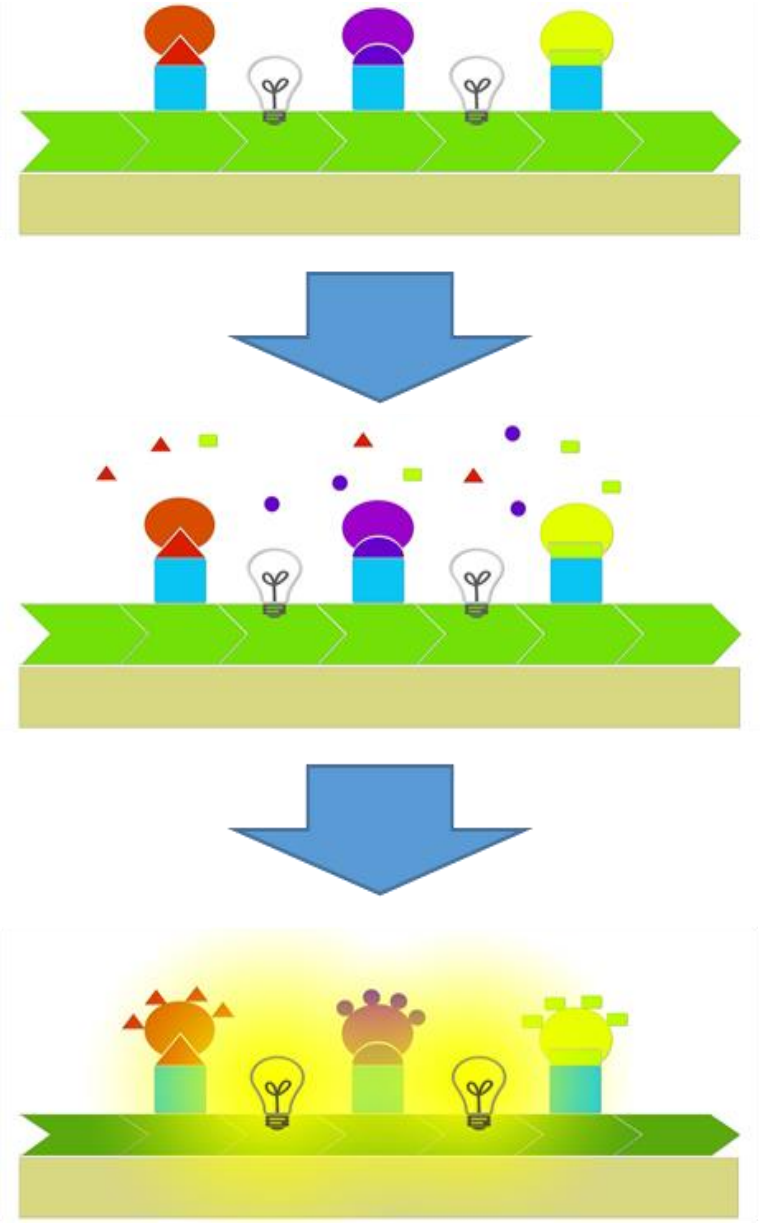

Figure 8: *Concept of a hydrogel sensor system with specific analyte binding moieties. Binding events cause a signaling cascade throughout the hydrogel, which collapses and induces signaling.*

In Figure 8 above, such a sensor is shown. The green bars represent the thermosensitive hydrogel, the shapes on top represent the binding points, for example peptides or proteins, which bind to their specific analytes. Different structures can be used to for the same analyte, too if available. The advantage of having different binding groups for the same target analyte should increase the specifity of the analyte binding, if the individual binding sites themselves are not specific enough. Clustering and pre-

orienting different binding sites together would be a possibility to enhance this effect even further, if enough knowledge about the analyte is available. The bulbs symbolize the signaling units, which may be integrated into the hydrogel, such as a solvatochromic dye. Alternatively be the hydrogel itself may show structural color. They might be integrated into the binding sites to interact with the analyte. The general principle stays the same: a fluid containing the analyte is brought onto or into the hydrogel, options would be static contact, like putting a drop onto a coated surface and letting it diffuse into the matrix. Another option is to use a more active method as pushing the fluid through a filter, for example a syringe filter, to increase the possible contact volume and giving a possibility of a concentration increase of the analyte within the matrix. It is only logical that the sensor needs some reaction time to accumulate enough binding events to cross over the LOD threshold and incur a reaction of the system. Hypothetically, a cascade could be induced by a contraction or expansion of the hydrogel mesh that would influence the adjacent mesh cells, so each singular signal would be multiplied by a certain factor. On the other hand, by using a purely additive signaling method, as a changing binding pocket that does not further influence the system at large, the LOD is higher. Thus, the first case – the interaction of the binding event with the whole system, is the more favorable case.

4. Carboxyl Based Coupling Systems

This chapter showcases the different factors that need to come together to gain a viable sensor system. The special requirements during monomer and polymer synthesis for the demonstrator hydrogel system are discussed. The focus lies on the hydrogel systems which are increasing in components and complexity. Different solid substrates are used to enable the analysis of binding reactions and recognition events.

4.1. Monomer Synthesis

The synthesis strategy for the carboxyl-functionalized monomers follows the same general ideas as the alkene and alkyne system, also utilizing very similar chemistry (Figure 9). A methacrylic polymerizable unit is connected to the coupling group for the recognition unit by an oligoethyleneglycol spacer. Due to polarity and potential reactivity of the carboxylic acid, a tert-butylic protecting group is integrated.

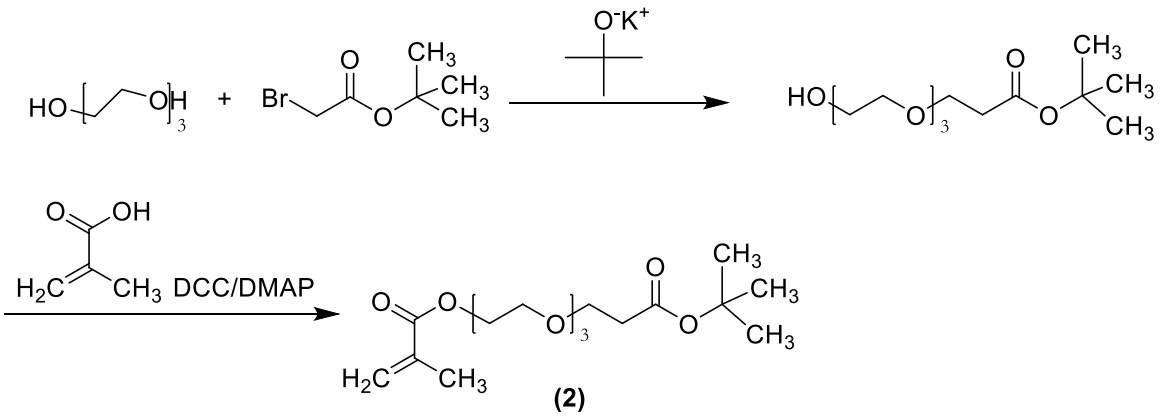

Figure 9: *Synthesis strategy for the 13,13-Dimethyl-11-oxo-3,6,9,12-tetraoxatetradecyl methacrylate (**2**) monomer*

The reasoning behind this synthesis route lies in the polymerization step. The monomer has to be completely free of contaminations from the triethylenglycol di-methacrylate species in order to avoid potential crosslinking at all costs as the aim will be to maximize the polymer chain length. The issue of impurities has to be pointed out, as the proposed pathway is not the most direct to the target monomer and simpler

ways without a protective group are readily imaginable. From the experience of this work, most impurities come from insufficient work up, whether the carboxylic group is integrated without the tert-butyl unit, is generated via oxidation, or if the synthetic route is started form the modification of methacrylic acid with the spacer first. As work up strategy a vast set of different eluent mixtures have been tried for column chromatography, as well as (high) vacuum distillation and ion exchange chromatography. In the end, taking the setback of having to remove a protective group was accepted as a necessity to keep the monomer available in decent quantities for polymerization.

4.2. Polymer Synthesis

In order to demonstrate the viability of the concept for as large as possible and available analytes, certain requirements for the polymer system have to be met. If possible hydrogels have to be driven to an as large as possible molar mass in order to keep the amount of necessary crosslinker concentration as low as possible. This in turn enables a larger mesh size of the resulting hydrogel and eases the penetration of the gel layer by the recognition unit and later on the analyte. From a statistical point of view, a polymer chain will need more than one crosslinker unit per chain to form a hydrogel, not accounting for loop formations or non-reacting crosslinker groups. This need for long, flexible chains is directly opposed to the need of mechanical stability of the resulting system.

Organic solvent based radical polymerization does have its limits in adjustability, so in order to improve on molecular size and to compare the viability of the approach, polymerizations are also performed in ionic liquids. This technique does not have an overly longstanding tradition in comparison to synthesis of “small” molecules, as a product purification via distillation is not viable for polymers (104). Ionic liquids still bring some advantages, having no vapor pressure, low toxicity and, if done properly, are recyclable, which is a positive aspect due to their high price in comparison to regular solvents. Due to their ionic nature, they are highly polar and many are water miscible as well as thermally stable.

Radical polymerization in ionic liquids has stirred some interest in the beginning of this century, as higher than otherwise usual molar masses for reactions in organic solvents or bulk have been achieved (105-107). The group of M. Haddleton performed pulsed laser polymerization experiments on methacrylic monomers in order to explain the effect better (104, 108). Their main findings were twofold – depending on the ionic liquid used in combination with the monomers, the rate of propagation (k_p) has increased due to a lowered activation energy mediated by from charge transfer effects in the transition state, caused by the ionic nature of the solvent. The other effect they put emphasis on was the rate of termination (k_t) of the polymerization, which seems to be significantly lowered due to the high viscosity of the reaction medium. While these effects are the ones targeted at in this chapter, caution has to be taken to not generalize or overestimate the possible results. Even for the narrowed down group of imidazolium based ionic liquids the resulting polymers made from methacrylic monomers vary widely (109, 110) while keeping reaction conditions identical. What seems to be a common denominator, though, is that the monomers and the resulting polymers should be decently soluble within the ionic liquid. While a pre-concentration of monomer units around the wrong polymer chain might be helpful or non-hindering to some extent, an actual full separation of reagents, polymer chains and reaction media is detrimental to the reaction.

Separation of the product and the ionic liquid as well as the recycling may not be neglected. In this work, a strategy of dissolving the polymer product and the ionic liquid in hot ethanol and then separating the two by cooling and recrystallization steps is employed.

4.3. Hydrogels

Independently of the chosen synthesis pathway, the functional polymers may be easier to analyze and handle immobilized on a surface. This is mostly due to the fact that the post polymer modifications consist of spacious macromolecules themselves. While working in solution might give an easier time binding to such molecules, the risk of simply wrapping a protein in a “hull” of polymer is high, making it inaccessible for potential analytes. From a handling perspective, hydrogels on surfaces are easy to

store in either dry or swollen state and are ready-to-use tools. In many cases, one surface can even be utilized for multiple experiments by simply washing off a reagent, switching a buffer and so on – this easy to clean prospect is especially valuable for post polymerization modifications. As mentioned in the introduction, benzophenone groups are used as main method for immobilization and crosslinking. The adjustment of layer thickness can be done by adjusting the amount of polymer brought on the surface and the spin coating speed and duration if utilized. The parameters for very similar polymer structures were described in detail by J. Buller (83, 84) and were used as a reliable starting point.

4.4. Activated Esters for Amide Bonds

Amide bonds are ubiquitous in nature, peptides and proteins use them as backbones. The idea to use those biomolecules to immobilize them on synthetic materials is not a new one, but has been around since the last half of the last century (111-113). Due to the nature of amino acids, using either their carboxylic acid or amine functionality for this cause was a logical choice.

While forming an amide is an equilibrium reaction, it may require significant activation to proceed as the equilibrium lies on the side of the hydrolysis(114). Thus, this condensation type reaction needs to be shifted in its equilibrium. This can be done either by heating and removal of water during the reaction (115), which might cause a series of unwanted side reactions especially with complex functional molecules like proteins. Or a more refined and selective method is utilized. The most common general method is to activate the carboxylic acid and transform it to a more reactive species in order to undergo an aminolysis with the target amine. While nature can rely on enzymes for peptide synthesis, common methods for the chemist are the formation of acyl chlorides with the aid of thionyl chloride (116), by formation of acyl azides (117) or utilizing anhydrides of carboxylic acids (118). A very popular way of using anhydrides is to react the carboxylic acid with carbodiimides, forming an acylurea in the intermediate step. Activation reagents are dicyclohexyl carbodiimide (DCC) or ethyl-dimethylaminocarbodiimide (EDC) (119, 120). These two compounds and their reaction can be made more efficient (and less prone to side reactions) by utilizing

activated ester intermediate, commonly referred to as activated ester. These, often aromatic, chemicals have the advantage of reacting under very mild conditions, with demanding coupling partners and with no or very few side reactions. The coupling with DCC and the aromatic partner 4-dimethylaminopyridine (DMAP) has been utilized in this work for monomer synthesis, the second example used is the combination of EDC and N-Hydroxysuccinimide (NHS). Both coupling strategies are widely known and used in organic synthesis as well as bioconjugation (11, 72, 121-130). While the combination of DCC and DMAP is commonly used in organic environments as the urea resulting of reaction is typically insoluble and can be removed by filtration, easing the work-up. EDC and NHS are often utilized in aqueous systems, as the resulting NHS-ester is more hydrolytically stable and can be isolated and stored. This coupling strategy has been published first by G. Anderson in 1963(131).

Coupling reactions using this type of chemistry are a prime example for click chemistry, as the reagents are readily available and easy to remove by aqueous work up. The requirements are mostly on the side of steric demands of the coupling partners, otherwise active esters are widely open to use with all kinds of substrates. The reactions can be driven to high yields and the materials used are non-toxic. For bioconjugation specifity and the lack of side reactions has to be viewed carefully though. Starting from small peptides to proteins other reactive groups like alcohols, thiols and amines that are not intended to couple are readily available. This is why a protective group strategy might be needed depending on the requirements of the resulting conjugate. An example of this strategy would be solid phase peptide synthesis where amino acid side chains that might interfere with the coupling are equipped with protective groups, and the terminal group attached to the resin is the only reactive partner remaining on the peptide after cleavage from the resin(80).

In this chapter, the reaction efficiency and the mild conditions of the coupling reactions are capitalized to the fullest in order to immobilize peptides and proteins as recognition units for virus and bacteria recognition, where a denaturalization of a protein might cause the whole sensor to fail.

4.5. Results

In this chapter a path to the development of a sensor system is proposed. Starting from trials in solution, the systems used will be adapted to the changing requirements of the more and more complex systems. Surface bound hydrogels will be modified in their macroscopic behavior to match the growing size of the sensor units as well as of the analytes.

4.5.1. Experiments in Solution

To discern the phase behavior and to gather experiences with the system, polymers **11** and **12a-d** were synthesized under standard conditions (Figure 10). Whereas polymer **11** consists of purely commercial monomers, the series of **12** was made to test copolymerization behavior of monomer **2.** Within the precision of the NMR analysis comparing methyl end groups (3,4 ppm) and protons of the t-butyl group (1,4 ppm) of the carboxyl functionality, the synthesis is a success and the monomers are integrated with the feed input ratio (between 15 and 30 %). In a first step, the efficiency of the oligoethyleneglycol spacer in polymer **12d** is put to the test as it represents the targeted concentration of functional groups in this work, balancing between a good amount of binding opportunities, but keeping the framework somewhat predictable in its behavior. While the spacer is longer than the MEO_2MA side chain, it is still open for discussion if this difference is paying off in solution, before going one step further and immobilizing the polymers on a surface. In order to remove the tert-butyl protective group, the polymer is treated with trifluoroacetic acid (TFA) and then dialyzed.

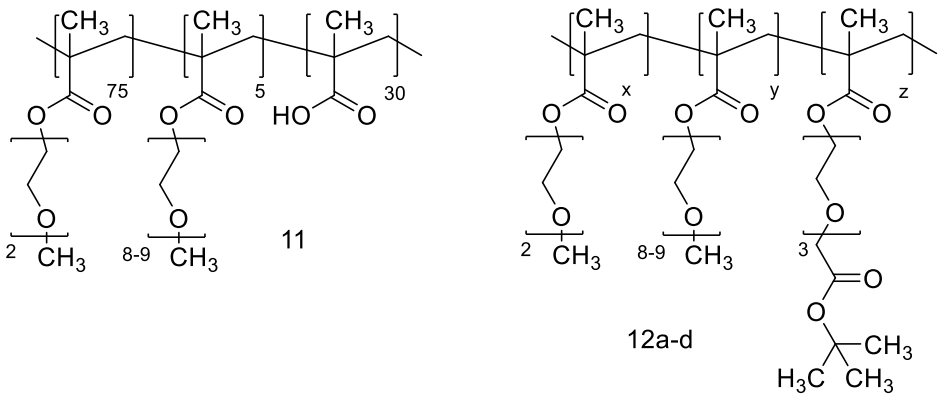

Figure 10: *Polymers 11 & 12a-d. Reaction conditions 55-60°C, 24-48 h, solvent: neat ethanol, initiator AIBN. Copolymer compositions ranged from 10-30 mol% of carboxylic monomer* ***2****, 5 mol% OEGMA*^{475}*, completed by MEO*$_2$*MA*

The polymers **11** and **12d** are coupled in aqueous solution to benzylamine with the help of active ester chemistry utilizing 3-(ethyliminomethyleneamino)-N,N-dimethylpropan-1-amine (EDC) and N-hydroxysuccinimide (NHS) as coupling agents(Figure 11). Benzylamine was chosen as a coupling partner due to being water soluble while having aromatic protons (7.2-7.5 ppm) that are easy to trace in the signals from the polymer background.

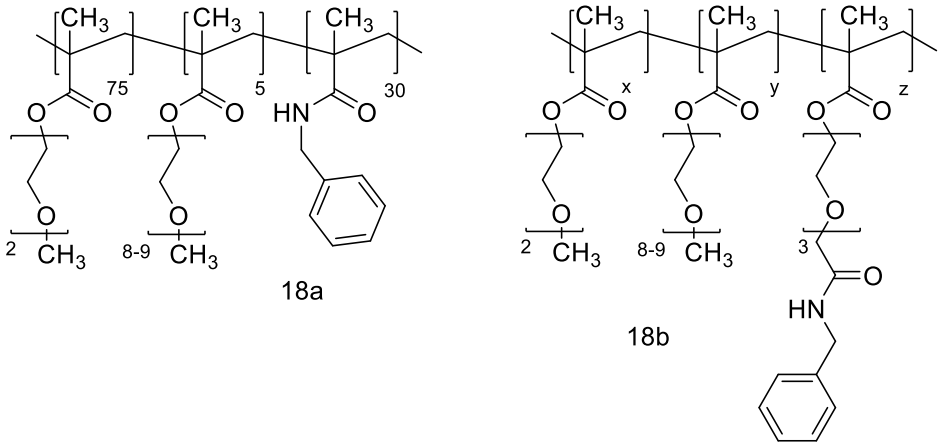

Figure 11: *Carboxyl group containing polymers* ***18a*** *and* ***18b*** *modified with benzylamine via EDC/NHS chemistry*

The resulting difference in coupling efficiency is quite pronounced. The polymer relying on methacrylic acid as coupling group (**18a**) only reached 50 % conversion of with benzylamine, whereas the customized functionality of polymer **12d** reached a 97% conversion (**18b**). The extent of these results is quite significant for the polymer design, as benzylamine is not very demanding from a sterical point of view. The exact cause

for the difference has not been discerned with these experiments but there are plausible options. First, the carboxylic group of polymer **18a** is in direct vicinity to the polymer backbone. This might hinder the nucleophile to get access to the electron deficient carbonyl carbon – this would follow the logic why methacrylics are more stable to hydrolysis as their acrylic counterparts. This point would hold up through all the steps of the Steglich esterification. The other way of driving the argument is to claim that the hindrance came from the barrier of the ethylene glycol chains in vicinity to the acid group. A possible way to discern the two hypothesis would have been to increase the $OEGMA^{475}$ ratio and to see if the coupling efficiency drops, or the other way around, increasing the content of methacrylic acid – if the coupling would rise proportional, so a 10 % increase in the feed would yield a 5 % higher coupling rate, one could guess at steric blockage from the methacrylic backbone –if the coupling ratio rises up unproportionally a point can be made for having made the polymer more accessible by removing the “fuzzy” oligoethyleneglycol chains.

Table 1: *Shift of phase transition temperatures upon reacting the polymers **11** (to **18a**) and **12d** (to **18b**) with benzylamine.*

Polymer	Phase transition temperature [°C]
11	53
18a	43
12d	40
18b	36

In Table 1 the results of the LCST screening are shown. It is clearly visible that the free acid groups of polymer **11** are the driving force for the high phase transition temperature. A drop of 10 °C takes place upon coupling the material with benzylamine. For the OEG spacer containing polymer **12d,** the starting point, with the hydrophobic protective group still attached, sits at 40 °C, the results for the unprotected polymer are not shown, as they were not yielding a measurable phase transition up to 80 °C. This point was chosen as a cut-off point for measurements, as the cuvettes were intentionally not airtight to prevent pressure building up and influencing the measurement, but evaporating solvent of course also changes possible results. It has to be noted though, that both results for the benzylated polymers are relatively close

together. This does not seem logical at a first glance due to the oligoethylenglycol chains that should promote solubility and increase the LCST of polymer **18b** over the one of polymer **18a.** A possible explanation is that three EO units are not yet increasing the water solubility by such a large extend as expected, being more neutral in the balance between hydrophobic and hydrophilic interactions. If the bonding efficiency is taken into account though it is clear that the free carboxylic groups have a big impact on the final phase behavior. One polymer has more or less none left, whereas the other has half of them still available. This contributes to the solubility due to the charged nature in solution. Accounting for all these factors is probably the most sensitive way to approach this system. The aid of the spacer glycols in the conjugation is undisputed though and can be taken as a sound proof to continue using spacers.

4.5.2. Hydrogel Formation

The second step after determining the general usability of the customized polymers from group **12** is to integrate a crosslinking agent so the polymer can be immobilized and crosslinked. Following up, the gel can be characterized and adjusted for further steps.

The most convenient way to integrate a crosslinker is to have an orthogonal functionality set up in the polymer to avoid unwanted or uncontrolled side reactions. Benzophenone ethylether methacrylate was kindly provided from the group as established working tool (84) and only needed to be integrated into the new systems at hand (Figure 12)

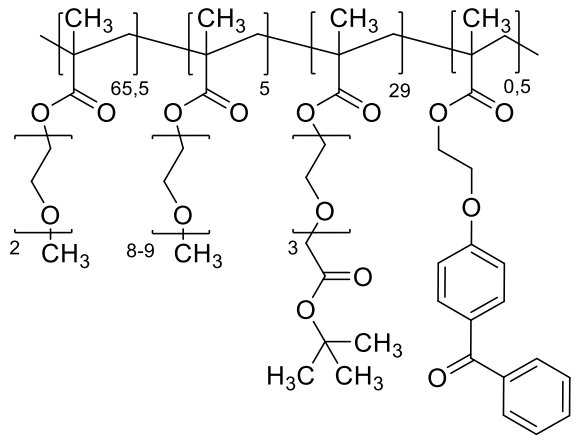

Figure 12: *Polymer **13**. Reaction conditions 50°C, 24 h, solvent: neat ethanol, initiator AIBN*

This polymer is used for spin-coating onto freshly prepared silicon slides in order to gain some predictability of film thicknesses. Thus the coating duration, speed and solution volume is kept steady, and only the polymer concentration changes. The films are crosslinked with the help of UV light. Then, the now immobilized surfaces get washed with water in order to remove any loose polymer chains that might interfere with later experiments or analysis. The results are shown in Figure 13: one can see that the thickness is growing stepwise, but not in a truly linear fashion. This is attributed to viscosity changes of the coating solution by increasing the viscosity of the mixture and thus flowing slower at the same coating speed, leaving behind a thicker layer to crosslink.

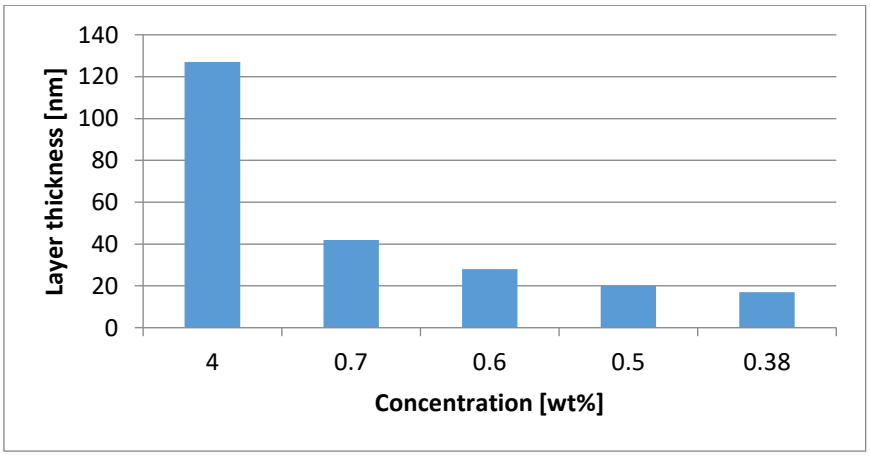

Figure 13: *Layer thickness of dry hydrogel films in relation to the coating solutions' polymer concentration*

The layers have to be characterized by their mesh size before attaching other materials in order to be able to better understand the results. Therefore, the swelling ratio (SR) is used. The swelling ratio has been introduced by equations 2 and 3 in the introduction, but for practical use it has to be expanded and connected to the mesh size ε (132).

$$\epsilon = SR^{1/3} * r \qquad \text{Equation 5}$$

$$r = d_{c-c} * (2N_c)^{\frac{1}{2}} * C_n^{1/2} \qquad \text{Equation 6}$$

The connection is made via the equations above, where the factor r defines the distance between two crosslinking points of the polymer. C_n is a static factor, for methacrylic polymers its value is 6.9; $d_{C\text{-}C}$ describes the distance bridged by C-C bonds while N_c is the amount of monomer units between two crosslinking points.

For polymer **13** a mesh size of 6 nm was determined this way for optimum conditions. The first coupling target on was the small protein Lysozyme with a maximum dimension of about 5x3x3 nm (133). As a precaution, the mesh size was considered to be too small, so a practical approach was chosen: polymer **13** was blended 1:1 with polymer **12d** as their main difference is the lack of a crosslinker. The goal was to reduce the crosslinker concentration and thus increase the distance N_c between two crosslinking units. The polymer blend was processed normally and then remeasured yielding a new mesh size of 11 nm. With these results at hand, gold chips were coated with the polymer blend in order to gain live insights into protein coupling. The targeted size for all hydrogels in the swollen state was between 400 and 500 nm. From a process point of view, safe for the coating and the crosslinking of the hydrogel, all further reactions are done in the SPR spectrometer as well as the deprotection of the carboxylic group and its activation, too. This means that the system shows a decent mechanical strength as the solvent is changed from water to acetate buffer and the different reagents which inflicts quite some osmotic stress on the hydrogel layer. The method of choice for the coupling reaction was the known EDC/NHS activate ester

coupling strategy at room temperature as Lysozyme contains an amine end functionality.

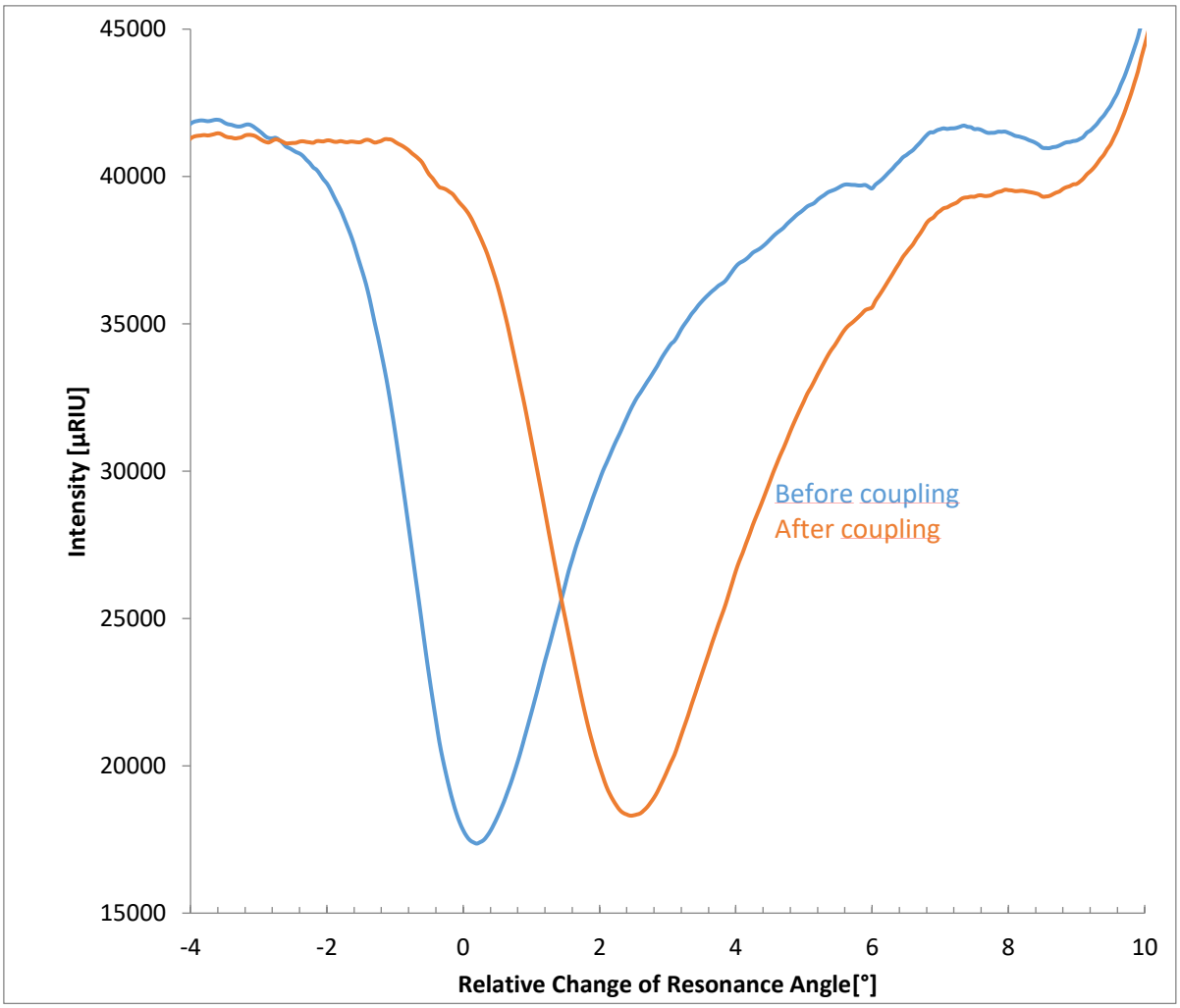

Figure 14: *Angle resolved intensity curve of the coupling of Lysozyme proteins on a hydrogel layer with carboxyl functionalization. The change in resonance angle is the equivalent of a layer growth of about 22 nm.*

In Figure 14 the resonance profile of the experiment is shown. The blue line represents the deprotected, swollen hydrogel on the chip, the red line is the same hydrogel after coupling with lysozyme and washing the chip with buffer. The change of the resonance angle, the minimum of the curve is what to look out for, a change of 0.1° represents roughly 1 nm in layer thickness. Here, the angle shifts over 2 °, representing a layer growth of about 22 nm in total. This growth does not represent a layer on top of the hydrogel, it has to be taken into account that lysozyme bound to the hydrogel increases the solubility of the layer and thus the swelling ratio of the layer. So it is a combination

of proteins penetrating the layer and attaching to it and then widening it up, as well as a top layer on the hydrogel surface, possibly even clogging the network structure to the remaining proteins in solution.

For the swollen, unreacted layer having about 70 nm of thickness, this is quite some considerable growth. While it has not been determined, how deep the layer was penetrated, it is assumed that the attachment of the protein does not increase the layer thickness in an additive way (safe for the top layer) but rather stretches the meshes to be properly hydrated and able to move as freely as possible due to entropy.

4.5.3. The Tailspike Protein – Salmonella Polysaccharide Recognition System

With the bonding ability of the synthesized polymers and hydrogels proven in the previous chapter, the experiments are continued with a more complex system and especially a system, where a recognition unit for the specific interaction with an analyte is available. The group of Prof. Seckler from the University of Potsdam kindly shared a system to work with within the framework of the project. The system consists of the tailspike protein NBD-P22TSP (Figure 15) from a bacteriophage, which is labeled with a fluorescent dye, N-((2-(iodoacetyl)ethyl)-N-methyl)amino-7-nitrobenz-2-oxa-1,3-diazol (IANBD).

Figure 15: *Fluorescent labeled tailspike protein of phage 22 (134, 135)*

The tailspike protein is intended to be bound to the hydrogel layer and with its binding pocket it is able to selectively bind to the T400C polysaccharide of Salmonella Typhimurium. This saccharide consists of fragments of 10, 20 and 60 kDA units. With this kind of selective bonding it should be possible to monitor the binding process via SPR spectroscopy but, due to the fluorescence label, also with different fluorescence methods as the fluorescence intensity is claimed to be up to ten times higher in a binding state than in a non-binding state at 540 nm (136).

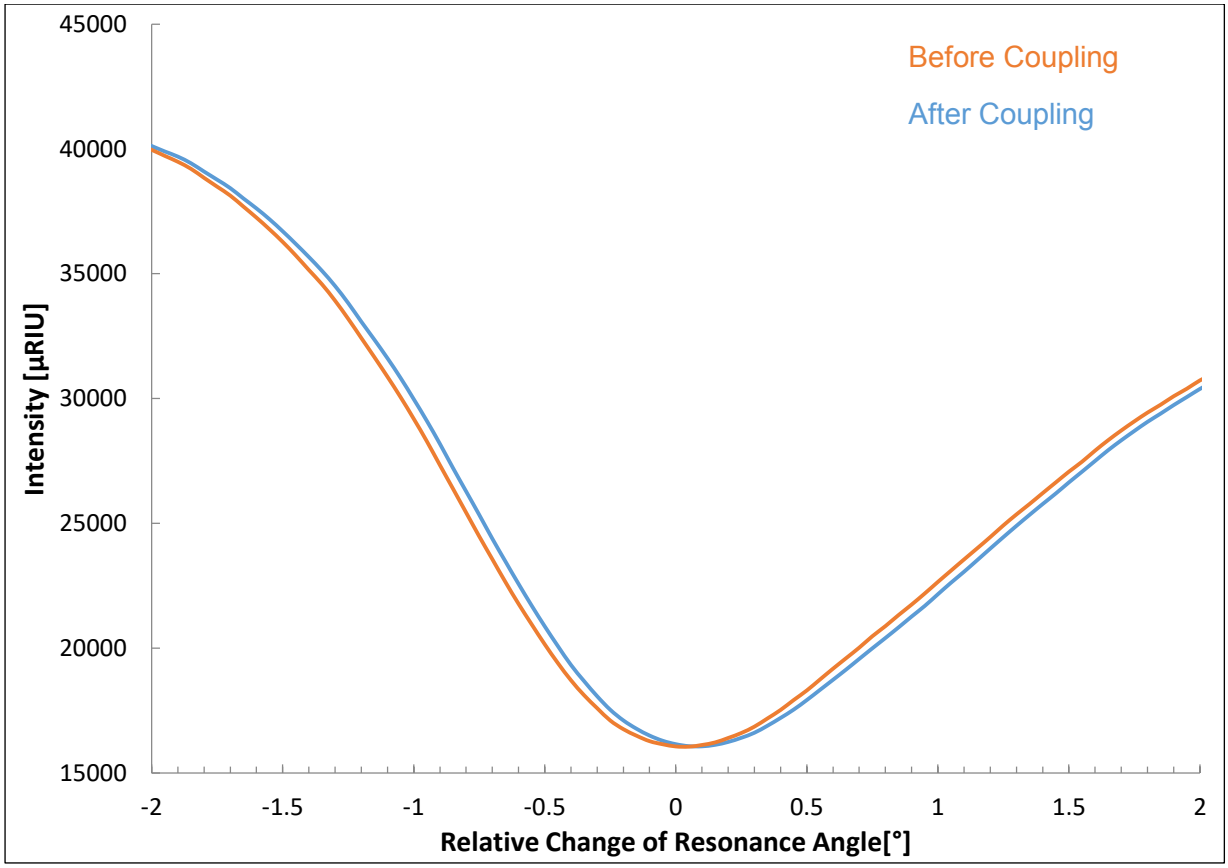

***Figure 16**: Resonance curve of the tailspike protein immobilization on a blended hydrogel made out of polymers **12d** and **13.** The change in angle is about 0.5 °, the equivalent of 1.5 nm.*

The exact same modified chips used in the last chapter to immobilize Lysozyme failed to do so for the tailspike protein as can be seen in Figure 16. During multiple trials, the result of the experiment stays the same. With a change in layer thickness of about 1.5 nm, there is a higher possibility of seeing the result of the activation with EDC/NHS and the deactivation with ethanolamine than anything else. While at least a monolayer on top of the hydrogel was expected, a possible explanation for this lack of binding would be that the binding site of the protein has higher sterical requirements, and therefore, needs either a more flexible network to bind to, or a more exposed binding group. This would mean that a different monomer with a longer oligoethyleneglycol spacer would be necessary. Synthetic challenges aside, this was not the path to be chosen due to the fact that the longer the spacer, the more the recognition unit would be detached from the whole hydrogel network, the less influence would a binding event have on the thermoresponsive behavior, making this property obsolete as this

requirement could be fulfilled with a monolayer on a surface, too. In order to design the hydrogel to be more flexible and to increase the mesh size, the starting material needs to be a much longer polymer than **12d** in order to be able to reduce the crosslinker content by a significant amount, allowing the mesh size to grow.

4.5.4. Hydrogel Systems Based on Improved Polymer Synthesis

In order to achieve this goal the polymerization data from previous polymerizations in ethanol were reviewed and found to be inconsistent as well as too low independently of the system. These polymers have molar masses around 20-100 kDa which is roughly between 50 and 200 monomers per chain. In order to resolve this limitation, the polymerization technique has to be modified. The method of choice was to rely on synthesis in ionic liquids, which would require no or very little changes from the other parameters and thus would give a better comparability between the standard polymerization and the ionic liquid based one. The reasoning for utilizing ionic liquids can be found in paragraph 4.2., leaving the question which ionic liquid to select. From literature screenings (106, 109, 110), the choice fell on 1-ethyl-3-methyl imidazolium hexaflourophosphate (EMIM PF_6, Figure 17), the reason being that due to its melting point of 62 °C, the polymerization temperature needs not to be increased too drastically from the standard 60°C and also, the viscosity will stay relatively high, pushing the polymer to larger chain lengths.

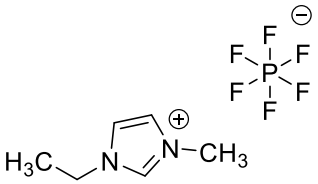

Figure 17: *1-Ethyl-3-methyl imidazolium hexafluorophosphate (EMIM PF6)*

The comparison in the mentioned literature also gives the highest molecular weight with a medium polydispersity. Polydispersity is mentioned because if a large quantity of short chains are in the resulting polymer material, it might weaken the hydrogel structure by “using up” crosslinking units without having own crosslinking points, making the hydrogel “fuzzy”. Another negative consequence would be that during the

washing steps, much of polymeric material could be lost, making the prediction of the hydrogel layer thickness unpredictable.

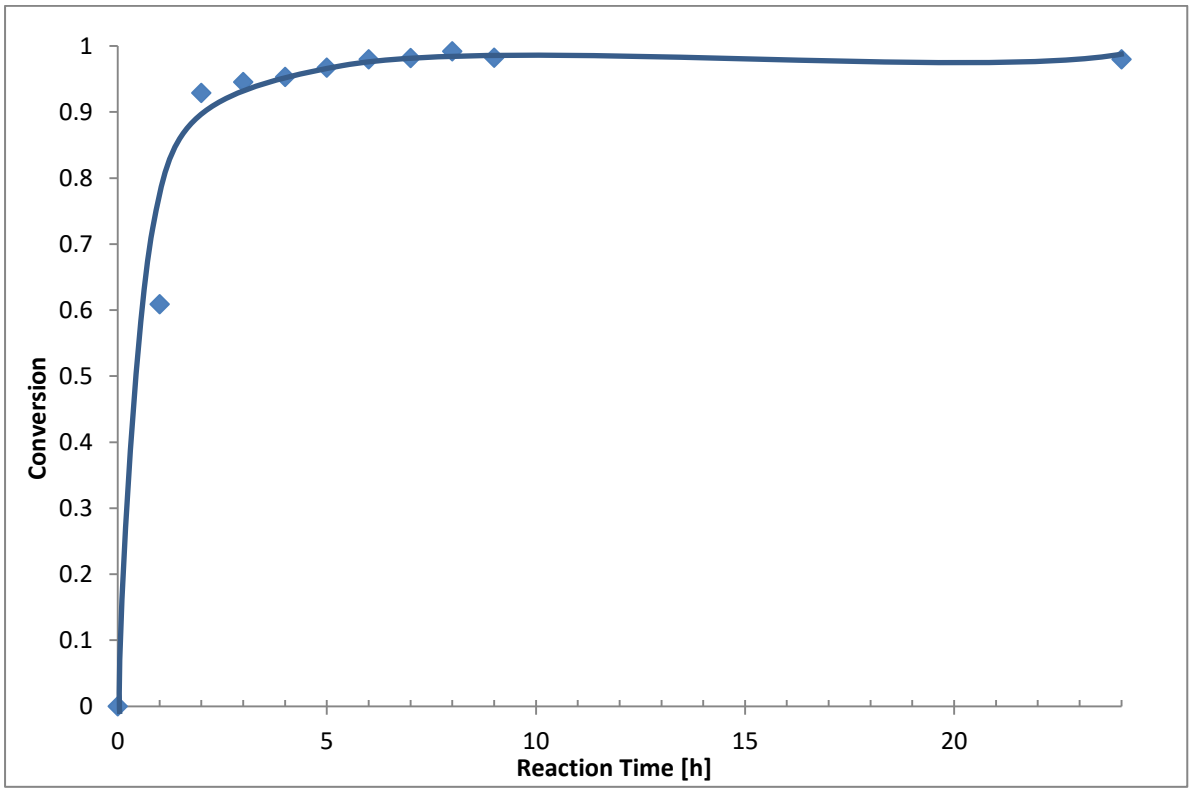

Figure 18: *Kinetics of the copolymerization of MEO_2MA and $OEGMA^{475}$ in EMIM PF_6. The conversion is controlled via ^{1}H-NMR spectroscopy.*

To get a better grasp on the specific system, a dummy test was performed to see if the ionic liquid harmonizes with the majority of the polymer system, using the simplified polymer **15** (Figure 19) as well as finding the required reaction time.

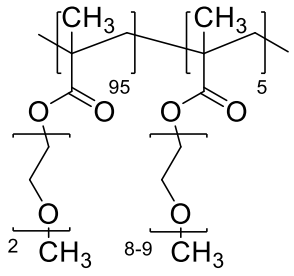

Figure 19: *Poly(oligo(ethylene glycol) methylether methacrylate475-stat-di(ethylene glycol) methylether methacrylate)(**15**)*

This is presented in Figure 18. The graph is the result of a simple reaction kinetics study with the goal of finding a point of high conversion with the minimum of reaction time to avoid unwanted gelation. The sampling was done from one and the same ongoing reaction, the turnover was determined by comparing the ratio of available

monomer, signified by the total available vinylic protons to the methyl protons of the ethylene glycol end cap. While the purification by crystallization of the ionic liquid from cold ethanol might give a certain error margin, this error should lie more on the side of trapped or unsolved polymer chains than on the freely soluble monomers. As can be seen from the graph, the polymerization is completed after 8 h. By going through the remaining time and taking a sample, the molar weight was determined to be 260 kDa by number average and 1100 kDa by weight average for this copolymer **15**. By comparison, polymer **13**, synthesized with standard conditions had a M_n of 50 kDa and a M_w of 70 kDa. So the polydispersity rose from 1.4 to 4.2 by using an ionic liquid, which is within the range reported in the literature(110). The gain in chain length is considerable and encourages the decision to use this more complicated synthesis procedure.

The reaction was repeated with an adapted feed containing both binding and crosslinking units. The resulting polymer **16** reached 42 kDA as number average and 100 kDa with a polydispersity of 2.5. This result was below the expectations but shows that in order to optimize the polymerization, a plug&play approach might not deliver the intended result. Still, the polymerization did advance to higher masses and of course the lower crosslinker concentration should help to extend the mesh size in comparison to the previous trials. Care has to be taken on how much of the polymer is lost during washing and deprotection steps. Measurements on Si-Wafers are compiled in Table 2.

Table 2: *Hydrogel layer analysis for the swelling ratio and mesh size of a polymer **16** based gel*

	Neat	Deprotected Functionalities
d (dry)	255 nm	138 nm
d (swollen)	1926 nm	1975 nm
Swelling Ratio	7.5	14.3
Mesh Size	25 nm	31 nm

By looking at the dry film thicknesses, the consequences of the molar mass and low crosslinker concentration are directly visible, by going from the dry film with protective groups to the deprotected, and at that point several times washed, hydrogel layer, 46% of its thickness is lost. While this has to be reflected in the planning of layer

thicknesses, it also shows that there are enough chains with sufficient crosslinker concentration to form a stable hydrogel. Also, the impact of the carboxylic group on the swelling ratio and the resulting layer thickness in the swollen state becomes obvious. Removing the t-butyl unit doubles the swelling ratio and puts the layer thickness on the same levels. At this stage, it is not possible to determine if the polymer chains that get washed out did have no, too little, or evenly distributed crosslinker concentrations in comparison to the properly immobilized chains of the hydrogel. So while the swelling ratio is very promising, it is certainly possible that the actual mesh size is not properly reflected in calculations according to equation 5-6.

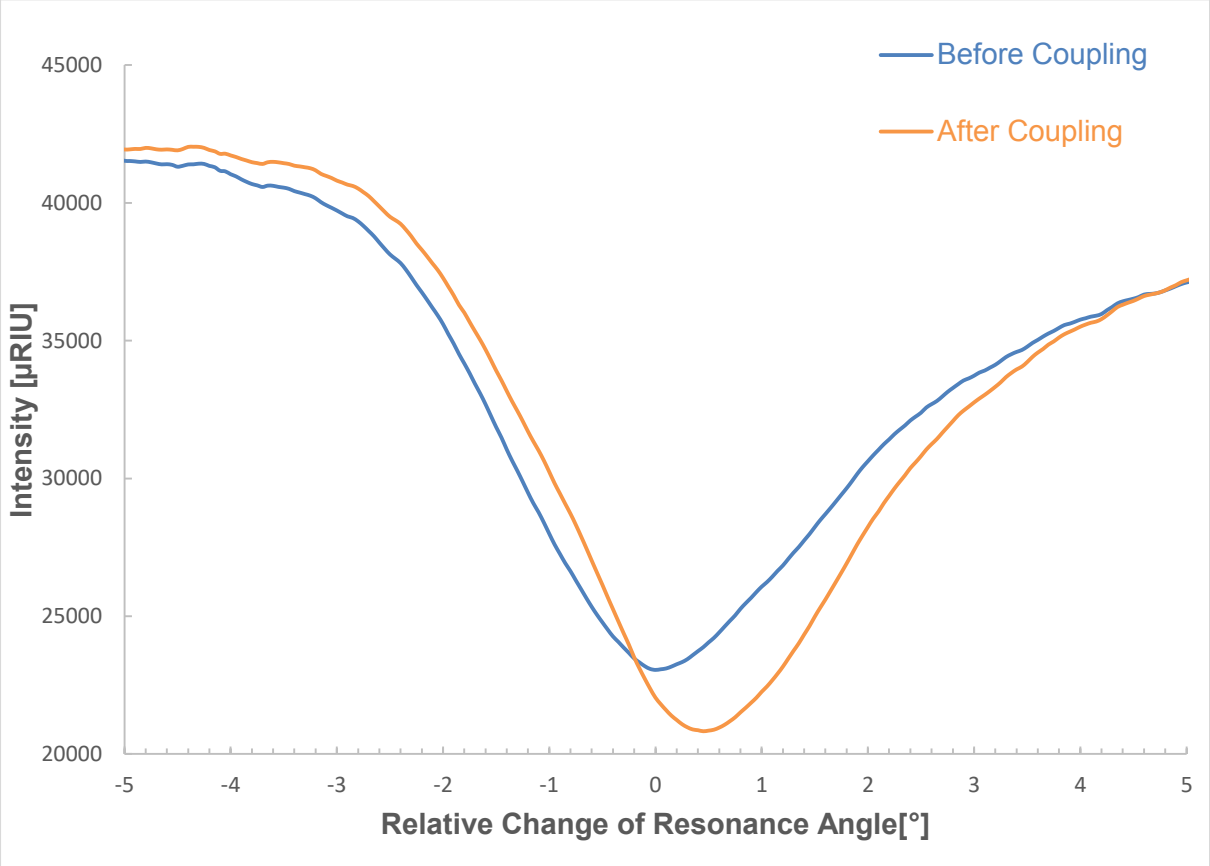

Figure 20: *SPR curve comparison before and after the immobilization of the tailspike protein recognition unit. This hydrogel base material was polymerized in an ionic liquid. The change in layer thickness is 5 nm*

With this polymer at hand, chips with in between 400 and 500 nm thin hydrogel layers were prepared. The SPR measurements show some changes in coupling behavior with the tailspike protein. The graph in Figure 20 indicates a larger shift in resonance angle for this hydrogel based on the ionic liquid utilizing polymer **16** as it has with the composite hydrogel formed out of polymers **12d** and **13,** see figure 16 for comparison**.**

The relatively small shift of 5 nm opens up the question of interpretation. In the worst case, no protein binding took place and instead, the results of surface deactivation are visible. This interpretation feels one sided, but still it seems to be a reasonable argument that the hydrogel is not highly modified with the recognition unit. A more sensible assessment would be to question if the hydrogel has been penetrated at all, or if there is a surface or near surface layer of immobilized protein. It is clear that the protein would not attach perpendicular to the surface, but more in a tilted conformation and that it would be moving as well. Portions of the protein could also penetrate into the hydrogel. While the lower “levels” of the hydrogel might be off limits due to hindered diffusion and the possibly smaller than measured mesh size, the binding sites close to the surface might be accessible. If it is assumed that the proteins are laying tilted on the surface, asking for the accessibility of the recognition moiety of the salmonella saccharide is of course justified. A given protein could be attached to the hydrogel at multiple points and make it impossible to get the binding pocket into the right position, while being too closed off from the surrounding liquid phase that the saccharide could find the pocket by diffusion.

In order to test the systems behavior, three different concentrations of the analyte were injected into the sampling loop and then sent onto the sample surface. The time resolved graph in Figure 21 shows that.

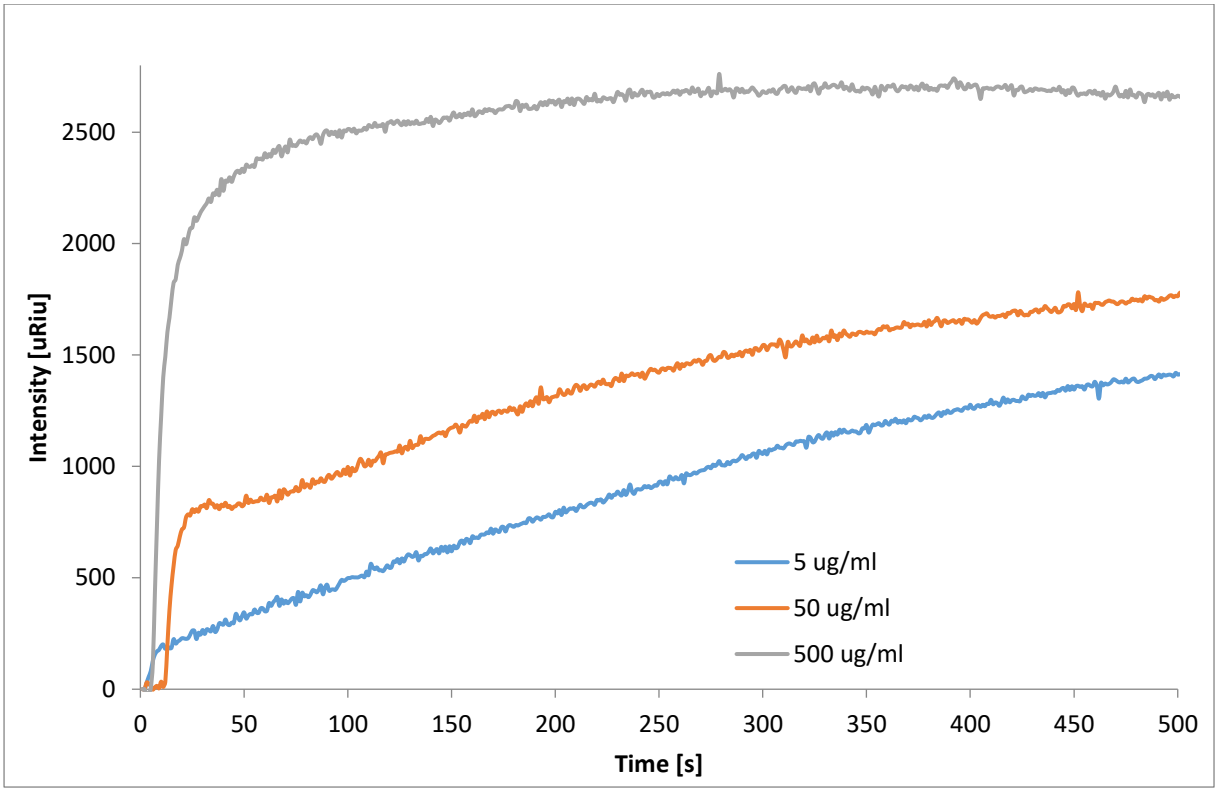

Figure 21: *Different concentrations of the Salmonella surface polysaccharide are flushed over the hydrogel surface. The time resolved intensity reaction of the gels refractive index is shown. Saturation of the gel is achieved for the 500 µg/ml sample.*

After the initial bump in intensity other features emerge. The intensity after integration of 5 and 50 µg/ml is ramping up over time, while after injecting 500 µg/ml, the values reach a plateau after about 3 min. Of course, there is an effect from purely injecting the sample solutions with different refractive indices. This offset has not been calculated out of the data. For the two lower concentrations, polysaccharide is accumulating on the hydrogel surface during the complete measurement. While the slope gets shallower, it does not reach a steady state of full saturation. For the 500 µg/ml sample, a kink can be identified about 2 min into the experiment, about the same time the slope gets more constant after the 50 µg/ml injection. Presumably, the saccharide starts to bind and accumulate in the tailspike proteins binding pockets instead of washing over the surface or sticking to it with unspecific interactions. For the lowest concentration of 5 µg/ml, this effect is not pronounced. Possibly, the concentration is low enough that either the saccharide attaches to a binding moiety on the tailspike protein, or it is in such a high dilution that it is not sticking to the surface by unspecific interactions to generate a bigger and more constant signal.

In order to get a better understanding how much of the signal is caused by unspecific binding events, and which parts of the signal are actually caused by the binding between the saccharide and the protein, more slides were prepared. The slide for this comparison treated again with 50 µg/ml injection of Salmonella saccharide T400C, then flushed with buffer and HCl solution to clean the binding pockets. Afterwards the slide was treated with the same concentration of a saccharide gained from E.Coli cell membranes.

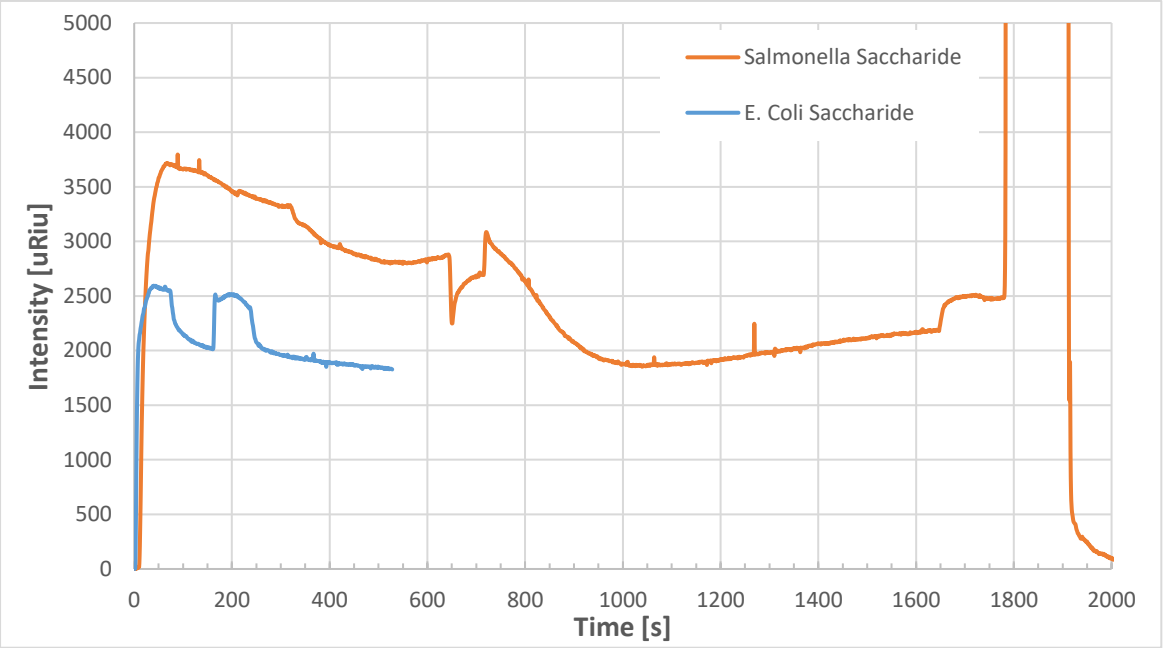

***Figure 22**: Comparative SPR-study of specifically (red) and unspecifically (blue) binding polysaccharides on the peptide modified hydrogel surface. The first injection(s) and their decrease of intensity over time show the difference between binding and nonbinding saccharides: The nonbinding saccharides intensity drops immediately after the injection stops, the binding saccharides drops much slower.*

As can be seen in Figure 22, the graphs look quite different despite being normalized to the same starting intensity. The first injection (0-50 s), the intended binding partner causes an almost 50 % higher intensity response. Furthermore, the injection lasts only 20 s in the beginning, the signal tapers off quite slowly and in an irregular pattern. The jagged curve may have come from air entrapments or some parts of the layer being unstable and getting washed off. Nevertheless, it takes about 15 min for the signal to reach a minimum, after which the surface seems to swell again slightly before HCl (0.01 mol/l) is injected to clear the binding pockets and the surface. As can be seen, the intensity drops rapidly back to the starting point. After this, the control saccharide is injected, showing a similar, high peak upon initial injection – but different from the

original analyte, the intensity drops off almost immediately after the injection was stopped, and falls down to a lower value. For a perfect theoretical system, this would mean that the intensity should fall back to its base value (here it would be normalized as 0); this step should be repeatable. Hypothetically, both saccharides should be removable completely, giving a long enough washing procedure even without HCl. In these experiments however, this seems not to be the case, which means unwanted processes are happening. The more obvious conclusion is that the hydrogel exhibits unspecific interactions with the analyte. The carboxylic groups should have been deactivated by the reaction with ethanolamine after the tailspike proteins immobilization. If the process is not complete, this might very well be the case. What might add up to this is the thickness of the gels – while standard inactivation procedures were utilized, they may have been not sufficient to ensure that the carboxylic groups within the hydrogel were fully inactivated (or activated in the first place even). Additionally, the surface layer of the chip is a hydrogel of considerable mesh size instead of a monolayer of polymers or a dense polymer layer, and the analyte is in comparison a quite small polysaccharide by pure dimensions. This could cause diffusion of the polysaccharides into the layer, where they get trapped and do not diffuse out of the hydrogel fast enough in relation to the used time scale.

Nevertheless, the graph of Figure 22 makes it clear that the hydrogels response is certainly different for the two different polysaccharides, with the targeted analyte having a much higher retention time on the layer than the control material. This shows that enough tailspike protein was bound to the gel to generate a signal and that the tailspike protein is not blocked off in a way that it can no longer interact with its analyte, meaning that this is a viable approach to detect the salmonella polysaccharide with this system, making up an already relative complex demonstrator.

These experiments were meant to be control experiments and used as a proof of concept before doing any further steps. The intention of this segment was to analyze the binding and recognition behavior of the tailspike protein – polysaccharide system with the help of fluorescence spectroscopy, as it is fitted with a chromophore that changes its fluorescence intensity upon binding. For this, glass slides were coated with the hydrogel system based on polymer **16** and prepared to the point of the tailspike protein being immobilized in two different concentrations and the layer deactivated with ethanolamine. As comparison, commercial Glymo and Epoxide slides

were spotted with the recognition unit as well as with their standard procedures. In summary, the analyte was used in different concentrations, the control polysaccharide, too, as well as polyvinylalcohol and blank fields were set up. Clearly, immobilization was taking place as there is no change in fluorescence for any of the slide types or the offered analyte at all. This leaves the question open if the chosen system was truly fitting for this kind of demonstrator. Of course handling errors cannot be fully excluded though the materials were handled with utmost care and by experienced application users. These results show that, while being promising, biosensors of such complexity are not as plug and play as other, simpler demonstrator systems and need a much more preparation to be viable as demonstrator tool for hydrogels.

4.5.5. Influenza Virus Detection Demonstrator System

The previous demonstrator system aiming for salmonella detection has shown some of the shortcomings of a large detector unit, namely a difficult integration onto the polymer or hydrogel system as well as the possibility of having a hard to control amount of inaccessible binding sites. Furthermore, with the fluorescent signaling unit being placed within the binding pocket, the spectroscopic detection can be problematic as well.

A different approach is to include the signaling unit into the polymer chain itself instead of at the receptor unit. This demands that there is an interaction that spans from the analyte to the detector unit to the polymer chain and then to the signaling unit.

H. Memczak from the former Fraunhofer IBMT kindly provided the basis of the system. MX-31 type influenza virus samples, a binding peptide specific to surface proteins of this virus stem as well as a control peptide that would work for other stems (compare Figure 23 for the sequence). The supplied peptides have their carboxylic groups protected by t-butyl protective groups, which were removed with TFA after coupling according to the standard procedure.

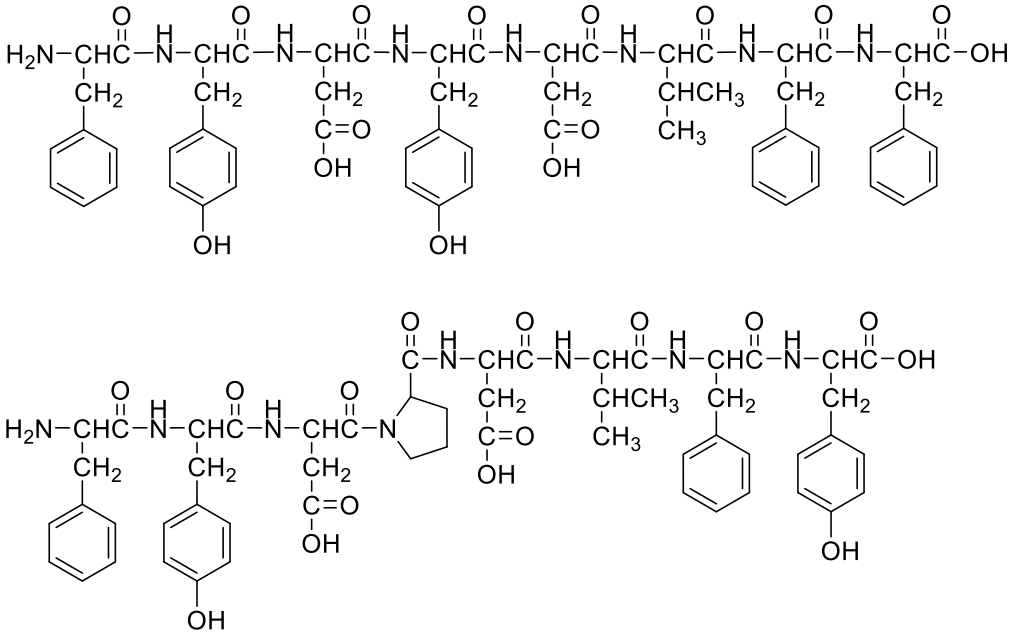

Figure 23: *Peptide systems for provided for the Influenza detection demonstrator. Top: FYGYDVFF as the selective binding unit and. Bottom: FYDPDVFY as control unit to prove specifity.*

As the detection of a complete virus cell is not a trivial matter, more proven parts are integrated to the planned polymer. A solvatochromic fluorescent dye from the naphtalimide family gets modified as a methacrylic monomer **8,** and instead of the combination of $OEGMA^{475}$ and MEO_2MA monomers as main components, the choice falls on N-isopropyl methacrylamide (NIPMAM). The reasoning behind this switch in polymer system lies in the solvatochromic behavior of the dye. J. Kölsch has proven that a higher spectral change can be achieved due to the sharper phase transition of NIPMAM-polymers over the ethyleneglycole modified ones(137). The assumption is that the dye does experience a bigger change in its environment by being heated over the LCST, and thus phase separating into a more hydrophobic environment. This was assumed to be caused by the better dehydration of NIPMAM in comparison to the longer and fuzzy OEGMA chains.

The idea of the demonstrator itself is to bring all the pieces together and aim for the following targets:

- The resulting polymer has to be thermoresponsive
- The polymer should be crosslinkable, so that surface inhibition and hydrogel formation is possible
- The dye should react by changing peak intensity or position in the spectra upon binding of the virus

- The spectral changes should happen upon heating /cooling

With these goals in mind the base polymers **14** and **17 (**Figure 24**)** was synthesized by polymerization with standard conditions (**14**) or in ionic liquid(**17**).

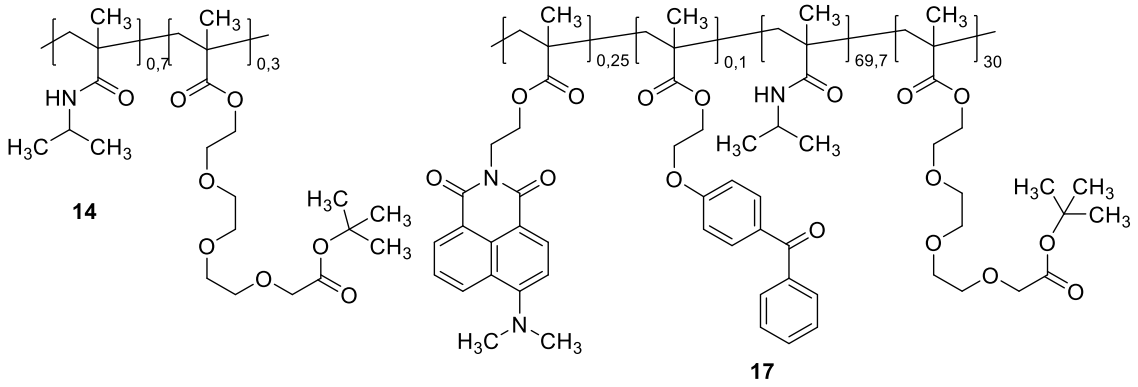

Figure 24: *The base-polymers for the virus studies,* ***left*** *: poly(N-isopropyl methacrylamide-stat- 13,13- dimethyl-11-oxo- 3,6,9,12- tetraoxatetradecyl methacrylate)(**14**);* ***right:*** *poly(N-isopropyl methacrylamide-stat- 13,13-dimethyl-11-oxo-3,6,9,12-tetraoxatetradecyl methacrylate- stat- 2-(4-benzoylphenoxy)ethyl methacrylate –stat -2-(6-(dimethylamino)-1,3-dioxo-1H-benzo[de]isoquinolin-2(3H)-yl)ethyl)methacrylate(**17**)*

At first, polymer 14 was used to check the viability of the concept in solution via turbidimetry. Therefore it was deprotected, then coupled with the receptor unit. After this, the receptor unit was deprotected as well and the whole polymer was purified and freeze dried again. In Figure 25, the results of the first test with the system can be seen. The base polymer with the recognition unit shows an onset point at 37 °C giving a rather broad transition. The neat virus shows some peculiar behavior –the starting temperature, it does not form a completely clear solution and as such, over a certain temperature range it becomes more soluble in the buffer solution. The virus itself has a cloud point as well, its onset is about 45 °C. Above that temperature, the turbidity rapidly increases. All virus related experiments are measured in PBS buffer solution. The virus is supposedly destroyed at temperatures above 50 °C, which limits the experimental window somewhat. When the virus dispersion is injected to the solution of the modified polymer **14**, the general behavior follows the one of the pure polymer closely until roughly 40 °C is reached, then shifting the onset of the phase transition by roughly 2 °C up to 39 °C.

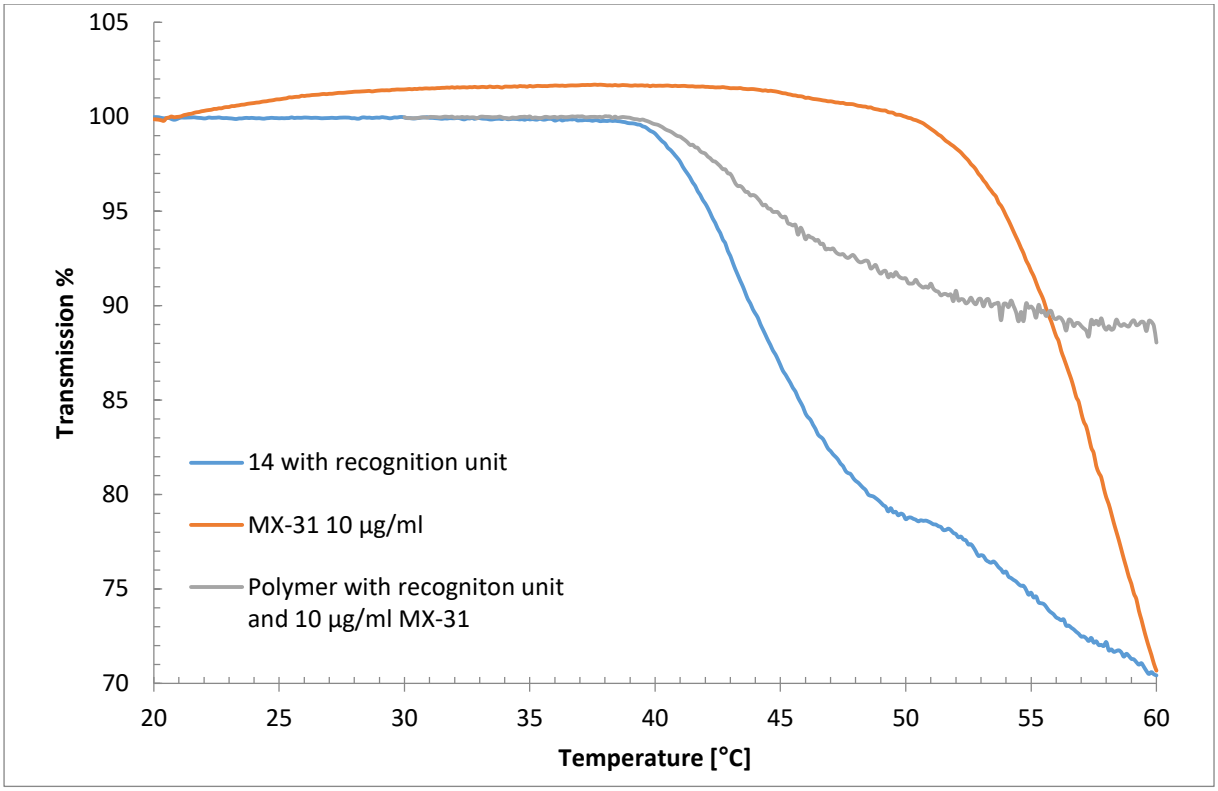

***Figure 25**: Temperature dependent turbidity measurements of polymer **14** modified with a recognition unit in comparison to the neat MX-31 virus, and the combination of **14** and MX-31. The cloud point of **14** shifts by 2 °C from 37 °C to 39 °C upon virus addition.*

The results of this first test were promising as they show an interaction between virus and polymer. Still, the targeted system is much more complex with two additional monomers being copolymerized. Furthermore, the roughly five times higher molar mass should affect the balance between the influence of the polymer and the viruses cloud points. The polymer **17,** when fully modified and deprotected, is significantly less water soluble than **14.** Possibly the integration of the aromatic groups favor the build-up of hydrophobic pockets or agglomerates. The hydrophobicity may be also increased by the higher amount of the peptide recognition unit which is a priori not hydrophilic. Also, the binding efficiency could no longer be determined, but this change in solubility suggests at a more efficient coupling for polymer **17** than for **14**. The result is a rather drastic decrease in the cloud point in Figure 26. Polymer **17** starts to cloud at 27 °C. For the measurements where the Influenza virus is added to the cuvette, the signal is very noisy in comparison to the other measurements. This may be caused by agglomerates of viruses that are crosslinked by the polymer, causing inhomogenities

within the sample. The cloud point that cannot be clearly determined anymore with high precision is between 40 and 42 °C.

This result seems interesting, because such a system could be the base for a detector. For example, a vial filled with this polymer solution is mixed with possibly infected body fluids (possibly with a filter system in place), and kept in the hand to heat it to body temperature or slightly below. If no virus material is present, the vial shall turn cloudy. If there is a significant virus concentration, the vial will stay clear. Such a test could be performed with the cuvette on the laboratory bench already.

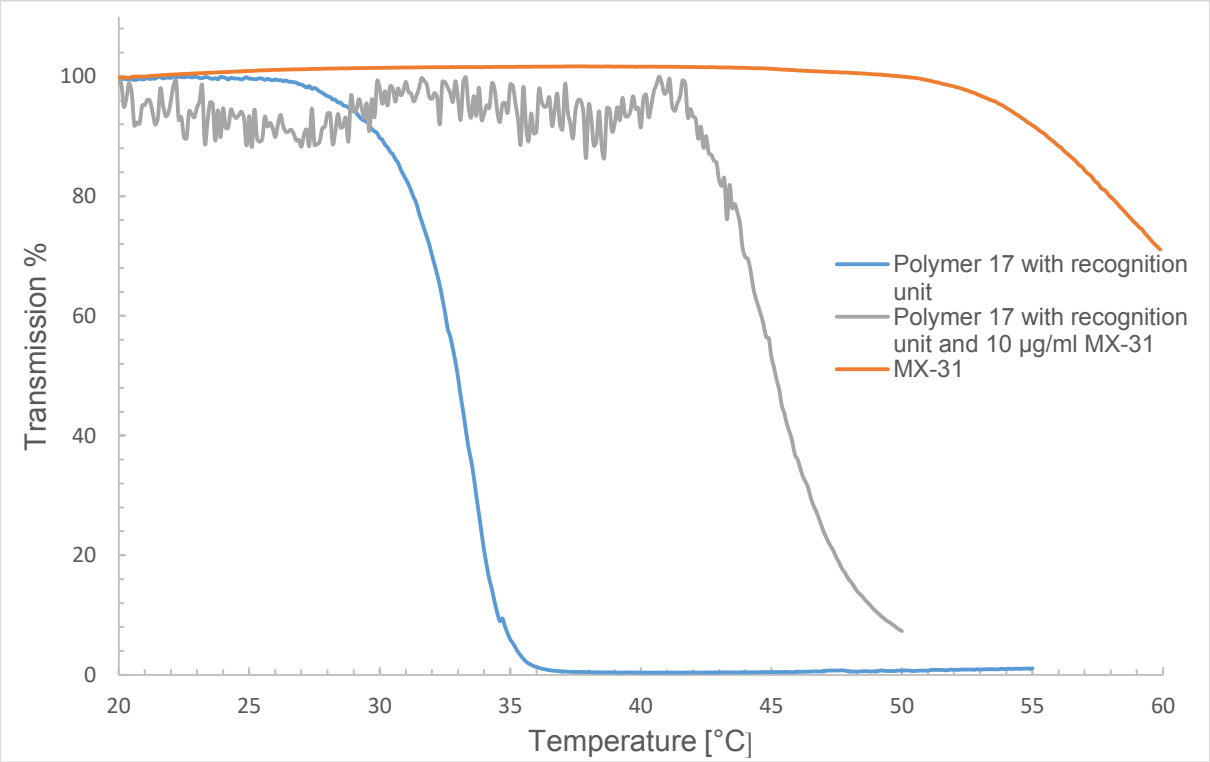

Figure 26: *Temperature dependent turbidity measurements of polymer **17** with and without virus added to the solution. The cloud point shifts from 27 °C to 40-42 °C upon virus addition.*

As already mentioned polymer **17** is not only than thermosensitive –The incorporated naphtalimide dye may exhibit a solvatochromic shift upon a binding event. The studies shown in the remainder of this chapter were made possible by Dr. C. Rötch and Dr. S. Inal (University of Potsdam), who provided the S-1 safety level laboratory and equipment as well as expertise in in designing and performing fluorescence experiments. The samples were measured at 10 °C unless otherwise noted on the graph to ensure a good polymer solubility.

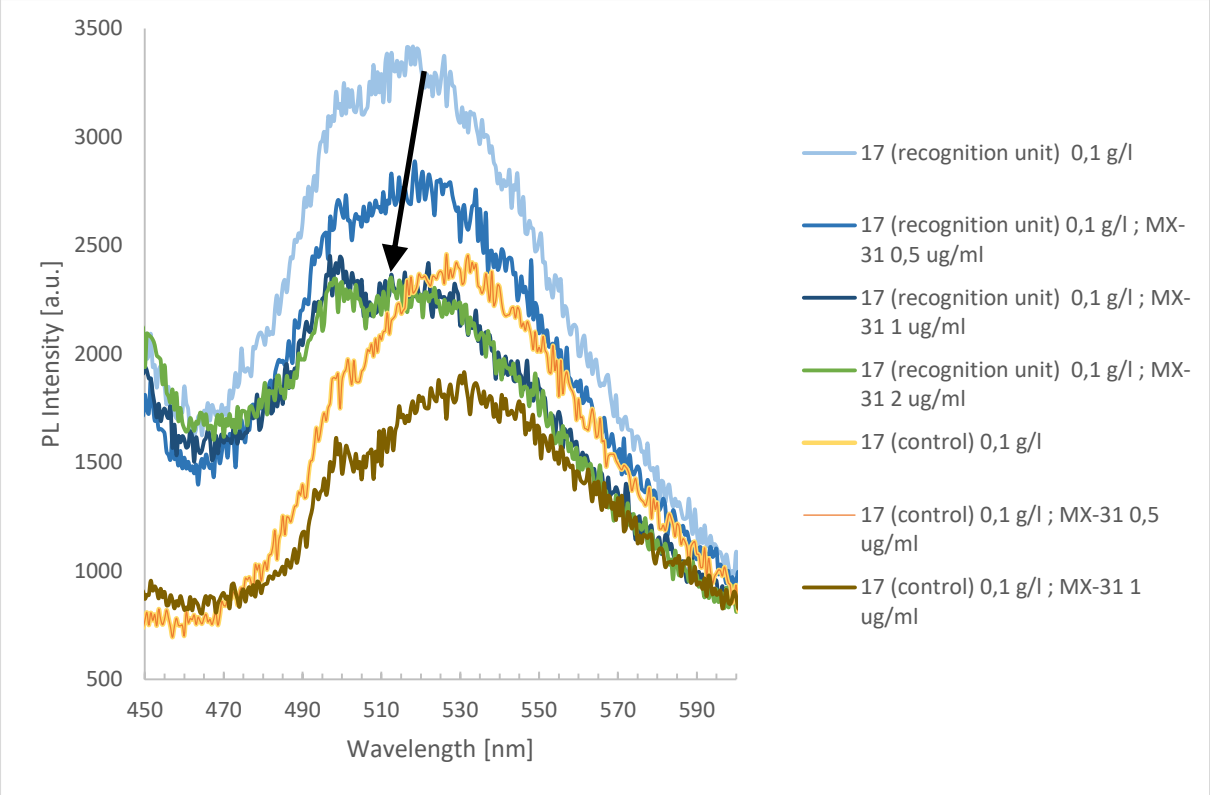

Figure 27: Fluorescence spectra of binding recognition unit and nonbinding control polymer 17 at 10 °C. Stepwise virus additions lower the fluorescence intensity, for the receptor polymer, there is a blue shift of about 10 nm. (PL Intensity is the absolute value of the fluorescences' intensity in arbitrary units)

Figure 27 is the cumulation of the experiments at constant temperature. For the polymer fitted with the binding peptide (blue/green curves) the fluorescence intensity decreases stepwise, the higher the virus concentration is. This decrease is not linear and stops for virus concentrations higher than 2 µg/ml. Moreover, the fluorescence maximum experiences a blue shift of about 10 nm. For the polymer modified with the nonbinding control peptide things are slightly different. The intensity also decreases with increasing concentration of the virus, but after a threshold is passed, the loss of intensity is lower than for the polymer with the binding peptide. Also, there is no shift of the emission maximum.

The loss of fluorescence intensity of the binding unit in combination with the hypsochromic shift means that even at low concentrations, the virus finds its binding surface protein and interacts. The fact that the change in intensity stops at 2 µg/ml means that after a certain point the environment of the dye no longer changes. A possible explanation is that all dye molecules that are able to bind are attached to one or more viruses, so the additional binding options at higher virus concentration goes

unnoticed due to the lack of free recognition units. Generally the drop of the intensity as well as the shift of the emission band mean that the environment of the dye becomes more polar upon binding. This is not surprising as virus surfaces rely on hydrophilic environments and interactions and thus have many polar surface groups and moieties. Thus, the dye feeling a local polar environment is plausible.

In comparison, the measurements of the non-binding peptide show no shift in the intensity maximum or curve shape. Still, there is a virus-concentration dependent shift, with the big difference that for this combination, the results suggest that a certain concentration threshold has to be overstepped before the fluorescence intensity drops. As the drop is smaller than found at with the comparable virus concentration for **17** bearing the binding protein, the interaction seems not overly favorable and is probably due to unspecific interactions between the polymer (and possibly the control peptide) and the virus surface. Further insights in the different behaviors were achieved by examining the scattering behavior over time for both systems at a high virus concentration.(Figure 28)

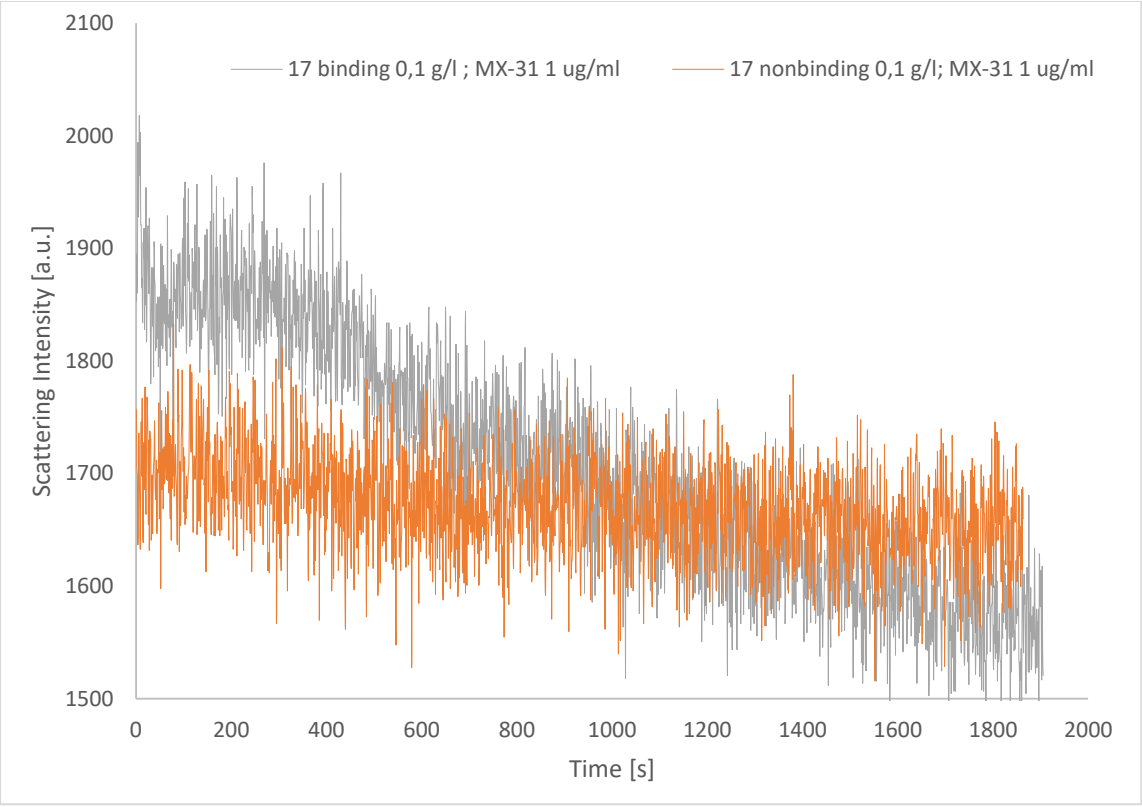

Figure 28: Scattering intensity over time of polymer 17 modified with binding and control peptides. A decrease in scattering means particles sinking or flocculating. The experiment was performed at 10 °C.

For the experiment, the polymer was pre-solved. While stirring, the virus was added. After 10 s for mixing, the stirrer was stopped. The orange line represents the control polymer without a selectively binding peptide you can see that there is quite a large amount of noise in the scattered signal, most probably due to the size of the viruses forming inhomogeneous zones in the cuvette. Still, over the course of roughly 30 min the signal remains more or less constant indicating that the virus dispersion is stable. Compared with Figure 28, at this virus concentration, some process are already well underway causing a change in fluorescence by hydrophilic interactions. This means that the loss of intensity is caused by minor or short termed interactions that are unspecific. This point is supported by taking the scattering behavior over time of the polymer with an attached recognition unit into account. While the scattering starts off higher it slowly drops over time. This would either mean that some material got dissolved and does no longer contribute to scattering, or that particles or aggregates were formed and caused the higher scattering intensity are either sedimenting or flocculating. By checking the sample, it became clear that sedimentation occurred. This behavior fits to the theory that the binding polymer acts like a glue to the virus cells, binding to them first, and then building a network structure that coagulates over time. The initial phase is dominated by peptide binding single chains to the virus and the binding moieties. The remainder of the now dangling polymer chain has the option to attach further peptide units to the same virus, forming a network on its surface – and losing entropy by each binding and “stiffening” of its chain. The other option for the polymer is to dangle in the solution and possibly at some point hitting another virus cell. When repeating this step, a network will form and separate from aqueous solution and keeping the connecting polymer chain flexible in movement.

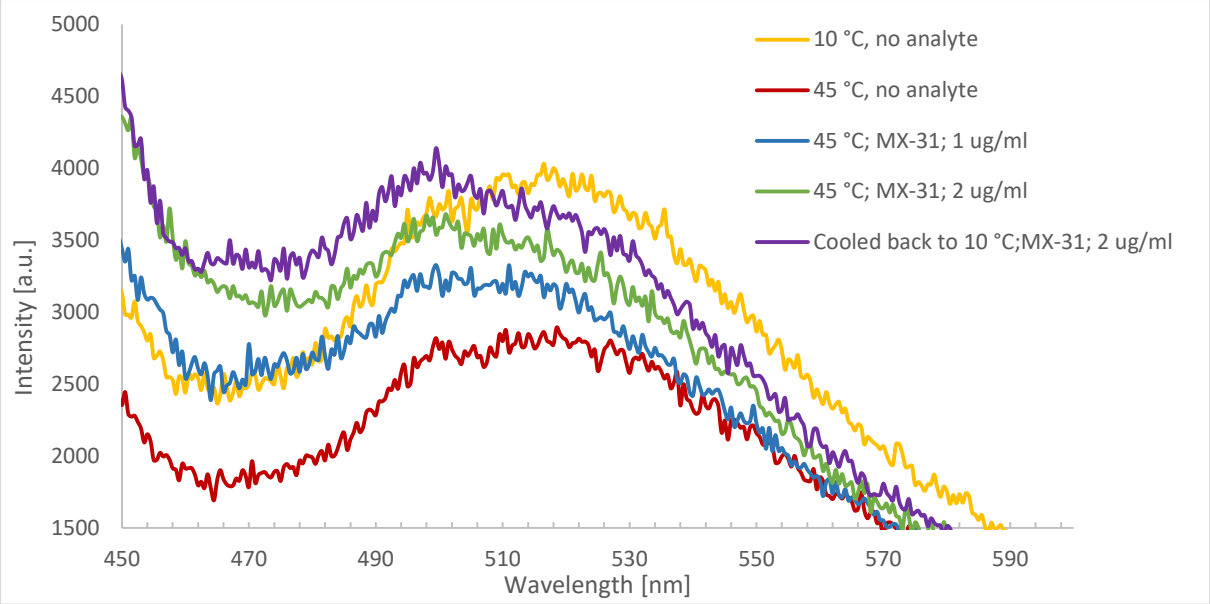

Figure 29: *Fluorescence intensity in correlation with temperature changes and analyte addition to a 1g/l solution of polymer* ***17*** *bearing recognition units.*

Temperature dependency of this complex system needs some further explanation. In pre-tests it was shown that with the attached recognition unit, the fluorescence intensity falls upon heating the polymer solution above the cloud point, which is again contrasts to the behavior of the polymer without an attached peptide. In the case of the pure polymer, the fluorescence intensity rises as anticipated, meaning that the near surroundings of the chromophores get more hydrophobic in nature. Figure 29 shows that heating the polymer with the attached recognition units lowers the fluorescence intensity, but the shape of the band remains the same. Possibly, this is caused by the fact that the peptide itself is hardly hydrophilic, and is dissolved only by the heating, thus interfering the collapse of the NIPMAM units and disturbing the dehydration of the polymer chain. Addition of the analyte to the solution brings the behavior back in line with what would be expected from the phase transitions influence on the fluorescence. The fluorescence rises in dependency of the virus concentrations. This means that the dye is feeling a more hydrophobic environment, it is assumed that the solubilized recognition peptide is still able to bind with the virus receptor moieties. With a certain percentage of the peptide trapped and is sitting in the binding pocket of the virus, the polymer is less influenced by the peptide and can now act “naturally” by collapsing, as the temperature is already above its cloud point. Without or with less interference of the peptide, the NIPMAM polymer can dehydrate properly, inducing the expected change of fluorescence behavior. If the sample is cooled back to 10 °C the

polymer does not dissolve or separate properly anymore. This lack of reversibility might be due to slow kinetics or the possible damage to the virus cells by the heating. In any case, aggregates that were formed during the heating of the sample do not break up anymore. The turbidity might be caused by lowering the solubility of the peptide further and other solvent effects.

4.6. Summary

In this chapter, a primitive biosensor demonstrator was prepared. Starting from building the basis of a thermoresponsive polymer system as well as identifying efficient coupling reactions a starting point to expand upon has been established. The incorporation of functional groups for immobilization makes the systems easier to prepare, opens up more methods for analysis, and also show how they could be used in real applications simply by being flexible on the surface used as well as portable, storable and easy to manufacture. It has been shown that the approach of using methacrylates as the backbone of the materials is indeed adaptable to the experimental conditions. Hydrogels and soluble polymers were prepared in manifold combinations. The thermoresponsive behavior has been shown to be an accessible way of detecting analytes, whereas fluorescence, while viable, requires more equipment to do so.

From a synthetic point of view, many options remain to be explored. Changing the spacer length of the carboxyl coupling group could improve the coupling yield; this would have to be balanced with setting binding and sensing groups not too far off the remaining system that is equipped with signal amplifiers or the signal units themselves. Also, the “backbone” is open for improvements – tuning the systems LCST closer to body temperature might help in applications with body fluids, while setting it lower would help scientific studies – in this case having more heating options or a larger safety margin for not destroying biological material. Polymerization is another issue discussed that has a wide-ranging impact. Polymerization in ionic liquid is not very widespread, especially not for complex copolymerization systems. This chapter has shown that is possible to improve free radical polymerization in solution by utilizing

ionic liquids, which generally tend to increase molar masses. For an optimized sensor system the hydrogel matrix the average chain lengths could be further improved, opening up more options for test systems and possibly increasing the mechanical strength, too. This could be achieved by further investigating polymerizations in ionic liquids. In order to get more out of the limited biological samples and recognition/control units available, miniaturization, e.g. utilizing a spotter for preparation would greatly increase the efficiency of the experiments. This way, more details like variants in the coupling chemistry, hydrogel composition on a macroscopic and molecular level and control experiments could be looked into to improve the overall system.

5. Alkene Based Systems

5.1. Thiol-Ene Reactions

Reactions of sulfur and unsaturated hydrocarbons are a long known reaction type, starting with Goodyears' famous vulcanization of natural rubber in 1844 (138). Discovering this important process by accident, Goodyear did not know the specific chemistry of the reaction. The chemistry of thiol compounds and unsaturated hydrocarbon has actually been documented over 100 years ago by Posner (139). He found that thiols add to double bonds not only in the vicinity of a ketone but also in regular unsaturated alkanes. While certainly far away from click chemistry conditions, he already found the reaction to be working out remarkably well. For the sake of simplicity, reactions between thiols and alkenes that are labeled as "thiol-ene type" mean in this work that the thiol part reacts as radical. The other very popular reaction that uses thiols and activated alkenes falls into the category of a hetero Michael type additions. While the latter type of reaction is certainly an interesting option, too, the focus here will be on the radical pathway. There has been a lot of research during the last century concerning the mechanism of the reaction, that is a multistep chain mechanism (140). The first step is radical generation. This can be done with initiators by a thermal pathway(141-143), by UV-light(90, 144-148) and most recently by sonification(149). These initial radicals start to abstract hydrogen from the thiol, thus forming the thionyl radical. This starts the cycle of the thionyl adding to the alkene, creating a carbon radical. In an ideal cycle, the carbon radical propagates by abstracting a hydrogen atom from a thiol, closing the cycle as schemed in figure 31

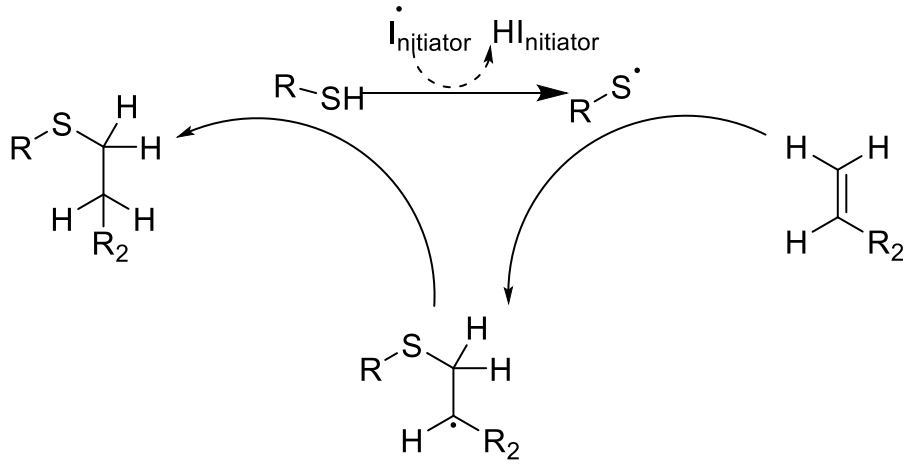

Figure 30: *Radical thiol addition to a double bond*

As in all radical reactions, this cycle is broken by the termination reactions. Roper and colleagues (150) did some extensive studies on the kinetics of the reaction, concluding that the rate determining step in the reaction is the hydrogen abstraction by the carbon radical. This suggests that the structure of the ene component defines the reaction, as detailed below. In particular, cis alkenes were found less reactive than trans alkenes, and a high degree of substitution lowered the reaction rates even when the electron densities increase (151-153).

This work was extended by Morgan (145)and others (154, 155) by correlating the reactivity to the structures of the thiol and the ene counterparts. The general findings were that the more electron density is on the alkene, the more reactive it is, in the following order

Norbornene > vinyl ether > propenyl > alkene >vinyl ester > allyl ether > acrylate > unsaturated ester > methacrylate > conjugated diene

Norbornene is special as ring strain is relieved during the reaction, and a highly reactive carbon radical is generated in the process (156). The last two entries in the list, methacrylates and conjugated dienes, generate rather stable radicals that don't abstract hydrogen easily.

The thiol component has received less attention. The mainly used compounds fall into the categories of alkyl 3-mercaptopropionates, alkyl thioglycolates and simple alkylthiols. While the reactivity of propionates is higher than for the other two types, especially alkylthiols, the discussion is still ongoing if this is a polarity effect (157) or if this is caused by a weakened H-S bond to the thiol by hydrogen bonding of the

carbonyl (158). Of course this is not an exhaustive thiol list. The structures used can be much more complex, especially in the application discussed later in this chapter. Literature agrees though that not all kinetic steps and processes involved are fully understood yet.

Importantly, the thiol ene reaction excels over many other radical chain reactions or polymerizations, to their robustness towards oxygen and water, to a point where presence of oxygen is not inhibiting the reaction at all. This is caused by the still effective abstraction of the hydrogen from the thiol even if oxygen reacts with the carbon radical formed from the alkene, thus allowing the cycle to continue (159). This is a very useful trait for the robustness of the coupling method, and broadens the possibilities for use.

5.2. Synthesis

5.2.1. Monomer Synthesis

As pointed out in the introduction, the goal of the monomer synthesis is to establish a modular pool of reactions that will see different iterations throughout this work. The polymerizable group through this thesis is the methacrylic moiety, which presumably is interchangeable with an acrylic moiety without too much change in the procedure. The spacer group consists of tetraethyleneglycol (TEG). This spacer was chosen due to its commercial availability as nearly pure compound. This point is important for analytical experiments and repeatability. Furthermore, TEG has the advantage that it can still be purified by fractioned distillation relatively easily, thus removing water and shorter glycols with the pre run while leaving longer glycols in the feed. The titular alkene unit is kept rather simple as allyl ether. The terminal double bond has a higher reactivity to the thiol radical addition than higher substituted analogs. The allylic structure does not provide a particularly high electron density, but clearly favors the radical reaction pathway of thiol addition.

The first reaction in the monomer synthesis is the nucleophilic substitution of allyl bromide by tetraethyleneglycole alcoholate in THF (**Figure 31**). From a practical point

of view, with polymerization as goal it is important to eliminate all possibilities of contaminating the final monomer with even trace amounts of methacrylic crosslinker.

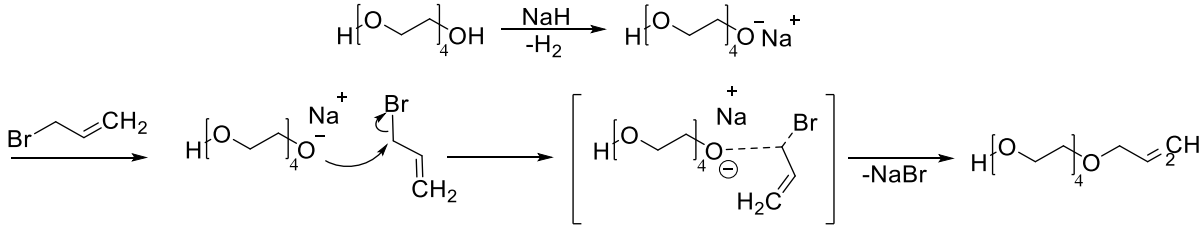

Figure 31: *S_N2 reaction to form 3,6,9,12-tetraoxapentadec-14-en-1-ol (**3**)*

The polar aprotic solvent THF will foster the reactivity of the nucleophile by leaving it “naked” due to its lack of hydrogen bonding ability. The second step in this monomer synthesis is the esterification of the intermediate **3** with methacrylate, the polymerizable group. The methacrylic residue can be introduced by a multitude of ways, starting from the long known and somewhat harsh acid catalyzed esterifications to the much more refined and milder ones such as the Steglich esterification using N,N'-dicyclohexylcarbodiimide (DCC) catalyzed by 4-dimethylaminopyridine (DMAP)(89, 123, 131). This was chosen due to the ease of use and good yields. It is also a very tolerant reaction when it comes to other functional group. In contrary to couplings with amines, the coupling of an alcohol with the carboxylic group does require DMAP to increase the reactivity.

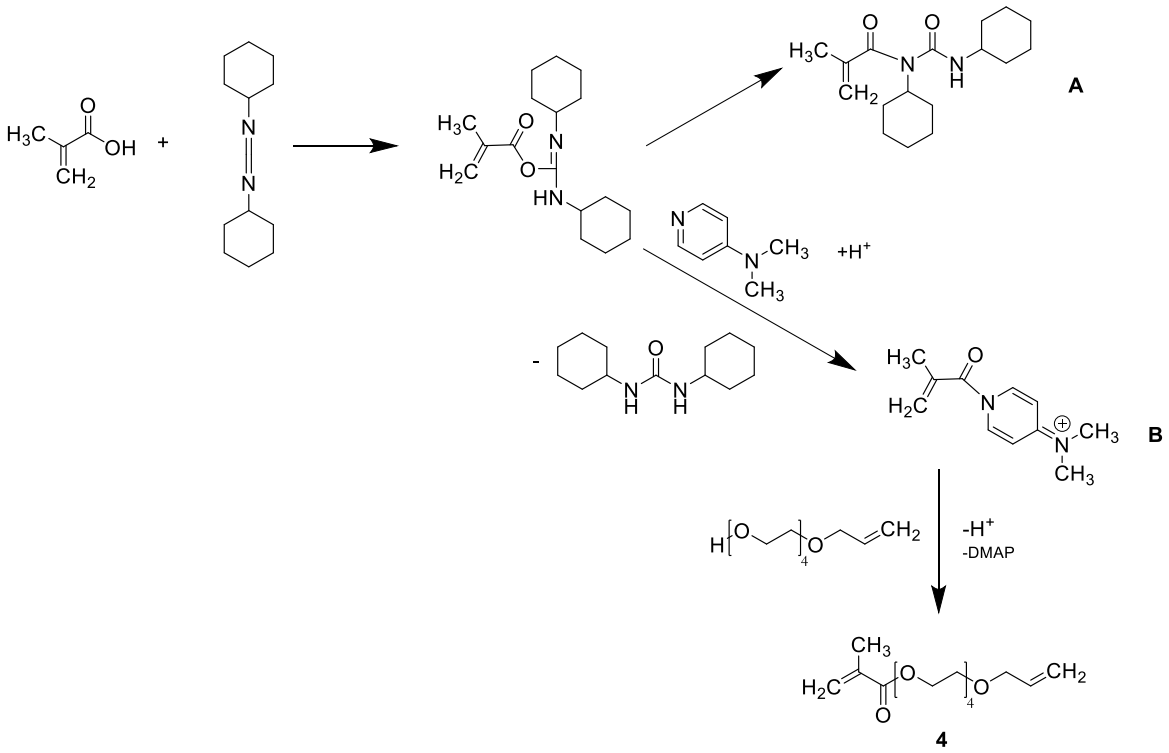

Figure 32: *Schematic Steglich esterification of methacrylic acid.*

It is thought that DCC forms an O-acylisourea intermediate with methacrylic acid, already much more reactive. However without any fast reacting amines in the reaction this intermediate is prone to a competitive side reaction, forming an N-acylurea side product. In the presence of DMAP though, which is a stronger nucleophile than the alcohol used for the esterification, the fastest reaction is the formation of the activated amide of the acid and DMAP, which in turn is highly reactive to the alcohol, thus forming the ester while regenerating DMAP. This reaction sequence outpaces the side reaction and drives the reaction to high yields. Particularly advantageous for the specific reaction is that the product of the reacted carbodiimide is an urea, which is insoluble in the chosen solvent and thus easily removed.

5.2.2. Polymer Synthesis

The development of the intended smart polymer depends on the polymerization. As already discussed, the goal is to polymerize the methacrylic group of the synthesized monomer via free radical polymerization. In order to introduce thermoresponsive

tunable properties, MEO_2MA and $OGMA^{475}$ are incorporated into to the polymer in different ratios to adjust the phase transition temperature.

The parameters of the various polymerizations are shown below Table 3. In short, the ratio of **4** and MEO_2MA is varied while the $OEGMA^{475}$ ratio stays at a constant 5 %. Pure ethanol is used as solvent and AIBN as initiator.

Table 3: *Copolymerization conditions of alkene containing thermoresponsive polymers. The relation of the feeds concentration of **4** and the found concentration after purification shows the loss of reactive groups to loop formation and, in the end, gelification.*

Polymer	MEO_2MA		$OEGMA^{475}$		**4**		AIBN		Ethanol	Yield	M_n	Functional group content
	eqv.	g	eqv.	g	eqv.	g	eqv.	g	g	g	kDA	eqv. (by NMR)
9a	90	0.8	5	0.1	5	0.07	0.5	0.004	7.6	0.9 (92%)	24	5
9b	85	0.8	5	0.1	10	0.15	0.5	0.004	7.6	0.8 (72%)	40	6
9c	80	0.7	5	0.1	15	0.21	0.5	0.004	7.6	0.8 (71%)	24	10
9d	75	0.7	5	0.1	20	0.29	0.5	0.004	7.6	0.7 (64%)	65	11
9e	65	0.3	5	0.1	30	0.19	0.5	0.002	3.7	-	-	-

The polymerization to obtain **9f** is symptomatic for the problems of this polymer class made by free radical polymerization. Whereas it is known that methacrylates are highly reactive, allylic moieties do not undergo polymerization easily (160). Still, they cause sufficient side reactions resulting either in a intra chain loop formation, or are a source of crosslinking (and gelification) of the polymer chains

The intrapolymer reaction may cause the radical propagation to stop, thus lowering the average molar mass of the polymer, as well as lowering the concentration of available functional groups for post polymerization reactions. This type of side reaction should occur most often at low concentrations of growing polymer chains in the mixture, as used for synthesizing high molar mass polymers with free radical polymerization. Nevertheless, the polymer per se is still usable as it is still soluble, at least on a macroscopic scale, and still contains a decent quantity of functional groups.

The interpolymer reaction is much more problematic, as eventually, it results in a crosslinked gel. Crosslinking probably occurs at the end of the polymerization, when most monomers are used, and the statistical chance of a radical to hit another growing polymer chain is the highest. Crosslinking is a big problem as it is impossible to

separate crosslinked and uncrosslinked material with a decent amount of work within the scope of the project needs.

In the light of these two side reactions one, the data from Table 3 may be explained: The general reaction conditions are the same. Only the concentration of functional monomer is varied. The more of the latter is in the feed, the lower is the amount of the OEGMA monomers. At low concentrations of the allylic monomer the reactions progress as intended. If polymers are synthesized with a higher starting concentration of allylic groups and the polymer was still able to be purified and are not gelled, then the allylic groups cannot be found in the intended concentration via NMR spectroscopy. At 10 % and 15 % overall concentration of **4** in the feed, roughly 40 % of the allyl groups are lost. The polymer with the highest content of **4** in the feed that could be isolated, **9d** had to be separated by first dialyzing and then dissolving in DMSO and filtrating the soluble polymer off from the remaining swollen gel pieces. This polymer lost already 90 % of its functionality by side reactions. Increasing the concentration of **4** in the feed further only led to completely gelled reaction vessels. If the double bonds found in the polymers are correlated with their molar masses, it is possible to see that the crosslinking step is the smaller (but deciding) factor. The first three polymers **9a** to **9c** give, using a very rough estimation, 50, 84 and 50 monomers units per chain. This translates to 2.5, 8.4 and 3.3 allylic double bonds expected per respective chain in theory. The experiment shows that 2.5, 5.0 and 2.2 discrete units remain. As the molar masses don't increase drastically, whereas the yield drops down much more prominently, the result suggests that loop formation is the more common reaction. The lowered yields suggest that a non-negligible amount of free radicals is lost due to the allylic groups' side reaction.

5.2.3. Thiol-Ene coupling and diversifying the polymer functionality

In order to prove the capabilities of the synthesized polymers a model reaction was needed. The conjugation partner was selected to couple in solution, for the ease of handling. Namely, mercaptopropionic acid was chosen for practical reasons: first, it is soluble in water as well as organic solutions, has little inclination towards side reactions and offers an easily accessible thiol group. Being a model system, the ease

of analysis and interpretation is also an important factor. For the experiments the commercially available photo initiator system Irgacure 2020 was used, which is of the acyl phospine type of initiator. This choice was made even though, other kinds of radical starters would work for this type of reaction and were tested, too. The UV-initiator was chosen over thermally induced radicals (using AIBN) as those caused gelification of the samples across the board with temperature ranges between 50 to 70 °C and varying polymer concentrations and despite the advantage of being able to stir and properly purge with nitrogen. While this phenomenon was not fully analyzed, a possible interpretation is that the heating caused the alkene groups to react before they could combine with the radicals generated by an AIBN initiator. As the gelification did not happen with the usage of the UV chamber is probably due to the fact that the reaction was done in flat dishes that were cooled to 14-18 °C from the water cooling system in the bottom of the box, thus it seems that the UV irradiation was selective enough to only drive the radical generation and reaction forward. The modified polymers could once again be purified by dialysis in almost quantitative yields.

The most efficient way to analyze of the product was by ^{1}H NMR spectroscopy. The relative amount of allylic end groups is obtained by comparing the vinylic proton integral (δ= 5.9 ppm) to the integral of the methoxy end groups of the OEGMA^{475} and MEO_2MA units (δ= 3.4 ppm) integrals. This procedure can be extended to the signal of the newly formed thio-ether bonds (δ ~ 2.6-2.8 ppm) integrals

5.3. Results

5.3.1. LCST Behavior

One of the most important features of the polymers explored in this work is the occurrence of a lower critical solution temperature in aqueous solution. As already stated much work has been done to quantify the range of temperature for copolymers having different OEGMA^{475} and MEO_2MA compositions(161). Even though the base polymers in this work are all water soluble below their LCST, integrating a ternary comonomer into these copolymers can drastically change the hydrophilic-hydrophobic balance, thus changing said LCST. While it is certainly possible to have an educated guess about the effect of the monomer in question, a reliable prediction is always

difficult. Considering the chemical structure of the alkene modified monomer **4**, the four EO groups are expected to promote the solubility at room temperature and the allyl ether group is expected to reduce it. To reveal the overall effect of the replacement of MEO_2MA by **4** in the copolymer, experiments were made in aqueous solution as summarized in Table 4. What can be seen is that by increasing the amount of **4** in the feed, the polymers cloud points are lowered step by step.

Table 4: *Evolution of the phase transition temperature of copolymers with 5 mol% $OEGMA^{475}$ and 95 –X mol% MEO_2MA, with X being the mol% of **4** in the feed. Measurements in aqueous solution, polymer concentration = 2 g/l*

Sample	**4** mol% feed	M_W	Cloud point
9a	5	24 kDa	29.7 °C
9b	10	40 kDa	28.9 °C
9c	15	24 kDa	27.0 °C
9d	20	65 kDa	25.1 °C

Although molar mass does affect the phase transition temperature, for the range of the samples studied, the effect is minor compared to the effect of the compositional change. What complicates the interpretation is the assumption of a partial loop formation by incorporated **4** since it is not clear to which extent loops cause the LCST to shift. On the one hand, one could expect that the LCST drops the more internal loops are formed as they provide a certain preorientation and possibly facilitate the collapse of the polymer coil by formation of hydrophobic pockets. On the other hand, one could argue that the dangling allyl moieties might favor such pocket formation, as they increase the hydrophobicity more than the methyl end caps for the oligoethyleneglycol methacrylates.

Whatsoever is the most probable explanation for the decrease of the cloud point, as seen in the table, the effects are moderate, reducing the transition temperature not more than 5 °C even for high concentrations of **4**.

After the post polymerization addition of the thiols however, there is a significant change (compare Table 5 and Fig. 34. Depending on the pH, the carboxylic groups are charged and create their own hydration sphere, which improves the water solubility of the group and probably of the overall macromolecule. Whereas thio ethers are much less hydrophilic than ether groups, the ionized carboxylates affect the phase transition more, when in order to keep up with the intended use as a bio-sensor, standard PBS is used for all measurements. (pH =7.4)

Table 5: *Comparison of the cloud points between the alkene-base polymer* ***9a*** *and its thiolated counterpart* ***21.*** *The increase of 7°C is largely due to the carboxylic group of the coupling reagent. Measurements in aqueous solution, polymer concentration = 2 g/l*

Sample	M_W	Cloud point
9a	24 kDa	29.7 °C
21	25 kDa	37.0 °C

As seen in table 5, the cloud point increases by roughly 7 °C, approaching human body temperature. This shows that even with a relatively small modification a rather big effect is achieved. This means that further increases in the molar content of mercaptopropanoic acid will drive the system out of a useful range rather quickly.

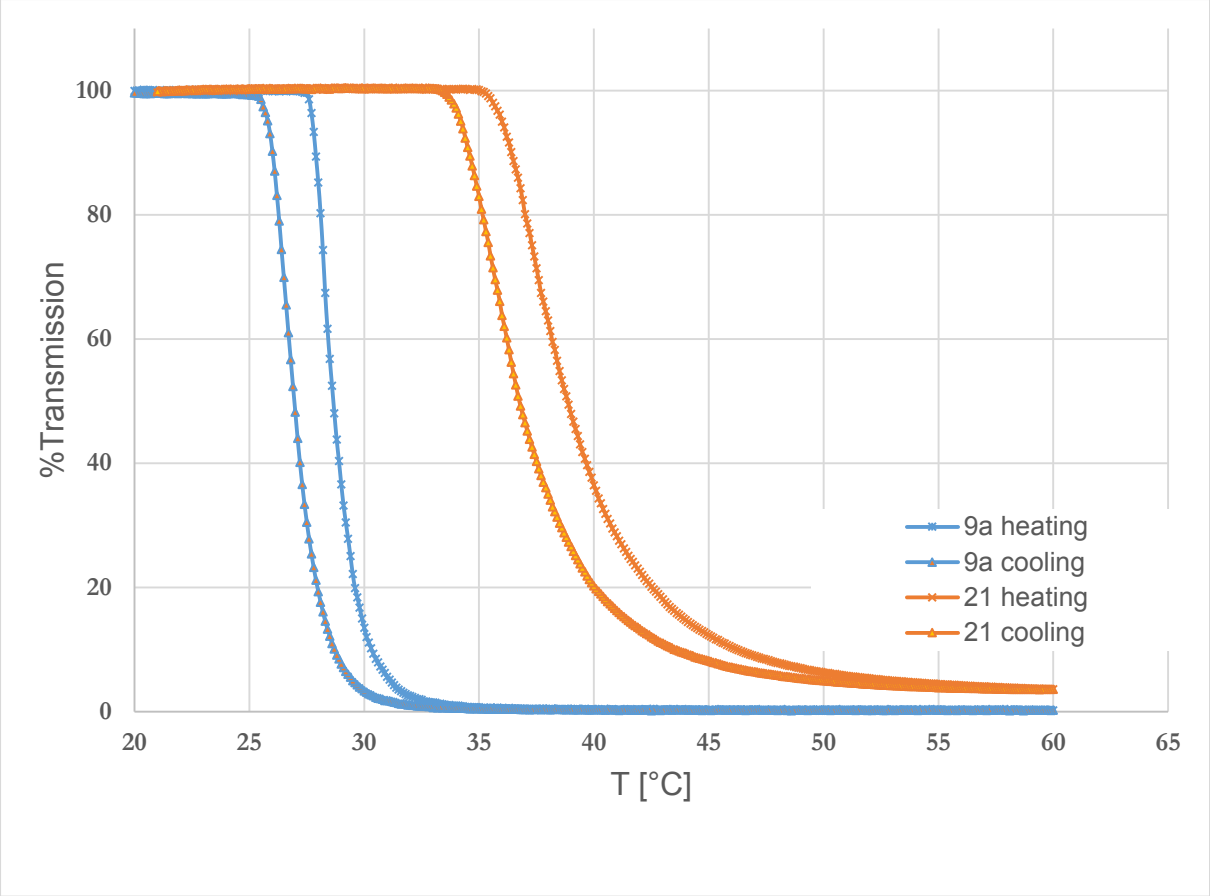

***Figure 33**: Temperature dependent turbidity measurements of polymers 9 and 21 in aqueous solution, demonstrating the marked effect of the incorporation of mercaptopropanoic acid on the cloud point. (c = 2 g/l, heating/cooling: 1 °C/min)*

Figure 34 shows the turbidity curves for heating and cooling. The phase transition process is reversible even if there is a small hysteresis. The hysteresis is presumeably due the rather fast heating and cooling rates, hydration and dehydration requiring more time.

5.3.2. Consequences for Bioconjugation

Considering the results from above with bioconjugation in mind, some further aspects have to be discussed. First, conjugation via thiol-ene reactions is shown as a viable approach, that is easy to realize and effective. The conditions are mild enough to be compatible with the presence of peptides or sugar-recognition units. Naturally, the more complex a potential receptor unit is, the higher the chance of cross-or side

reactions. In the case of large recognition units, steric hindrance has to be taken into account as well –hindering the coupling reaction, or requiring the utilization of a spacer; which, in turn sets the recognition unit further apart from the polymer, and thus might decouple the binding event of an analyte from influencing the LCST transition that is needed for signaling. This means the compromise between ease of access and influence on the phase transition has to be found.

5.3.3. Outlook

Using a relatively simple allyl capped monomer as co-monomer for a potential biosensor has some drawbacks, mostly due to the side reactions of the double bonds which limit the extend of usability for this project's goals down to an example of what could be instead of a true model system or even a workhorse system to truly expand on. On the flipside– the reaction efficiency of the, in itself limited, number of coupling groups within the polymer and the ease of the modification step via the UV induced coupling surely fulfills the requirement of a click reaction usable for this kind of biosensor. How could this monomer concept be improved? Generally searching a better compromise between the thiol-ene reactivity and the stability during polymerization is the way to go. This would enable a higher content of coupling groups, making the system more viable for demonstrator experiments with large biomolecules or cells. One possibility would be to use a 2-butene ether kind of end-cap adding a small steric hindrance to possibly ward of the side reaction during polymerization without stabilizing the radical further and somewhat slowing down the thiolation as well, possibly not to an extend that would block the reaction from being efficient enough. This would also have the benefit of not adding too much complexity to the system that might have more unwanted side effects on the polymer or hydrogel like changing the LCST too much or adding potential reactive partners and so on.

6. Alkyne Based Coupling Systems

6.1. Introduction

This chapter discusses another option for bioconjugateable base polymers that is in close relation to alkene systems. The alkyne based polymers have the option to either undergo a thiol-yne reaction, similar to the thiol –ene reaction, but with a two-step addition process that adds two reaction partners to the triple bond(90). The other option is to utilize the 3+2 dipolar cycloaddition with an azide compound, also known as Huisgen cycloaddition. The polymers will be reacted with simple model molecules in order to show the viability of this approach for rendering hydrogel systems more complex and for adjusting them to the challenges of bio-sensor application.

6.1.1. Radical Thiol Additions to Triple bonds

With their C-C triple bonds, alkynes show some common features with the alkenes, sharing many reactions and their reactive behavior to a certain extent. Terminal alkynes are more acidic than typical hydrocarbons due to their sp-hybridization (162). Thiols undergo a radical addition with alkynes just as to alkenes, though with certain differences, as described by K. Griesbaum(143):

The rate of radical addition to triple bonds is generally slower than for the double bonds of alkene compounds with similar structure and under the same reaction conditions. The addition converts the alkyne to an alkene that can react further. Dependent on the coupling partner used, the reactivity of this second addition step can be higher or lower. The first addition produces the anti-Markovnikov product, as do alkenes, and as expected for a radical addition. The second reaction step, adding a thiol to a newly formed vinylether compound, is faster. This difference in reactivity has been used to perform stepwise additions to mixed alkene-alkyne materials(163, 164). The beauty of the reaction is that it is catalyst-free, tolerant to many other chemical species and environments, yet sensitive to oxygen(165). The reaction technique has been used to synthesize star polymers(164), end-capping and modification of RAFT polymers(163), photo pattering of surfaces with brush polymers(166), biomimetics(167, 168), for the

synthesis of block-copolymers(169) as well as bioconjugation(170) ,to name a few recent applications.

In order to utilize the thiol-yne chemistry, the requirements are pleasantly similar to those of the thiol-ene reactions discussed in the previous chapter, but the reaction has the benefit of being able to react with the same thiol twice in order to create a branched structure (165, 168, 169) or possibly to react stepwise with the help of stoichiometric control of the reagents to create two functionalities out of one alkyne functionality(163, 170). It is expected that this flexibility will increase the popularity of this reaction as a click-chemistry type of reaction(146).

6.1.2. Huisgen Cycloadditions

The currently most widespread click reaction is the 1,3 dipolar cycloaddition of an azide and an alkyne compound developed and explored by R. Huisgen (171), while first published by A. Michael in 1893. This cycloaddition produces 1,4 or 1,5 substituted triazole rings. The reaction can be conducted without catalysts at elevated temperature, lacking regioselectivity (29). When utilizing copper catalysts, the reaction occurs at room temperature and yields exclusively the 1,4 substituted triazole (172). The copper catalyzed variant relies on an additional reducing agent to generate the active Cu(I) species. This cyclization reaction is most commonly mentioned in connection to Sharpless' "click chemistry" branding, and as such has found a widespread audience. The reaction has been successfully used to functionalize polymerization initiators(92) or polymer end groups(173), and has found a broad acceptance in post polymerization modifications (9, 89, 93, 174, 175). Moreover it is used in polymerizations (95, 96) as well as for bioconjugation (9, 129, 176)

While ligands are not essential for the copper catalyst, the reaction rates are reportedly higher when triphenyl phospine or tris(triazolyl) methylamine are utilized as ligands (177, 178). A typical reducing agent to activate the catalyst of choice is sodium ascorbate. While literature often describes this reaction as a plug&play type tool, this is not true - to make it truly a "click" reaction, a lot more effort and optimization has to be invested it to optimize the various conditions.

6.2. Synthesis

The synthesis of the materials used in this chapter are straight forward, using the modular approach outlined in Chapter 1. The main monomer that is used in this chapter is shown in Figure 34. Almost the same reactions as in the previous parts could be used, with similar conditions and work up as well, delivering three very different custom monomers to add to methacrylic systems. The substitution reactions to hetero-substitute the ethylene glycols are reliable and easy to conduct. The main source of error is still insufficient purification which would cause unwanted crosslinking. With this in mind, lowered yields are accepted in exchange for purity, which means longer chromatographic columns are always used which will irreversibly bind some product, causing said losses in yield.

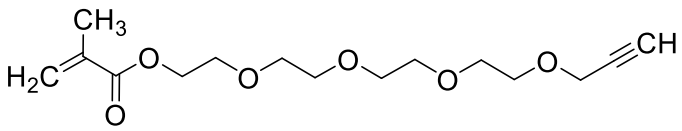

Figure 34: *Structure of 3,6,9,12-tetraoxapentadec-14-yn-1-yl methacrylate (**6**)*

Polymerization was done under standard conditions in ethanol using AIBN as initiator. The set of polymers **10a-d (**Figure 35**)** was synthesized using varying amounts of the functional monomer **6**, giving good yields. It has to be pointed out that in comparison to the alkene based systems no gelation occurred and no loss of functionality could be measured afterwards. So it seems that this polymer system is c more robust in synthesis when it comes to unwanted side reactions such as crosslinking or loop formation. The molar masses achieved by the polymerization are all in the region of 50 kDa, which is more in the average range compared to the alkene counterpart ranging from 24 to 64 kDa and considering the mass was increased by crosslinking.

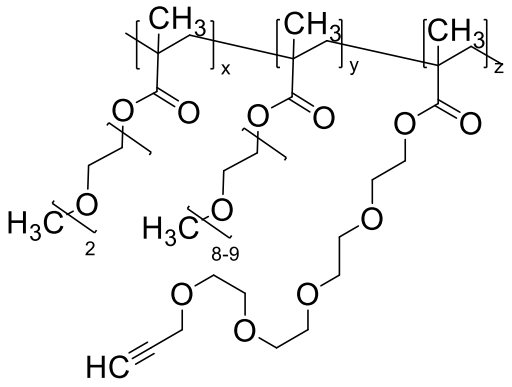

Figure 35: *Alkyne functionalized base polymers* ***10a-d*** *with a degree of functionalization between 14 and 28 %, OEGMA^{475} is fixed at 5 %mol and the MEO$_2$MA content is varied to make up the remainder, details are in chapter 8.2.2*

6.2.1. Radical Addition to Alkyne Functionalized Polymers

Radical addition of thiols to copolymers of series **10** is done with the identical setup as in chapter 3, circumventing the initiation of the reaction by heating completely by focusing on the UV-induced radical addition.

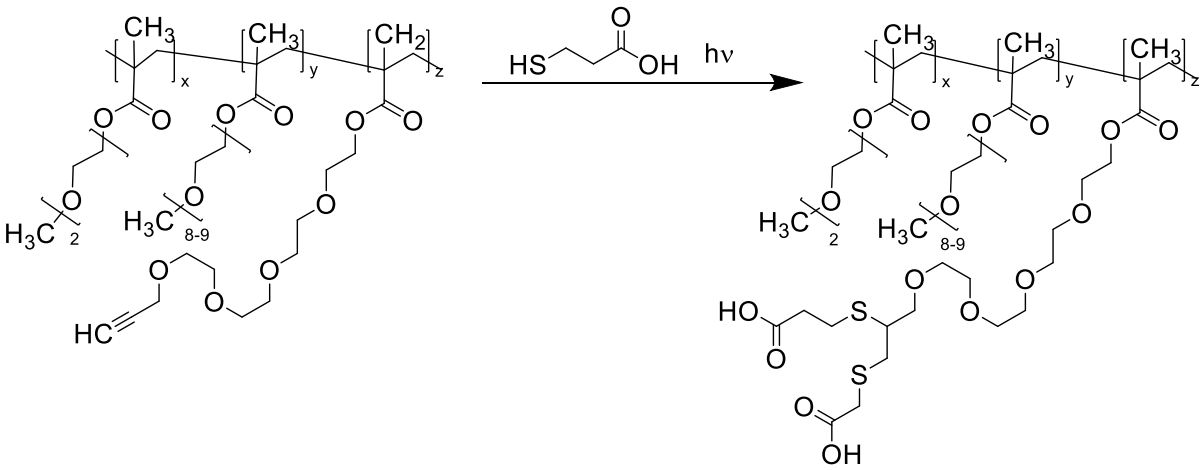

Figure 36*: Thiol-yne radical addition to the polymer bound alkyne functionality of the series 10 polymers*

With polymer **10c** as an example, having an average of 0.12 mmol of triple bonds per 100 mg of polymer and getting reacted with 1 mmol thiol per 100 mg. This is a fivefold excess of reagent to the total reactivity (triple and the consecutive double bonds). The reactions turnover is identified by the thioether signal generated by the ^{1}H NMR spectrum (δ= 2.6-2.8 ppm). The reaction has a high coupling rate, with 90 % of all

possible triple bonds turning out to be thiolated twice after the reaction. The remaining 10 % are groups that did not react at all or are only substituted once could not be determined by NMR spectroscopy as no allylic or alkyne protons can be found. Overall this is a very effective post polymerization modification that exemplifies well the degrees of functionalization or bioconjugation that can be achieved.

6.2.2. Huisgen Cycloadditions to Alkyne Functionalized Polymers

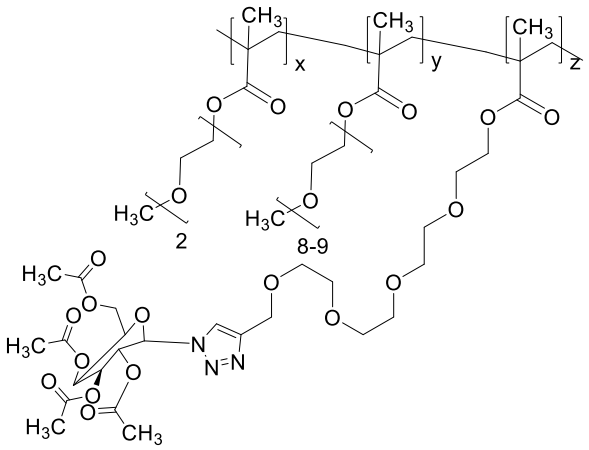

***Figure 37**: Product of the cycloaddition between the alkyne functionalized polymers **10** and azidoglucose.*

For the Huisgen cycloaddition reactions, two exemplary catalyst systems are utilized - copper(II) sulfate/ sodium ascorbate and tris(triphenylphosphine)copper(I)bromide. For both cases, the polymer was dissolved in water:DMF 1:1,4 mixtures to increase their solubility. An azido glucose was used as coupling reagent. Reactions were started simultaneously to allow a better comparability and proceeded for 24 h at room temperature. After purification, the products were analyzed via 1H-NMR spectroscopy, using the proton signal of the triazole ring (δ~ 8.4 ppm) as an indicator of successful coupling. In summary, the reaction proceeded to 54 % of completion with the copper(II)sulfate/ sodium ascorbate catalysis, and up to 43 % with the tris(triphenylphosphine)copper(I)bromide catalyzed reaction. This shows that both reaction pathways are viable, but do not achieve very high yields, it is questionable if those reactions fulfill the “click requirements”. The difference between the catalysts of this experiment can be explained by the steric situation – in comparison to the triphenylphospine ligand copper(II) sulfate is much less sterically demanding. It is

better soluble, too, which might help to cope with the generally hydrophilic environment of the polymer.

6.3. Outlook

This chapter has shown that starting from the same base polymers two completely different reactions can be used to couple potential binding groups. The radical thiol-yne addition, is highly efficient and very easy to use, in agreement to the spirit of the “click” principles. In the future, it should be possible to integrate this system into hydrogel based structures. Given the availability of suited recognition units and analytes, this appears to be the next logical step. Furthermore, the reaction using mercaptopropioic acid seems also an ideal starting point for carboxyl based recognition units, if an increased local concentration of binding units is wanted. Another approach is to use this dual-addition to halve the amount of long ethylene glycol units in order to keep the LCST of the polymers low, or to facilitate its modulation.

The Huisgen cycloaddition leaves room for systematic improvements. On the one hand, steric reasons may be the reason for the rather low yields. On the other hand, effects of solvent or reactant could also play a role. As eliminating the catalyst and using the purely thermally activated reaction variant might be hard to realize for LCST polymers, a solvent-based system would be needed which would cause this reaction to lose some viability with the aspects of bioconjugation. Careful optimization of the reaction conditions and reagent screening are probably the best way to proceed. In any case, the results certainly show that alleged click reactions are not always easy to use and require a certain degree of optimization, instead of working straight out of the box as often insinuated in literature.

7. Summary and Conclusion

The goal of this work was to show an exemplary pathway of how a sensor for biologically relevant analytes can be designed. Two major systems are the result. (1) A surface bound sensor that is able to detect the binding of a surface saccharide of salmonella bacteria with the help of SPR spectroscopy. (2) A hydrogel coated on a quartz surface that is able to change the fluorescent behavior when in contact with a specific influenza virus.

Monomer synthesis was done by forming alcoholates of tri- or tetraethyleneglycol chains that undergo a nucleophile substitution with the bromide of the desired functionality. This was done for t-butyl bromoacetate, allylbromide and propargylbromide. In a second step the polymerizable group was introduced either by DCC/DMAP coupling or by utilizing methacryloylchloride as reaction partner. Utmost care has to be taken with the purification steps to exclude any possibly crosslinking species for the polymerization. To form thermoresponsive polymers, the new functional monomers were copolymerized with MEO_2MA and $OEGMA^{475}$ for water soluble systems. In order to immobilize and crosslink the polymer into a hydrogel BPMA was added in small concentrations. Carboxyl functionalized systems were also synthesized in combination with NIPMAM and a napthalimide dye. Most of the polymerizations underwent free radical polymerization in ethanol initialized by AIBN. In order to increase the polymers chain length and molar mass, polymerization in the ionic liquid EMIM PF_6 was done with good results, achieving molar masses of over 1000 kDA.

Hydrogels were characterized by their swelling ratio in order to get an estimated mesh size and to tailor them better to binding groups and analytes. The deposition thickness was also tested in dependence of the applied polymer amount. The hydrogels were immobilized on SPR chips to follow the coupling of a small protein, Lysozyme. After successful experiments, a tailspike protein extracted from a phage that selectively binds to a surface bound salmonella polysaccharide was utilized as conjugation partner. The protein was only immobilized in a low concentration and probably only in the surface layer. Nevertheless this demonstrator system showed a concentration depended reaction and a much smaller (and non-binding) reaction to an E.Coli surface saccharide.

By utilizing a solvatochromic napthalimide dye as an indicator, a carboxyl containing polymer was modified with a peptide or a non-binding control peptide to target the MX-31 influenza stem. The binding has shown to be specific by scattering and fluorescence experiments. Binding with the detection polymer, a temperature dependent solvatochromic shift and a change in fluorescence can be detected even at very low virus concentrations. Binding occurs in solution or with hydrogels bound to surfaces. Furthermore, utilizing turbidimetry, the virus binding induces a temperature shift of the cloud point making it possible to identify the virus by simply warming up a virus – polymer mixture.

The flexibility of the chosen approach was demonstrated by the alkene and alkine functionalized polymers. They showed a high coupling efficiency towards radical thiol reactions that can be used to diversify the polymers or to increase a localized concentration of, for example, carboxylic groups. The possibility to attach an azido saccharide with the aid of a 2+3 copper catalyzed cycloaddition was also shown, diversifying the potential binding partners. With these four independent and orthogonal coupling options, a number of possibilities for different hydrogel applications are given. The polymers can be photocrosslinked easily even if only one polymer of the blend contains benzophenone crosslinkers.

From a practical point of view, the biggest limiting factor is the availability of test substrates in combination with recognition units and control units to check for specifity. Furthermore, an important point to focus on in the future would be the optimization of the polymerization in ionic liquids. Reaching reliably ultra-high molar masses should be a major goal, as the longer chain polymers offer more possibilities for receptor units and analytes to penetrate the hydrogels by allowing lower crosslinker concentrations. Obviously, there will be a lower limit due to reduced mechanical robustness that has not yet been reached though. More detailed research in singular systems and methods are certainly an approach to optimization that can follow up on the results presented in this thesis

8. Experimental Part

Chemical	CAS	Purity %	Supplier
(3-Aminopropyl)dimethylethoxysilane	3179-76-8	97	Aldrich
AIBN	78-67-1	98	Aldrich
Allyl bromide	106-95-6	99	Aldrich
Aminoethanol	141-43-5	98	Aldrich
Benzylamine	100-46-9	99	Aldrich
BHT	128-37-0	99	Aldrich
Copper(II) Sulfate	7758-98-7	99	Alfa Aesar
Copper(II)bromide	7789-45-9	99	Alf Aesar
DCC	538-75-0	99	Alfa Aesar
Dichlormethane	75-09-2		J.T.Baker
DMAP	1122-58-3	98	Fluka
EDC	25952-53-8	98	Aldrich
EMIM PF_6	155371-19-0	99	TCI
Ethanol	64-17-5	99.5	Chemsolute
Irgacure 2020	-	-	Ciba
MEO_2MA	7328-17-8	95	Aldrich
Mercaptopropioic acid	107-96-0	99	Aldrich
Methacrylic acid	79-41-4	99	Aldrich
Methacryloylchloride	213-058-9		Aldrich
NHS	6066-82-6	98	Aldrich
$OEGMA^{475}$	26915-72-0	-	Aldrich
Potassium tert-butoxide	865-47-4	98	Aldrich
Sodium Hydride	7646-69-7	60	Fluka
TEA	121-44-8	99.5	Aldrich
tert.Butyl bromoacetate	5292-43-3	98	Aldrich
tert-Butyl alcohol	75-65-0	99	Riedel de Hän
Tetraethylenglycole	112-60-7	99	Aldrich
TFA	76-05-1	99	Aldrich
Triethylenglycole, dry	112-27-6	99	Aldrich
Triphenylphosphine	603-35-0	99	Fluka

Non-commercial biomaterials provided by cooperation partners

Substance	Supplied Form	Source / Institution
NBD-P-22 tailspike protein	22.8 µm/ml in acetate buffered solution	Provided by Dr. K. Tang/ University of Potsdam
T400C polysaccharide	30 µm/ml in HEPES buffered solution	Provided by Dr. K. Tang/ University of Potsdam
E. Coli saccharide (unspecified)	30 µm/ml in HEPES buffered solution	Provided by Dr. K. Tang/ University of Potsdam
FYGYDVFF detector peptide	pure substance, solid phase synthesis	Provided by H. Memczak/ Fraunhofer IBMT
FYDPDVFY control peptide	pure substance, solid phase synthesis	Provided by H. Memczak/ Fraunhofer IBMT
MX-31 virus	10 µg/ml dispersed in PBS buffered solution	Provided by H. Memczak/ Fraunhofer IBMT

8.1. Monomer Synthesis

8.1.1. tert-Butyl 2-(2-(2-(2-hydroxyethoxy)ethoxy)ethoxy)acetate (1)

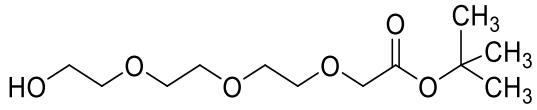

A dry three neck flask is filled with 300 g (~250 ml) of dried tert-butyl alcohol and 9.3 g of dry triethylenglycole (62 mmol) under nitrogen atmosphere. After melting the solvent 14.6 g of potassium tert-butoxide (129 mmol) are added while stirring vigorously. The mixture is heated for 3 h under refluxing conditions at 95 °C until fully solved. In order to add the tert. butyl bromoacetate the mixture is cooled back to 30 °C, then 14.9 g (74.9 mmol, 98%) of the acetate are added slowly under nitrogen atmosphere. The reaction mixture is refluxed for 3 h. 100 ml of toluene are added to the cooled suspension to keep it liquid. The mixture is filtrated to remove the KBr formed and evaporated afterwards. The resulting sticky oil is diluted with 150 ml of water and extracted with 50 ml of a 1:1 mixture of diethylether and hexane to remove any double alkylated side product. The remaining aqueous phase is extracted with DCM until no further trace of the product is detected via TLC in the aqueous phase. The collected DCM phases are evaporated. The yellow oil is purified by column chromatography with a 20:1 ethylacetate: methanol eluent. The product phase is dried with magnesium sulfate, filtrated and evaporated. 7.1 g (26.9 mmol; 39 %) of a yellow tinted clear oil are gained.

R_f: 0.4 in 20/1 EtAc/MeOH

^{1}H-NMR (300 MHz, $CDCl_3$) δ(ppm): 1.5 (s, 9H, -OC(CH_3)$_3$); 4.0 (s, 2H, -OCH_2COOR); 3.7 -3.8 (m, 10H, HO-CH_2-C$\underline{H}_2$-O-(C$\underline{H}_2$-C$\underline{H}_2$-O)$_3$-), 4.1(m,2H, HO-CH_2R), 2.9 (b, 1H, HO-R)

8.1.2. 13,13-Dimethyl-11-oxo-3,6,9,12-tetraoxatetradecyl methacrylate (2)

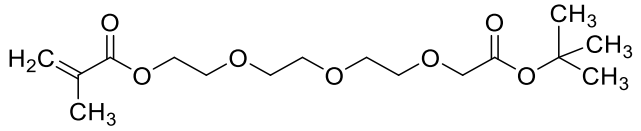

A dried Schlenk flask with nitrogen atmosphere is filled with 100 ml of dry DCM, 6.0 g (22 mmol) of **1**, 2.9 g (33.8 mmol) of dry methacrylic acid, 0,25 g (2,8 mmol) of DMAP and a small pinch of BHT. This mixture is chilled in an ice bath to 0 °C, then 7,0 g (33.8 mmol) of DCC solved in 15 ml of dry DCM are added slowly with a dropping funnel. The mixture is allowed to warm up to ambient temperature and stirred overnight. The resulting suspension is filtered and evaporated. Purification is achieved by a column chromatography using a 5:2 ratio of ethylacetate: hexane as eluent. After evaporation 6.7 g (20 mmol, 91%) of a waxy colorless substance are collected. R_f of the product is 0.5.

^{1}H-NMR (300 MHz, $CDCl_3$) δ(ppm): 1.5 (s, 9H, -OC(CH_3)$_3$); 1.9(dd, 3H, CH_2=C(C$\underline{H}_3$)-COO-R), 4.0 (s, 2H, -OCH_2COOR); 3.7 -3.8 (m, 10H, HO-CH_2-C$\underline{H}_2$-O-(C$\underline{H}_2$-C$\underline{H}_2$-O)$_3$-), 4.3(t, 1H, Methacrylic acid-O- C$\underline{H}_2$-CH_2-R), 5.6(m, 1H, trans-CH_2=CR-CH_3), 6.1(m, 1H, cis -CH_2=CR-CH_3)

8.1.3. 3,6,9,12-Tetraoxapentadec-14-en-1-ol (3)

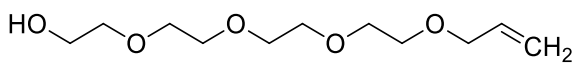

A dried flask with nitrogen atmosphere is filled with 400 ml of dry tetrahydrofurane (THF), then 19.0 g (97.8 mmol) of tetraethylene glycole are added. The mixture is cooled to 0 °C with an ice bath. 2.8 g (117.4 mmol) of sodium hydride is added carefully while stirring vigorously, preventing massive foam build up. Then, the mixture is left to reach room temperature and stirred continuously for 1 h. Via a dropping funnel 5.9 g (48.9 mmol) of allylic bromide in 50 ml of dry THF are added dropwise. The reaction is completed after 4 h. The suspension is filtered and evaporated. The residue is diluted with 200 ml of water and extracted at least five times with 75 ml of diethylether each. This extract containing the disubstituted side product as well as the product is evaporated and purified by column chromatography using 19:1 DCM to methanol as the eluent. The product is a transparent, yellow viscous oil (5.102 g, 58.5%. R_f: 3.2).

^{1}H-NMR (300 MHz, $CDCl_3$) δ(ppm): 3.5 -3.8 (m, 14H, HO-CH_2-C$\underline{H}_2$-O-(C$\underline{H}_2$-C$\underline{H}_2$-O)$_3$-), 4.0(d,2H, R-O-C$\underline{H}_2$-CH=CH_2), 5.2(m, 2H R-O-CH_2-CH=C$\underline{H}_2$), 5.9(m, 1H, R-O-CH_2-C$\underline{H}$=CH_2), 4.1(m,2H, HO-CH_2R), 2.9 (b, 1H, HO-R)

8.1.4. 3,6,9,12-Tetraoxapentadec-14-en-1-yl methacrylate (4)

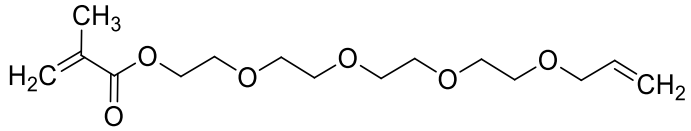

A dried Schlenk flask with nitrogen atmosphere is filled with 25 ml of dry Dichloromethane, 2.0 g (8.5 mmol) of **3**, 1.1 g (12.3 mmol) of dry methacrylic acid, 0.1 g (21.5 mmol) of DMAP and a small pinch of BHT. This mixture is chilled in an ice bath to 0 °C, then 2.6 g (12.6 mmol) of DCC dissolved in 5 ml of dry DCM are added slowly with a dropping funnel. The mixture is allowed to warm up to room temperature and stirred overnight. The resulting suspension is filtered and evaporated. Purification is achieved with a column chromatography using a 5:1 ratio of ethylacetate: hexane as

eluent. After evaporation 2.3 g (7.7 mmol, 89.9%) of a waxy yellow substance is obtained. R_f of the product is 0.56.

^{1}H-NMR (300 MHz, $CDCl_3$) δ(ppm): 1.9(dd, 3H, CH_2=C($C\underline{H}_3$)-COO-R), 3.5 -3.8 (m, 14H, HO-CH_2-$C\underline{H}_2$-O-($C\underline{H}_2$-$C\underline{H}_2$-O)$_3$-), 4.0(d,2H, R-O-$C\underline{H}_2$-CH=CH_2), 4.1(m,2H, HO-CH_2R), 2.9 (b, 1H, HO-R), 5.2(m, 2H R-O-CH_2-CH=$C\underline{H}_2$), 5.9(m, 1H, R-O-CH_2-$C\underline{H}$=CH_2), 4.3(t, 1H, Methacrylic acid-O- $C\underline{H}_2$-CH_2-R), 5.6(m, 1H, trans-CH_2=CR-CH_3), 6.1(m, 1H, cis -CH_2=CR-CH_3))

8.1.5. 6,9,12-Tetraoxapentadec-14-yn-1-ol (5)

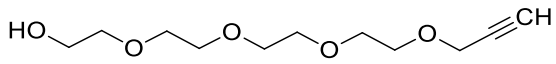

A dried flask with nitrogen atmosphere is filled with 150 ml of dry THF, then 11.1 g (57.2 mmol) of tetraethylene glycole are added. The mixture is cooled to 0 °C with an ice bath. In the next step 2.1 g (87.7 mmol) of sodium hydride are added slowly while stirring vigorously, preventing massive foam build up. After the addition, the mixture is left to gain room temperature and stirred continuously for 1 h. With the help of a dropping funnel 7.7 g (51.9 mmol) of propargylbromide (80 % in Toluene) in 25 ml of dry THF are added dropwise. The reaction is completed after 4 h. The suspension is filtered and evaporated. The crude product is purified by column chromatography using neat ethylacetate as eluent. The product is a transparent, yellow viscous oil (4.9 g, 21.1 mmol 40.7 %. R_f: 0.19).

^{1}H-NMR (300 MHz, $CDCl_3$) δ(ppm): 3.56-3.7 (m, 14H, HO-CH_2-$C\underline{H}_2$-O-($C\underline{H}_2$-$C\underline{H}_2$-O)$_3$-), 4,2(s,2H, R-O-$C\underline{H}_2$-CCH), 2.4(t, 1H R-O-CH_2-C$C\underline{H}$), 4.1(m,2H, HO-CH_2R), 2.9 (b, 1H, HO-R)

8.1.6. 3,6,9,12-Tetraoxapentadec-14-yn-1-yl methacrylate (6)

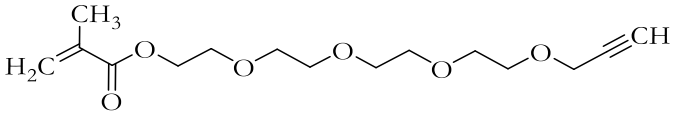

A dried Schlenk flask with nitrogen atmosphere is filled with 20 ml of dry DCM, 2.4 g (10.2 mmol) of **5**, 1.2 g (15.0 mmol) of pyridine and a small pinch of BHT. This mixture is chilled in an ice bath to 0 °C, then 3.4 ml (15.0 mmol) of methacryloylchloride are added dropwise with a syringe. The mixture is allowed to warm up to ambient temperature and stirred for 4 h. The resulting suspension is filtered and evaporated. Purification is achieved with a column chromatography using neat ethylacetate as eluent. After evaporation 2.1 g (7.0 mmol, 69.0%) of a waxy yellow substance are acquired. R_f of the product is 0.62.

^{1}H-NMR (300 MHz, $CDCl_3$) δ(ppm): 1.9(s, 3H, CH_2=C($C\underline{H}_3$)-COO-R), 3.5-3.7 (m, 14H, HO-CH_2-$C\underline{H}_2$-O-($C\underline{H}_2$-$C\underline{H}_2$-O)$_3$-), 4.2(s,2H, R-O-$C\underline{H}_2$-CCH), 2.4(t, 1H R-O-CH_2-$C\underline{C}$H), 4.1(m,2H, HO-CH_2R), 2.9 (b, 1H, HO-R), 4.3(t, 1H, CO-O- $C\underline{H}_2$-CH_2-R), 5.6(m, 1H, trans-CH_2=CR-CH_3), 6.1(m, 1H, cis -CH_2=CR-CH_3),

8.1.7. 6-(Dimethylamino)-2-(2-hydroxyethyl)-1H-benzo[de]isoquinoline-1,3(2H)-dione (7)

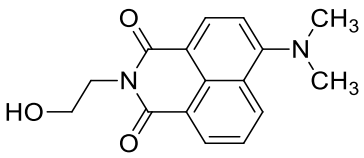

34 mg (0.14 mmol) of 6-(dimethylamino)benzo[de]isochromene-1,3-dione (supplied by Dr. Viet Hoang) and 21 mg (0,35 mmol) of aminoethanol are dissolved in 10 ml of ethanol. The mixture is refluxed at 100 °C for 12 h, then the solvent is evaporated. The crude product is purified by washing it thoroughly with distilled water. After drying in vacuo at 40 °C, 38 mg (0.13 mmol, 98 %) of product are obtained as a bright orange solid.

^{1}H-NMR (300 MHz, $CDCl_3$) δ(ppm): 3.1 (s,6H, ($C\underline{H}_3)_2$N-C(aromatic)), 3.4 (t, 2H, HO-CH_2-$C\underline{H}_2$-N), 3.6 (m, 2H, HO-$C\underline{H}_2$-CH_2-N), 4.8 (b, 1H, HO-), 7,1 (d, 1H, C-CH-C$\underline{H}$-$CN(CH_3)_2$)), 7.6 (dd, 1H, C-CH-C$\underline{H}$-CH-C-C), 8.5 (m, 1+1H, -C$\underline{H}$-C-C-C-C$\underline{H}$-), 8.6 (d, 1H, C-CH-CH-C$\underline{H}$-C-C)

8.1.8. 2-(6-(Dimethylamino)-1,3-dioxo-1H-benzo[de]isoquinolin-2(3H)-yl)ethyl methacrylate (8)

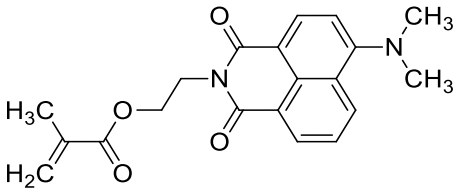

38 mg (0.13 mmol) of **7** and 55.4 mg (0.55 mmol) of dry TEA are dissolved in 5 ml dry DCM in a Schlenk flask with nitrogen atmosphere and cooled to 0°C. Via syringe, 27.2 mg (0.26 mmol) of methacryloyl chloride are added. The reaction mixture was brought to ambient temperature and stirred overnight, then evaporated. The crude product is dissolved in the minimum amount of acetone and precipitated into water. The product is isolated by filtration. After drying in vacuo, 35 mg (0.1 mmol 78%) of bright orange solid are isolated.

^{1}H-NMR (300 MHz, $CDCl_3$) δ(ppm): 1.9(s, 3H, CH_2=C($C\underline{H}_3$)-COO-R) 3.1 (s,6H, ($C\underline{H}_3)_2$N-C(aromatic)), 4.5 (m, 4H, COOO-$C\underline{H}_2$-$C\underline{H}_2$-N), 7.1 (d, 1H, C-CH-C$\underline{H}$-$CN(CH_3)_2$)), 7.6 (dd, 1H, C-CH-C$\underline{H}$-CH-C-C), 8.5 (m, 1+1H, -C$\underline{H}$-C-C-C-C$\underline{H}$-), 8.6 (d, 1H, C-CH-CH-C$\underline{H}$-C-C), 5.5(m, 1H, trans-CH_2=CR-CH_3), 6.0(m, 1H, cis -CH_2=CR-CH_3)),

8.2. Polymerizations in Ethanol

All radical polymerizations in this subchapter were performed with the following general procedures. The commercially available monomers inhibitors were removed by filtering them through basic aluminiumoxide directly before the polymerization. The freshly destabilized monomers, the synthesized monomers and the initiator are filled into a Schlenk tube and diluted with the pre-set amount of absolute ethanol (typically 90 %wt). The flask is sealed with a septum cap, in which two syringe capillaries are inserted. One capillary leads to the bottom of the flask, the other one ends about 1 cm below the cap. Then nitrogen is slowly passed through the lower one in order to purge the oxygen out of the solution and the reaction vessel. This purging continues for 20 min, after which the upper syringe is removed first in order to keep a slight nitrogen overpressure. The reaction vessel is then placed in a preheated oil bath and stirred constantly for the duration of the polymerization. The polymerization is stopped by removing the cap and diluting the mix with deionized water. The polymers are cleaned by dialysis with a 12-13.5 kg/mol cutoff dialysis tube in deionized water for 4 days and isolated by freeze drying.

The polymers were characterized via ^{1}H-NMR, SEC and turbidity measurements

8.2.1. Poly(oligo(ethylene glycole) methylether methacrylate^{475} -stat-di (ethylene glycol) methylether methacrylate-stat-3,6,9,12-tetraoxapentadec-14-en-1-yl methacrylate) (9)

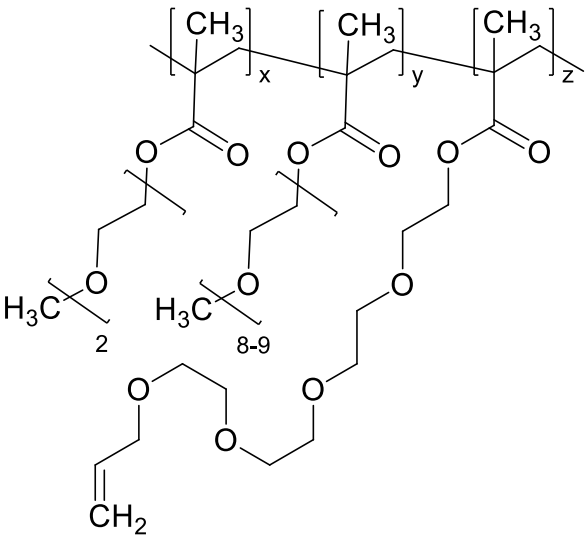

Table 6: *Overview of the polymer synthesis and results of polymer* ***9***

Polymer	MEO_2MA		$OEGMA^{475}$		**4**		AIBN		Ethanol	Yield	M_n	Functional group content
	eqv.	g	eqv.	g	eqv.	g	eqv.	g	g	g	kDA	eqv.
9a	90	0.8	5	0.1	5	0.07	0,5	0.004	7.6	0.9 (92%)	24	5
9b	85	0.8	5	0.1	10	0.15	0,5	0.004	7.6	0.8 (72%)	40	6
9c	80	0.7	5	0.1	15	0.21	0,5	0.004	7.6	0.8 (71%)	24	10
9d	75	0.7	5	0.1	20	0.29	0,5	0.004	7.6	0.7 (64%)	65	11
9e	65	0.3	5	0,1	30	0.19	0,5	0.002	3.7	-	-	-

Polymerization temperature: 60 °C

Reaction duration: 24 h

Functional group content was determined via ^{1}H-NMR

8.2.2. Poly(oligo(ethylene glycole) methylether methacrylate^{475}-stat-di(ethylene glycol) methylether methacrylate-stat-3,6,9,12-tetraoxapentadec-14-yn-1-yl methacrylate) (10)

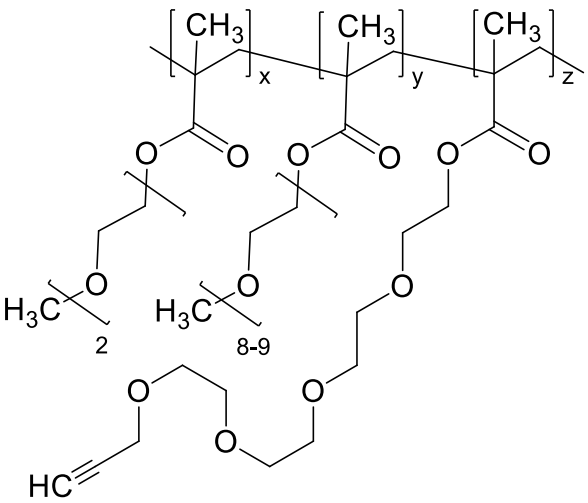

Table 7: *Overview of the polymer synthesis and results of polymer* ***10***

Polymer	MEO_2MA		$OEGMA^{475}$		**6**		AIBN		Ethanol	Yield	M_n	Functional group content
	eqv.	g	eqv.	g	eqv.	g	eqv.	g	g	g	kDA	eqv.
10a	80	0.7	5	0.1	15	0.2	0.5	0.004	5.7	0,6 (58%)	59	14
10b	75	0.6	5	0.1	20	0.3	0.5	0.004	5.7	0.5(45%)	65	20
10c	70	0.6	5	0.1	25	0.4	0.5	0.004	5.7	0.4 (79%)	53	27
10d	65	0.7	5	0.1	30	0.4	0.5	0.004	5.7	0.5 (40%)	51	28

Polymerization temperature: 60 °C

Reaction duration: 24 h

Functional group content was determined via ^{1}H-NMR

8.2.3. Poly(oligo(ethylene glycole) methylether methacrylate^{475}-stat-di(ethylene glycol) methylether methacrylate-stat- methacrylic acid) (11)

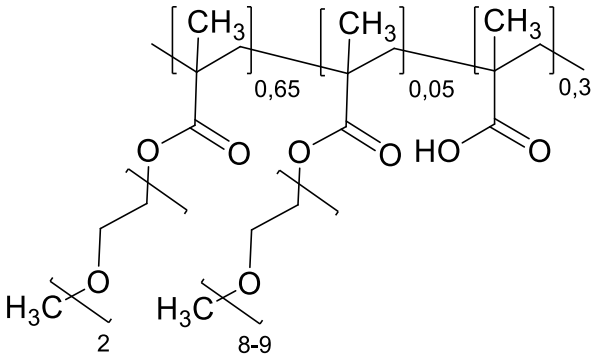

Table 8: *Overview of the polymer synthesis and results of polymer* ***11***

Polymer	MEO_2MA		$OEGMA^{475}$		**MA**		AIBN		Ethanol	Yield	M_n	Functional Groups content
	eqv.	g	eqv.	g	eqv.	g	eqv.	g	g	g	kDA	eqv.
11	65	1.0	5	0.2	30	0.2	0.3	0.007	4.2	1.0 (72%)	82	30

Polymerization temperature: 65 °C

Reaction duration: 48 h

Functional group content was determined via ^{1}H-NMR

8.2.4. Poly(oligo(ethylene glycole) methylether methacrylate^{475}-stat-di(ethylene glycol) methylether methacrylate-stat- 13,13-Dimethyl-11-oxo-3,6,9,12-tetraoxatetradecyl methacrylate) (12)

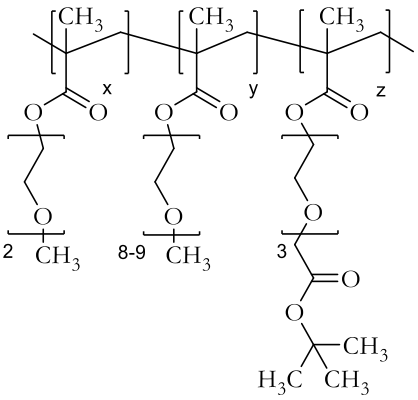

Table 9: *Overview of the polymer synthesis and results of polymer* ***12***

Polymer	MEO_2MA		$OEGMA^{475}$		**2**		AIBN		Ethanol	Yield	M_n	Functional Groups content
	eqv.	g	eqv.	g	eqv.	g	eqv.	g	g	g	kDA	eqv.
12a	80	0.7	5	0.1	10	0.2	0.5	0.004	5.7	0.5(49%)	74	11
12b	75	0.6	5	0.1	15	0.3	0.5	0.004	5.7	0.5 (50%)	75	15
12c	65	0.5	5	0.1	22	0.4	0.5	0.004	5.7	0.5(44%)	80	23
12d	65	0.3	5	0.1	30	0.4	0.03	0.003	2.1	0.7(84%)	82	36

Polymerization temperature: 60 °C (a-c)

55 °C (d)

Reaction duration: 24 h (a-c)

48 h (d)

Functional group content was determined via ^{1}H-NMR

8.2.5. Poly(oligo(ethylene glycole) methylether methacrylate^{475}-stat-di(ethylene glycol) methylether methacrylate-stat- 13,13-Dimethyl-11-oxo-3,6,9,12-tetraoxatetradecyl methacrylate –stat- 2-(4-benzoylphenoxy)ethyl methacrylate)(13)

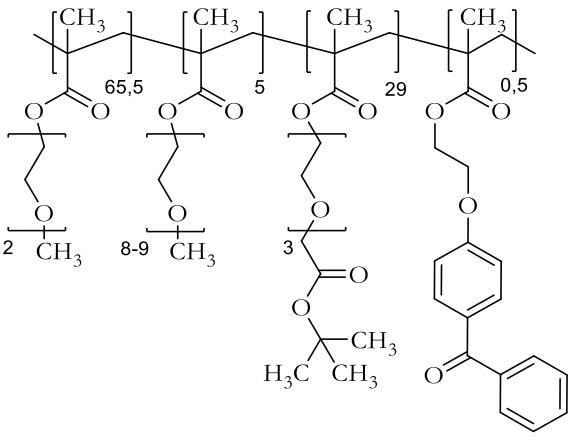

Table 10: *Overview of the polymer synthesis and results of polymer* ***13***

Polymer	MEO_2MA		$OEGMA^{475}$		**2**		BPEMA		AIBN		Ethanol	Yield	M_n	Functional Groups content
	eqv.	g	eqv.	g	eqv.	g	eqv.	g	eqv.	g	g	g	kDA	eqv.
13	64.5	0.61	5	0.12	30	0.45	0.5	0.01	0.1	0.004	4.9	0.9 (74%)	50	27

Polymerization temperature: 50 °C

Reaction duration: 24 h

Functional group content was determined via ^{1}H-NMR

8.2.6. Poly(N-isopropyl methacrylamide-stat- 13,13-dimethyl-11-oxo-3,6,9,12-tetraoxatetradecyl methacrylate)(14)

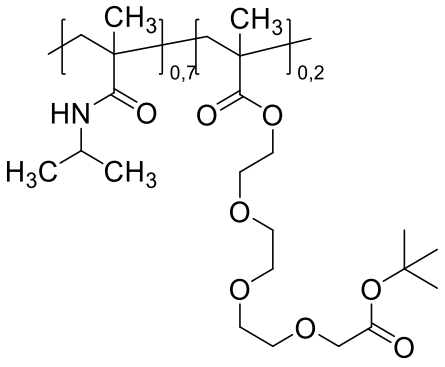

Table 11: *Overview of the polymer synthesis and results of polymer* ***14***

Polymer	NPMAM		**2**		AIBN		Ethanol	Yield	M_n	Functional Groups content
	eqv.	g	eqv.	g	eqv.	g	g	g	kDA	eqv.
14	80	0.3	20	0.2	0.5	0.004	1.5	0.3 (69%)	14	18

Polymerization temperature: 65 °C

Reaction duration: 48 h

Functional group content was determined via ^{1}H-NMR

8.3. Polymerizations in Ionic Liquids

Polymerizations in ionic liquids often require different procedures as those in ethanol. The ionic liquid (IL) used, generally 1-ethyl-3-methyl imidazolium hexafluorophosphate has to be molten at 70 °C in an oil bath while being purged with nitrogen. After the IL is liquefied, all the used monomers (freed of inhibitors) are added. The weight ratio of added monomers is 10% in relation to the IL. The monomer addition has to be done very carefully in order to keep the IL in the reaction vessel molten and not forming clumps on the walls and so on. If possible monomers are added via syringe. The mixture has to be stirred vigorously at all times, watching carefully to keep the complete solution liquid. The nitrogen purging continues for 2 h. After this time the initiator, AIBN, is added. It is imperative that the material is properly pushed into the solution and not blown out or on the walls of the reaction vessel. Afterwards the nitrogen purging syringes are removed and the vessel is properly sealed. The reaction time was 8 h, in order to stop the reaction, and to isolate the product the still hot IL solution is poured into a beaker. With the help of a minimum amount of 30°C warm ethanol, the last residues can be procured. The ionic liquid is regained by solving it in said beaker with small amounts of ethanol at 30°C – then the solution is cooled in the refrigerator at 4 °C and filtrated. The remaining liquid can be cooled again, the filtered solids can be recrystallized 3 times each to gain the IL back. Afterwards it is dried at 50° in a vacuum oven with Sicapent for 2 days. This way about 80 % of the IL can be recovered.

The ethanol-polymer mixture is dialyzed for a week with a 12 kDa cutoff tube (Zellutrans) against deionized water and freeze dried to yield the pure polymer.

8.3.1. Poly(oligo(ethylene glycole) methylether methacrylate^{475}-stat-di(ethylene glycol) methylether methacrylate)(15)

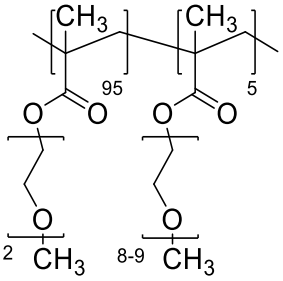

Table 12: *Overview of the polymer synthesis and results of polymer* ***15***

Polymer	MEO_2MA		$OEGMA^{475}$		AIBN		IL	Yield	M_n	M_w
	eqv.	g	eqv.	g	eqv.	g	g	g	kDA	kDA
15	95	1.8	5	0.2	1	0.016	7.8	-	260	1100

The polymerization was surveyed to gain information on the reaction kinetics. Every hour a small sample of the mixture was removed with a spatula and purified according to the work up procedure for NMR spectroscopy, the freeze drying was skipped in lieu of evaporation of all solvent. Therefore the yield is not representative.

Yield: 1.48 g (71%)

Polymer content was determined via ^{1}H-NMR

8.3.2. Poly(oligo(ethylene glycole) methylether methacrylate^{475}-stat-di(ethylene glycol) methylether methacrylate-stat- 13,13-dimethyl-11-oxo-3,6,9,12-tetraoxatetradecyl methacrylate –stat- 2-(4-benzoylphenoxy)ethyl methacrylate)(16)

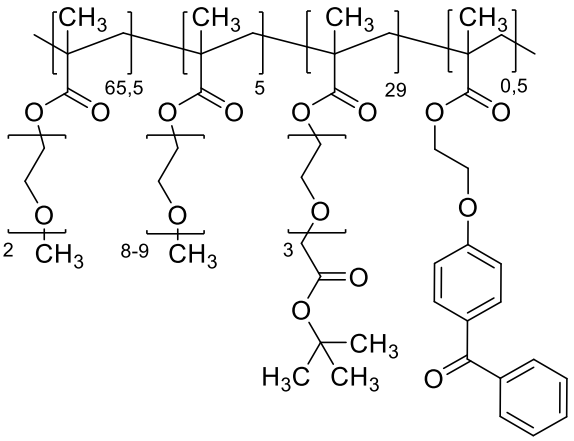

Table 13: *Overview of the polymer synthesis and results of polymer* ***16***

Polymer	MEO_2MA		$OEGMA^{475}$		**2**		BPEMA		AIBN		IL	Yield	M_n	Functional Group content
	eqv.	g	eqv.	g	eqv.	g	eqv.	g	eqv.	g	g	g	kDA	eqv.
16	64.5	0.4	5	0.1	30	0.3	0.1	0.01	1	0.01	7.	0.9 (74%)	42	28

Functional group content was determined via ^{1}H-NMR

8.3.3. Poly(N-isopropyl methacrylamide-stat- 13,13-dimethyl-11-oxo-3,6,9,12-tetraoxatetradecyl methacrylate stat- 2-(4-benzoylphenoxy)ethyl methacrylate –stat -2-(6-(dimethylamino)-1,3-dioxo-1H-benzo[de]isoquinolin-2(3H)-yl)ethyl)(17)

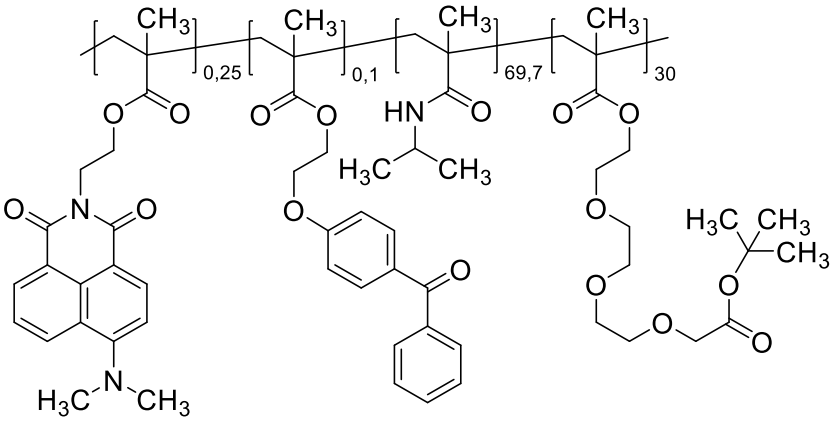

Table 14: *Overview of the polymer synthesis and results of polymer* ***17***

Polymer	NIPMAM		**2**		**8**		BPEMA		AIBN		IL	Yield	M_n
	eqv.	g	eqv.	g	eqv.	g	eqv.	g	eqv.	g	g	g	kDA
17	69.7	0.5	30	0.5	0.25	0	0.1	0.01	1	0.01	8.9	0.8 (78%)	75

8.4. Post Polymerization Reactions

8.4.1. Coupling Reactions with Benzylamine (18a-b)

The coupling reactions of the polymers with benzylamine are performed under identical conditions in order to gain comparability. The following reaction solutions are freshly prepared: 0.8 g of 3-(ethyliminomethyleneamino)-N,N-dimethylpropan-1-amine (EDC, 0.5 mmol) dissolved in 10 ml of deionized water and a solution of 0.2 g of N-hydroxysuccinimide (NHS, 2 mmol) in 10 ml of deionized water is prepared separately. A third solution is prepared by mixing 0.2 g of benzylamine (0.002 mol) with 20 ml deionized water. The polymers used for the reaction are dissolved separately in deionized water, as specified below.

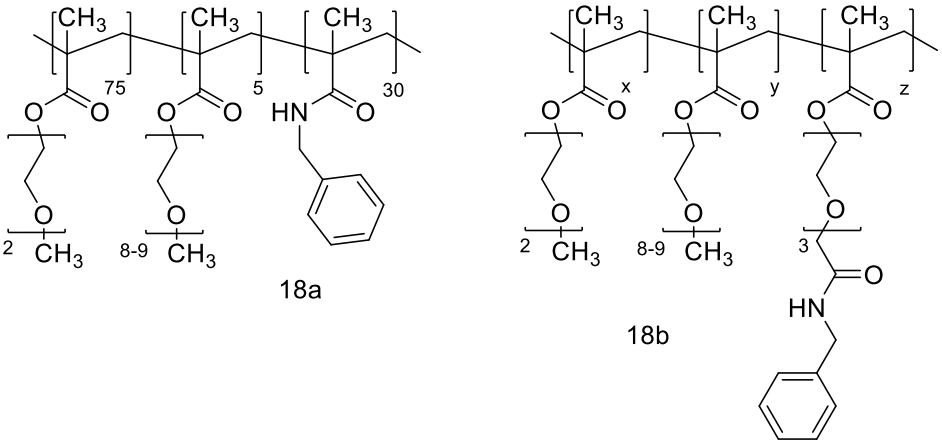

Figure 38: *Polymer structures of the polymers **18a** and **b** used as comparison of the coupling efficiency in dependence of spacer length*

The flasks with the dissolved polymer are equipped with a stirring bar, then 6 ml of the benzylamine solution are added to each. Immediately before use, the NHS and EDC solutions are mixed together and 6 ml of said mixture is added to the polymer solutions at room temperature. The reactions are completed by stirring overnight. The work up procedure includes five days of dialysis with 12 kDa cutoff tubes (Zellutrans) against deionized water and freeze dried to yield the pure polymer products. The products are analyzed via NMR spectroscopy.

8.4.2. General Procedure for Deprotecting Carboxylic Groups

The removal of the tert-butyl protective group is done as a post polymerization step. If applicable, it can be done after immobilizing the polymer on a substrate or after crosslinking. For best results, the material has to be as dry as possible. The deprotecting agent is a 1 vol% solution of trifluoroacetic acid in dry DCM. The polymer is dissolved in this freshly prepared mixture. The deprotecting mix is added in excess, approximately 5 ml per 100 mg of polymer. The solution is stirred for 8 h, then it is poured into distilled water. The DCM is evaporated, the aqueous polymer solution is dialyzed (Zellutrans) for one week against deionized water. After freeze drying the polymer is ready for further use.

8.4.3. Active Ester Couplings with Peptides (19)

The coupling reactions of the carboxyl containing polymers with peptides are performed under standard conditions. Exemplary, 178 mg of **13** in its deprotected state is dissolved under a nitrogen atmosphere in 10 ml of dried DCM. 50 mg (0.04 mmol) of peptide are added, as well as 11.6 mg of DMAP (94.7 mmol). While stirring, the solution is cooled in an ice bath to 0 °C. 183 mg of DCC (887 mmol), dissolved in 1.5 ml of dry DCM are added slowly with a dropping funnel. The solution is allowed to reach room temperature and stirred overnight. For ease of handling, the solution is filtered with a Büchner funnel, then the solvent is evaporated in vacuo. The residue is diluted with water as needed and transferred into a dialysis tube, then it is dialyzed (Zellutrans) against deionized water for a week and freeze dried. This precursor polymer is deprotected in order to remove the protective groups of the peptide. The functionalized polymer can be analyzed with NMR and turbidity measurements.

8.4.4. UV Induced Thiol-Ene Coupling (21)

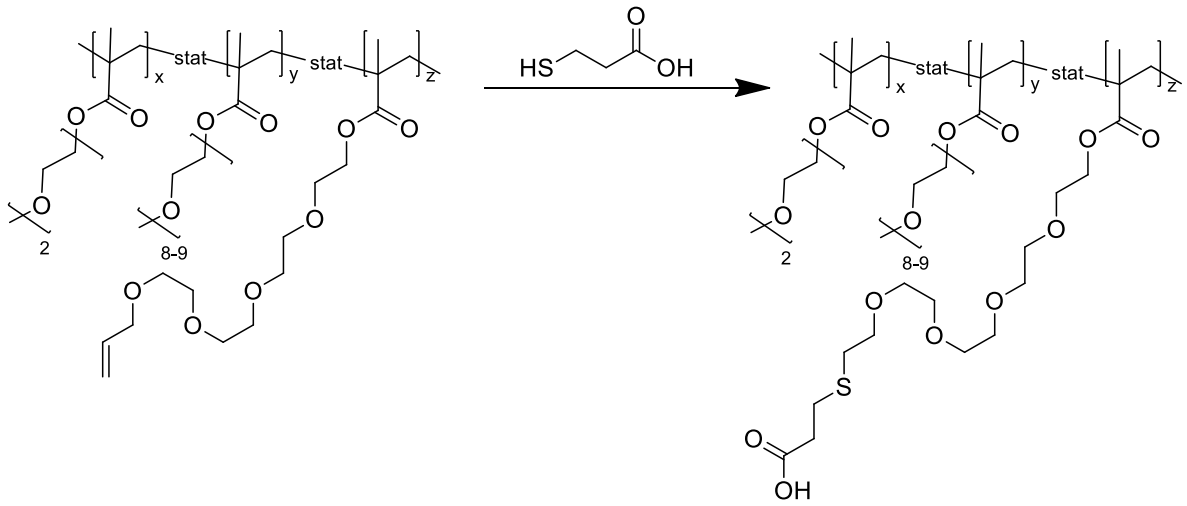

For the click reaction of polymer **9,** 500 mg of the material are dissolved in 4 g of DMF in a flat bottomed petri dish. 268 mg of mercaptopropionic acid (2.5 mmol) are added, then protected from environmental light, 29 mg of commercial Irgacure 2020 solution are added. The vessel is placed into the UV chamber which is purged with nitrogen for 15 mins, this time is used to pre-heat the lamp. The mix is then irradiated for 2h while the nitrogen purging is continued. The bottom of the vessel is water cooled to approximately 14-16 °C. After the reaction time, the mix is dialyzed for a week (Zellutrans) against deionized water, then freeze dried. The polymer is analyzed with NMR spectroscopy.

8.4.5. UV Induced Thiol-Yne Coupling (22)

Polymer **10c** is coupled with mercaptopropioic acid in the same way as described in 7.7.: 500 mg of the material are dissolved in 4 g of DMF in a flat bottomed petri dish. 536 mg of mercaptopropionicacid (5 mmol) are added. Then protected from environmental light, 60 mg of the Irgacure 2020 solution are added. The vessel is placed into the UV chamber which is purged with nitrogen for 15 mins, this time is used to pre-heat the lamp. The mix is then irradiated for 2h while the nitrogen purging is continued. After the reaction the mix is dialyzed for a week (Zellutrans) against deionized water, then freeze dried. The polymer is analyzed with ^{1}H-NMR spectroscopy.

8.4.6. Cycloadditions of Azido-Sugars to Alkyne Containing Polymers (23)

Variant A

Polymer **10c** (100 mg) is dissolved in 1.75 ml of DMF. 32 mg of azide-sugar are added (azidoglucose ((2R,3R,4S,5R,6S)-2-(acetoxymethyl)-6-azidotetrahydro-2H-pyran-3,4,5-triyl triacetate) , 0.1 mmol, supplied by Robert Bernin) to the solution as well as 1 mg of sodium ascorbate (0.005 mmol) and 0.12 mg of copper(II)sulfate (0.5 µmol) dissolved in 125 ml of deionized water. This mixture was stirred on a stirring plate for 12 h, then purified via dialysis (Zellutrans) against deionized water for a week. The resulting polymer was freeze dried, then analyzed via ^{1}H-NMR spectroscopy.

Variant B

Polymer **10c** (100 mg) is dissolved in 1.75 ml of DMF. To the solution, 32 mg of azide-sugar (azidoglucose ((2R,3R,4S,5R,6S)-2-(acetoxymethyl)-6-azidotetrahydro-2H-pyran-3,4,5-triyl triacetate), 0.1 mmol) as well as the catalyst **24** dissolved in 125 ml of deionized water are added. This mixture was stirred on a stirring plate for 12 h, then purified via dialysis (Zellutrans) against deionized water for a week. The polymer was freeze dried, then analyzed via ^{1}H-NMR spectroscopy.

8.4.7. Tris(triphenylphosphine)Copper(I)-Bromide (24)

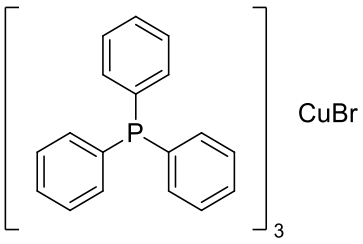

24.22 g of triphenylphosphine (92 mmol) are dissolved in 150 ml of refluxing methanol. In the next step, 5.15 g of copper(II)bromide (23 mmol) are slowly added. The mix is refluxed for 30 more minutes, then cooled to room temperature. The white precipitate is filtered off and washed with ethanol (3x50 ml), then diethyl ether (3x 50 ml). Yield 93 %.

8.5. Preparation of Silicon Wafers and Glass Surfaces for Polymer Coatings

Silicon wafers (2x2 cm), glass slides and quartz cuvettes are prepared for polymer coatings according to this standard procedure: The slides are checked for a clean, unscratched surface, placed in a soilent green solution made up from 100 mg of $KMnO_4$ 40 ml of sulfuric acid for 24 h. After the cleaning step the platelets are rinsed with ultrapure water three times. Afterwards, they are rinsed three times each with pure ethanol (p.a) and toluene. The pieces are then placed into a 1 vol% solution of (3-aminopropyl)dimethylethoxysilane in toluene for 24 h. Then, the slides are rinsed three times each in the following order: toluene, pure ethanol, ultrapure water. After drying the slides with nitrogen, they can be stored for use in tightly closed containers.

8.6. Preparation of Gold Chips for Polymer Coatings

Gold chips (1,2 cm x1,2 cm; Ssens, Netherlands) coated with a 50 nm gold layer are prepared for polymer coatings according to this standard procedure: The chips are checked for a clean, unscratched surface, placed in a “piranha acid” solution made up a 1:1 vol% mix of concentrated hydrogen Peroxide in water and concentrated sulfuric acid for 24 h. After the cleaning step the platelets are rinsed with ultrapure water three times. Afterwards, they are rinsed three times each with pure ethanol. The pieces are now placed in a 1 mM solution of mercaptopropioic acid in ethanol for 24 h. Then the slides are rinsed three times each in the following order: pure Ethanol, ultrapure water. After drying the slides with nitrogen, they can be stored for use in tightly closed containers.

8.7. Ellipsometry

All ellipsometric measurements were done with an Optrel Multiscope (Germany) in a rotating analyzer setup. Measurements done with solvents were transduced with a 60 ° flow cell provided by Optrel. All measurements were performed at a fixed angle of 60 °. The silicon wafers used in all experiments were bought from Si-Mat and had a defined SiO_2 layer with a thickness of 1 nm.

All data were processed with the Elli software provided by Optrel. The layer thickness calculations followed the assumption of a four layer system. In dry measurements, layers were as follows; layer 1 – air (n=1.000; k=0), layer 2 polymer layer (n=1.4800; k=0), layer 3 SiO_2 (n=1.4580; d=1.0 nm), layer 4 silicone (n=3.8858; k=-0.02). For all measurements with the flow cell layers 1 and 2 were adjusted: layer 1 water (n=1.3323; k=0), layer 2 swollen polymer layer (n=1.3700; k =0). For all experiments with the flow cell, the samples were left submersed in the cell for 30 min prior to measurements to adjust to the solvent environment.

8.8. Gel Permeation Chromatography (GPC)

All GPC measurements were processed on a setup consisting of a single channel degasser (WEG Dr. Bures, Germany), an isocratic pump P 1000 (Spectra Physics, USA), PolarGel columns (Guard 7,5 x 75 mm, PolarGel L 7,5 x 300 mm; Polymer Laboratory, USA) and detection by a UV/vis-detector SEC-3010 and refractometer SEC 3010 (WEG Dr. Bures). Measurements were done with a flow rate of 1ml/min at 50 °C using polystyrene standards in DMF (PSS, Germany)

8.9. Nuclear Magnetic Resonance Spectroscopy (NMR)

NMR spectra were recorded on an Avance 300 spectrometer (Bruker, USA), fitted with an automatic sampler. ^{1}H spectra were recorded at 300 MHz, ^{13}C at 75 MHz. The peak used for reference was either the TMS signal if added or the typical solvent peak.

8.10. Surface Plasmon Resonance Spectroscopy (SPR)

Surface plasmon resonance experiments were conducted on a dual channel SR7000DC unit (Reichert, USA). The standard flow used was 50 µL/min, the injection of reagents was done via a 1 ml injection loop. The sample chamber was kept at a constant temperature of 25 °C. Samples were immobilized on SPR chips (Ssens, Netherlands) with a gold layer thickness of 50 nm

8.11. Spin Coating

Spin coating of silicon wafers, glass slides and gold chips was done with a KL-SCV coater (Schaefer Technologie GmbH, Germany). Samples were fixed to the plate by vacuum, then revved to a constant 50 rps before the polymer solutions were dropped onto the surface. The treated samples were spun for 30 s before removal and further treatments.

8.12. Turbidity Measuremnts

Turbidity was measured on a Cary 50 UV-Vis spectrometer (Agilent, Germany) fitted with a Peltier element for heating and cooling. If not noted otherwise, the heating/cooling rate was 1 °C per minute. Measurement wavelength was 700 nm and the standard polymer concentration was 2 g/l.

8.13. UV-Crosslinking

UV induced crosslinking was performed with a UVA Cube 100 (Hönle, Germany), fitted with a 100 W Iron- doped mercury lamp, which was filtered with a 315 nm cut-off window. A nitrogen hose was used to purge and fill the chamber constantly with nitrogen

9. Literature

1. Jochum FD, Theato P. Temperature-and light-responsive polyacrylamides prepared by a double polymer analogous reaction of activated ester polymers. Macromolecules. 2009;42(16):5941-5.
2. Kungwatchakun D, Irie M. Photoresponsive polymers. Photocontrol of the phase separation temperature of aqueous solutions of poly-[N-isopropylacrylamide-co-N-(4-phenylazophenyl) acrylamide]. Die Makromolekulare Chemie, Rapid Communications. 1988;9(4):243-6.
3. Mi P, Chu LY, Ju XJ, Niu CH. A Smart Polymer with Ion-Induced Negative Shift of the Lower Critical Solution Temperature for Phase Transition. Macromolecular Rapid Communications. 2008;29(1):27-32.
4. Jia Y-g, Zhu X, Liu L-y, Li J. Multi-responsive properties of a poly (ethylene glycol)-grafted alternating copolymers of distyrenic monomer with maleic anhydride. Langmuir. 2012;28(9):4500-6.
5. Pietsch C, Hoogenboom R, Schubert US. Soluble polymeric dual sensor for temperature and pH value. Angewandte Chemie International Edition. 2009;48(31):5653-6.
6. Li D, He Q, Yang Y, Möhwald H, Li J. Two-stage pH response of poly (4-vinylpyridine) grafted gold nanoparticles. Macromolecules. 2008;41(19):7254-6.
7. Schmaljohann D. Thermo-and pH-responsive polymers in drug delivery. Advanced drug delivery reviews. 2006;58(15):1655-70.
8. Harada A, Johnin K, Kawamura A, Kono K. Preparation of temperature-responsive polymer gels physically immobilizing core-shell type bioconjugates. Journal of Polymer Science Part A: Polymer Chemistry. 2007;45(24):5942-8.
9. Li M, De P, Gondi SR, Sumerlin BS. Responsive Polymer-Protein Bioconjugates Prepared by RAFT Polymerization and Copper-Catalyzed Azide-Alkyne Click Chemistry. Macromolecular Rapid Communications. 2008;29(12-13):1172-6.
10. Hanyková L, Spěváček J, Radecki M, Zhigunov A, Šťastná J, Valentová H, et al. Structures and interactions in collapsed hydrogels of thermoresponsive interpenetrating polymer networks. Colloid and Polymer Science. 2015;293(3):709-20.
11. Laschewsky A, Rekaï ED, Wischerhoff E. Tailoring of Stimuli-Responsive Water Soluble Acrylamide and Methacrylamide Polymers. Macromolecular Chemistry and Physics. 2001;202(2):276-86.
12. Gao W, Xu D, Lim DW, Craig SL, Chilkoti A. In situ growth of a thermoresponsive polymer from a genetically engineered elastin-like polypeptide. Polymer Chemistry. 2011;2(7):1561-6.
13. Robinson JW, Secker C, Weidner S, Schlaad H. Thermoresponsive Poly(N-C3 glycine)s. Macromolecules. 2013;46(3):580-7.
14. Wischerhoff E, Zacher T, Laschewsky A, Rekaï ED. Direct Observation of the Lower Critical Solution Temperature of Surface-Attached Thermo-Responsive Hydrogels by Surface Plasmon Resonance. Angewandte Chemie International Edition. 2000;39(24):4602-4.
15. Heskins M, Guillet JE. Solution Properties of Poly(N-isopropylacrylamide). Journal of Macromolecular Science: Part A - Chemistry. 1968;2(8):1441-55.
16. Irie M. Photochromism: Memories and SwitchesIntroduction. Chemical Reviews. 2000;100(5):1683-4.
17. Ju HK, Kim SY, Kim SJ, Lee YM. pH/temperature-responsive semi-IPN hydrogels composed of alginate and poly (N-isopropylacrylamide). Journal of applied polymer science. 2002;83(5):1128-39.
18. Acharya G, Shin CS, McDermott M, Mishra H, Park H, Kwon IC, et al. The hydrogel template method for fabrication of homogeneous nano/microparticles. Journal of Controlled Release. 2010;141(3):314-9.

19. Oliveira MB, Mano JF. Natural-Based and Stimuli-Responsive Polymers for Tissue Engineering and Regenerative Medicine. Polymers in Regenerative Medicine: John Wiley & Sons, Inc; 2014. p. 49-90.
20. Hoffman AS. The origins and evolution of “controlled” drug delivery systems. Journal of Controlled Release. 2008;132(3):153-63.
21. Jhaveri SJ, Hynd MR, Dowell-Mesfin N, Turner JN, Shain W, Ober CK. Release of nerve growth factor from HEMA hydrogel-coated substrates and its effect on the differentiation of neural cells. Biomacromolecules. 2008;10(1):174-83.
22. Liu Z, Calvert P. Multilayer hydrogels as muscle-like actuators. Advanced Materials. 2000;12(4):288-91.
23. Mendes PM. Stimuli-responsive surfaces for bio-applications. Chemical Society Reviews. 2008;37(11):2512-29.
24. Tokarev I, Minko S. Stimuli-responsive hydrogel thin films. Soft Matter. 2009;5(3):511-24.
25. Anker JN, Hall WP, Lyandres O, Shah NC, Zhao J, Van Duyne RP. Biosensing with plasmonic nanosensors. Nature materials. 2008;7(6):442-53.
26. Cheng G, Xue H, Zhang Z, Chen S, Jiang S. A switchable biocompatible polymer surface with self-sterilizing and nonfouling capabilities. Angewandte Chemie International Edition. 2008;47(46):8831-4.
27. Trmcic-Cvitas J, Hasan E, Ramstedt M, Li X, Cooper MA, Abell C, et al. Biofunctionalized protein resistant oligo (ethylene glycol)-derived polymer brushes as selective immobilization and sensing platforms. Biomacromolecules. 2009;10(10):2885-94.
28. Gautrot JE, Trappmann B, Oceguera-Yanez F, Connelly J, He X, Watt FM, et al. Exploiting the superior protein resistance of polymer brushes to control single cell adhesion and polarisation at the micron scale. Biomaterials. 2010;31(18):5030-41.
29. Kolb HC, Finn MG, Sharpless KB. Click Chemistry: Diverse Chemical Function from a Few Good Reactions. Angewandte Chemie International Edition. 2001;40(11):2004-21.
30. Ponnuswamy SR, Penlidis A, Kiparissides C. Batch solution polymerization of methyl methacrylate: Parameter estimation. The Chemical Engineering Journal. 1988;39(3):175-83.
31. Kuchta F-D, van Herk AM, German AL. Propagation Kinetics of Acrylic and Methacrylic Acid in Water and Organic Solvents Studied by Pulsed-Laser Polymerization. Macromolecules. 2000;33(10):3641-9.
32. Graeme Moad DHS. The Chemistry of Radical Polymerization. 2nd ed. Netherlands: Elsevier; 2006.
33. Carswell TG, Hill DJT, Londero DI, O'Donnell JH, Pomery PJ, Winzor CL. Kinetic parameters for polymerization of methyl methacrylate at 60°C. Polymer. 1992;33(1):137-40.
34. Beuermann S, Buback M, Davis TP, Gilbert RG, Hutchinson RA, Olaj OF, et al. Critically evaluated rate coefficients for free-radical polymerization, 2.. Propagation rate coefficients for methyl methacrylate. Macromolecular Chemistry and Physics. 1997;198(5):1545-60.
35. Zhang D, Lahasky SH, Guo L, Lee C-U, Lavan M. Polypeptoid Materials: Current Status and Future Perspectives. Macromolecules. 2012;45(15):5833-41.
36. Zhang N, Salzinger S, Rieger B. Poly(vinylphosphonate)s with Widely Tunable LCST: A Promising Alternative to Conventional Thermoresponsive Polymers. Macromolecules. 2012;45(24):9751-8.
37. Gandhi A, Paul A, Sen SO, Sen KK. Studies on thermoresponsive polymers: Phase behaviour, drug delivery and biomedical applications. Asian Journal of Pharmaceutical Sciences. 2015;10(2):99-107.
38. Feoktistova N, Stoychev G, Puretskiy N, Leonid I, Dmitry V. Porous thermo-responsive pNIPAM microgels. European Polymer Journal. 2015;68:650-6.
39. Lutz J-F, Akdemir Ö, Hoth A. Point by Point Comparison of Two Thermosensitive Polymers Exhibiting a Similar LCST: Is the Age of Poly(NIPAM) Over? Journal of the American Chemical Society. 2006;128(40):13046-7.
40. Roy D, Brooks WLA, Sumerlin BS. New directions in thermoresponsive polymers. Chemical Society Reviews. 2013;42(17):7214-43.

41. Liu R, Fraylich M, Saunders BR. Thermoresponsive copolymers: from fundamental studies to applications. Colloid and Polymer Science. 2009;287(6):627-43.
42. Puoci F, Iemma F, Picci N. Stimuli-Responsive Molecularly Imprinted Polymers for Drug Delivery: A Review. Current Drug Delivery. 2008;5(2):85-96.
43. Aoshima S, Kanaoka S. Synthesis of Stimuli-Responsive Polymers by Living Polymerization: Poly(N-Isopropylacrylamide) and Poly(Vinyl Ether)s. Wax Crystal Control · Nanocomposites · Stimuli-Responsive Polymers. Berlin, Heidelberg: Springer Berlin Heidelberg; 2008. p. 169-208.
44. Djokpé E, Vogt W. N-Isopropylacrylamide and N-Isopropylmethacryl-amide: Cloud Points of Mixtures and Copolymers. Macromolecular Chemistry and Physics. 2001;202(5):750-7.
45. Winnik FM. Phase transition of aqueous poly-(N-isopropylacrylamide) solutions: a study by non-radiative energy transfer. Polymer. 1990;31(11):2125-34.
46. Suzuki A, Kojima S. Phase transition in constrained polymer gels. The Journal of Chemical Physics. 1994;101(11):10003-7.
47. Zhang Y, Furyk S, Bergbreiter DE, Cremer PS. Specific Ion Effects on the Water Solubility of Macromolecules: PNIPAM and the Hofmeister Series. Journal of the American Chemical Society. 2005;127(41):14505-10.
48. Plamper FA, Steinschulte AA, Hofmann CH, Drude N, Mergel O, Herbert C, et al. Toward Copolymers with Ideal Thermosensitivity: Solution Properties of Linear, Well-Defined Polymers of N-Isopropyl Acrylamide and N,N-Diethyl Acrylamide. Macromolecules. 2012;45(19):8021-6.
49. Lutz J-F, Weichenhan K, Akdemir Ö, Hoth A. About the Phase Transitions in Aqueous Solutions of Thermoresponsive Copolymers and Hydrogels Based on 2-(2-methoxyethoxy)ethyl Methacrylate and Oligo(ethylene glycol) Methacrylate. Macromolecules. 2007;40(7):2503-8.
50. Miasnikova A, Laschewsky A. Influencing the phase transition temperature of poly(methoxy diethylene glycol acrylate) by molar mass, end groups, and polymer architecture. Journal of Polymer Science Part A: Polymer Chemistry. 2012;50(16):3313-23.
51. Skrabania K, Kristen J, Laschewsky A, Akdemir Ö, Hoth A, Lutz J-F. Design, Synthesis, and Aqueous Aggregation Behavior of Nonionic Single and Multiple Thermoresponsive Polymers. Langmuir. 2007;23(1):84-93.
52. Lutz J. Sci. Part A: Polym Chem. 2008;46:3459-70.
53. Han S, Hagiwara M, Ishizone T. Synthesis of thermally sensitive water-soluble polymethacrylates by living anionic polymerizations of oligo (ethylene glycol) methyl ether methacrylates. Macromolecules. 2003;36(22):8312-9.
54. Weber C, Hoogenboom R, Schubert US. Temperature responsive bio-compatible polymers based on poly (ethylene oxide) and poly (2-oxazoline) s. Progress in Polymer Science. 2012;37(5):686-714.
55. Aseyev V, Tenhu H, Winnik FM. Non-ionic Thermoresponsive Polymers in Water. In: Müller AHE, Borisov O, editors. Self Organized Nanostructures of Amphiphilic Block Copolymers II. Berlin, Heidelberg: Springer Berlin Heidelberg; 2011. p. 29-89.
56. Lutz J-F, Börner HG. Modern trends in polymer bioconjugates design. Progress in Polymer Science. 2008;33(1):1-39.
57. Singh N, Blackburn WH, Lyon A. Bioconjugation of Soft Nanomaterials: John Wiley & Sons, Inc.; 2007. 61-91 p.
58. Peppas NA, Keys KB, Torres-Lugo M, Lowman AM. Poly(ethylene glycol)-containing hydrogels in drug delivery. Journal of Controlled Release. 1999;62(1–2):81-7.
59. Knop K, Hoogenboom R, Fischer D, Schubert US. Poly(ethylene glycol) in Drug Delivery: Pros and Cons as Well as Potential Alternatives. Angewandte Chemie International Edition. 2010;49(36):6288-308.
60. Dong Y, Feng S-S. Methoxy poly(ethylene glycol)-poly(lactide) (MPEG-PLA) nanoparticles for controlled delivery of anticancer drugs. Biomaterials. 2004;25(14):2843-9.
61. Sousa-Herves A, Riguera R, Fernandez-Megia E. PEG-dendritic block copolymers for biomedical applications. New Journal of Chemistry. 2012;36(2):205-10.

62. Harris JM, Dust JM, McGill RA, Harris PA, Edgell MJ, Sedaghat-Herati RM, et al. New Polyethylene Glycols for Biomedical Applications. Water-Soluble Polymers. ACS Symposium Series. 467: American Chemical Society; 1991. p. 418-29.
63. Shalaby SW, McCormick CL, Butler GB. Water-Soluble Polymers: American Chemical Society; 1991. 548 p.
64. Harris JM, Zalipsky S. Poly(ethylene glycol): American Chemical Society; 1997. 508 p.
65. Zalipsky S, Harris JM. Introduction to Chemistry and Biological Applications of Poly(ethylene glycol). Poly(ethylene glycol). ACS Symposium Series. 680: American Chemical Society; 1997. p. 1-13.
66. Geever LM, Nugent MJD, Higginbotham CL. The effect of salts and pH buffered solutions on the phase transition temperature and swelling of thermoresponsive pseudogels based on N-isopropylacrylamide. Journal of Materials Science. 2007;42(23):9845-54.
67. Du H, Wickramasinghe R, Qian X. Effects of Salt on the Lower Critical Solution Temperature of Poly (N-Isopropylacrylamide). The Journal of Physical Chemistry B. 2010;114(49):16594-604.
68. Bruck SD. Aspects of three types of hydrogels for biomedical applications. Journal of Biomedical Materials Research. 1973;7(5):387-404.
69. Caló E, Khutoryanskiy VV. Biomedical applications of hydrogels: A review of patents and commercial products. European Polymer Journal. 2015;65:252-67.
70. Kopeček J. Hydrogel biomaterials: A smart future? Biomaterials. 2007;28(34):5185-92.
71. Annabi N, Tamayol A, Uquillas JA, Akbari M, Bertassoni LE, Cha C, et al. 25th Anniversary Article: Rational Design and Applications of Hydrogels in Regenerative Medicine. Advanced Materials. 2014;26(1):85-124.
72. Van Vlierberghe S, Dubruel P, Schacht E. Biopolymer-Based Hydrogels As Scaffolds for Tissue Engineering Applications: A Review. Biomacromolecules. 2011;12(5):1387-408.
73. Hoffman AS. Hydrogels for biomedical applications. Advanced Drug Delivery Reviews. 2012;64, Supplement:18-23.
74. Flory PJ, Rehner J. Statistical Mechanics of Cross-Linked Polymer Networks II. Swelling. The Journal of Chemical Physics. 1943;11(11):521-6.
75. Flory PJ. Statistical Mechanics of Swelling of Network Structures. The Journal of Chemical Physics. 1950;18(1):108-11.
76. Laschewsky A, Ouari O, Mangeney C, Jullien L. Reactive hydrogels grafted on gold surfaces. Macromolecular Symposia. 2001;164(1):323-40.
77. Minko S. Grafting on Solid Surfaces: “Grafting to” and “Grafting from” Methods. In: Stamm M, editor. Polymer Surfaces and Interfaces: Characterization, Modification and Applications. Berlin, Heidelberg: Springer Berlin Heidelberg; 2008. p. 215-34.
78. Halliwell CM, Cass AEG. A Factorial Analysis of Silanization Conditions for the Immobilization of Oligonucleotides on Glass Surfaces. Analytical Chemistry. 2001;73(11):2476-83.
79. Brzoska JB, Azouz IB, Rondelez F. Silanization of Solid Substrates: A Step Toward Reproducibility. Langmuir. 1994;10(11):4367-73.
80. Merrifield RB. Solid Phase Peptide Synthesis. I. The Synthesis of a Tetrapeptide. Journal of the American Chemical Society. 1963;85(14):2149-54.
81. Barbey R, Lavanant L, Paripovic D, Schüwer N, Sugnaux C, Tugulu S, et al. Polymer Brushes via Surface-Initiated Controlled Radical Polymerization: Synthesis, Characterization, Properties, and Applications. Chemical Reviews. 2009;109(11):5437-527.
82. Pengo P, Broxterman QB, Kaptein B, Pasquato L, Scrimin P. Synthesis of a Stable Helical Peptide and Grafting on Gold Nanoparticles. Langmuir. 2003;19(6):2521-4.
83. Buller J. Entwicklung neuer stimuli-sensitiver Hydrogelfilme als Plattform für die Biosensorik: Universitätsbibliothek der Universität Potsdam; 2013.
84. Buller J, Laschewsky A, Wischerhoff E. Photoreactive oligoethylene glycol polymers - versatile compounds for surface modification by thin hydrogel films. Soft Matter. 2013;9(3):929-37.

85. Boundless. Boundless Microbiology2016 2016/05/26.
86. and HNS, Jørgensen BB. Big Bacteria. Annual Review of Microbiology. 2001;55(1):105-37.
87. Buntgarn/Stannered. Ellipsometry setup.jpg www.wikipedia.com2008 [cited 2016 11/13/2016]. Available from: https://en.wikipedia.org/wiki/File:Ellipsometry_setup.svg.
88. Schasfoort RB, Tudos AJ. Handbook of surface plasmon resonance: Royal Society of Chemistry; 2008.
89. Binder WH, Sachsenhofer R. 'Click' Chemistry in Polymer and Materials Science. Macromolecular Rapid Communications. 2007;28(1):15-54.
90. Gokmen MT, Brassinne J, Prasath RA, Du Prez FE. Revealing the nature of thio-click reactions on the solid phase. Chemical Communications. 2011;47(16):4652-4.
91. Lowe AB. Thiol-ene "click" reactions and recent applications in polymer and materials synthesis. Polymer Chemistry.1(1):17-36.
92. Mansfeld U, Pietsch C, Hoogenboom R, Becer CR, Schubert US. Clickable initiators, monomers and polymers in controlled radical polymerizations - a prospective combination in polymer science. p. -.
93. Sumerlin BS, Vogt AP. Macromolecular Engineering through Click Chemistry and Other Efficient Transformations. Macromolecules. 2009;43(1):1-13.
94. Hoyle CE, Bowman CN. Thiol–Ene Click Chemistry. Angew Chem, Int Ed. 2010;49:1540.
95. Golas PL, Matyjaszewski K. Marrying click chemistry with polymerization: expanding the scope of polymeric materials. Chemical Society Reviews. 2010;39(4):1338-54.
96. Qin A, Lam JWY, Tang BZ. Click Polymerization: Progresses, Challenges, and Opportunities. Macromolecules. 2010;43(21):8693-702.
97. Barner-Kowollik C, Du Prez FE, Espeel P, Hawker CJ, Junkers T, Schlaad H, et al. "Clicking" Polymers or Just Efficient Linking: What Is the Difference? Angewandte Chemie International Edition. 2011;50(1):60-2.
98. Hoshino A, Ohnishi N, Yasuhara M, Yamamoto K, Kondo A. Separation of Murine Neutrophils and Macrophages by Thermoresponsive Magnetic Nanoparticles. Biotechnology Progress. 2007;23(6):1513-6.
99. Tatsuma T, Mori H, Takahashi H, Fujishima A. Activity Control of a Heme Peptide-Modified Electrode by an Inhibitor Bound to a Thermoresponsive Polymer. Electrochemical and Solid-State Letters. 2001;4(2):E5-E7.
100. Toma M, Jonas U, Mateescu A, Knoll W, Dostalek J. Active Control of SPR by Thermoresponsive Hydrogels for Biosensor Applications. The Journal of Physical Chemistry C. 2013;117(22):11705-12.
101. Ding Z, Fong RB, Long CJ, Stayton PS, Hoffman AS. Size-dependent control of the binding of biotinylated proteins to streptavidin using a polymer shield. Nature. 2001;411(6833):59-62.
102. Ayi T-C, Tong JM-M, Lee PV-S, editors. Optically tunable hydrogel biosensor material2006.
103. Jeníková G, Pazlarová J, Demnerová K. Detection of Salmonella in food samples by the combination of immunomagnetic separation and PCR assay. International Microbiology. 2010;3(4):225-9.
104. Harrisson S, Mackenzie SR, Haddleton DM. Unprecedented solvent-induced acceleration of free-radical propagation of methyl methacrylate in ionic liquids. Chemical Communications. 2002(23):2850-1.
105. Carmichael AJ, Haddleton DM, Bon SA, Seddon KR. Copper (I) mediated living radical polymerisation in an ionic liquid. Chemical Communications. 2000(14):1237-8.
106. Hong K, Zhang H, Mays JW, Visser AE, Brazel CS, Holbrey JD, et al. Conventional free radical polymerization in room temperature ionic liquids: a green approach to commodity polymers with practical advantages. Chemical communications. 2002(13):1368-9.
107. Rogers RD, Seddon KR, editors. Ionic liquids(industrial applications for green chemistry). A C S symposium series; 2002: American Chemical Society.

108. Harrisson S, Mackenzie SR, Haddleton DM. Pulsed Laser Polymerization in an Ionic Liquid: Strong Solvent Effects on Propagation and Termination of Methyl Methacrylate. Macromolecules. 2003;36(14):5072-5.
109. Schmidt-Naake G, Woecht I, Schmalfuß A, Glück T. Free Radical Polymerization in Ionic Liquids – Solvent Influence of New Dimension. Macromolecular Symposia. 2009;275–276(1):204-18.
110. Strehmel V, Laschewsky A, Wetzel H, Görnitz E. Free Radical Polymerization of n-Butyl Methacrylate in Ionic Liquids. Macromolecules. 2006;39(3):923-30.
111. Drobník J, Vlasák J, Pilař J, Svec F, Kálal J. Synthetic model polymers in the study of protein immobilization on glycidyl methacrylate carriers. Enzyme and Microbial Technology. 1979;1(2):107-12.
112. Chang TMS. Removal of endogenous and exogenous toxins by a microencapsulated absorbent. Canadian Journal of Physiology and Pharmacology. 1969;47(12):1043-5.
113. Campbell DH, Luescher E, Lerman LS. Immunologic adsorbents I. Isolation of antibody by means of a cellulose-protein antigen. Proceedings of the National Academy of Sciences. 1951;37(9):575-8.
114. Stryer L. Biochemistry. 4th ed. New York: W H Freeman; 1995.
115. Jursic BS, Zdravkovski Z. A simple preparation of amides from acids and amines by heating of their mixture. Synthetic communications. 1993;23(19):2761-70.
116. Zabicky J. chemistry of amides. 1970.
117. Curtius T. Synthetische Versuche mit Hippurazid. Berichte der deutschen chemischen Gesellschaft. 1902;35(3):3226-8.
118. Wittenberger SJ, McLaughlin MA. Preparation of endothelin antagonist ABT-627. Tetrahedron Letters. 1999;40(40):7175-8.
119. Sheehan J, Cruickshank P, Boshart G. Notes-A Convenient Synthesis of Water-Soluble Carbodiimides. The Journal of Organic Chemistry. 1961;26(7):2525-8.
120. Sheehan JC, Hess GP. A new method of forming peptide bonds. Journal of the American Chemical Society. 1955;77(4):1067-8.
121. Ryu Y, Scott AI. Self-condensation of activated malonic acid half esters: a model for the decarboxylative Claisen condensation in polyketide biosynthesis. Tetrahedron letters. 2003;44(40):7499-502.
122. Devouge S, Salvagnini C, Marchand-Brynaert J. A practical molecular clip for immobilization of receptors and biomolecules on devices' surface: Synthesis, grafting protocol and analytical assay. Bioorganic & medicinal chemistry letters. 2005;15(13):3252-6.
123. Mädler S, Bich C, Touboul D, Zenobi R. Chemical cross-linking with NHS esters: a systematic study on amino acid reactivities. Journal of mass spectrometry. 2009;44(5):694-706.
124. Zhao X, Milton Harris J. Novel degradable poly (ethylene glycol) hydrogels for controlled release of protein. Journal of pharmaceutical sciences. 1998;87(11):1450-8.
125. Elia G. Biotinylation reagents for the study of cell surface proteins. Proteomics. 2008;8(19):4012-24.
126. Wojtyk JT, Morin KA, Boukherroub R, Wayner DD. Modification of porous silicon surfaces with activated ester monolayers. Langmuir. 2002;18(16):6081-7.
127. Cengiz N, Kabadayioglu H, Sanyal R. Orthogonally functionalizable copolymers based on a novel reactive carbonate monomer. Journal of Polymer Science Part A: Polymer Chemistry.48(21):4737-46.
128. Swamy KCK, Kumar NNB, Balaraman E, Kumar KVPP. Mitsunobu and Related Reactions: Advances and Applications. Chemical Reviews. 2009;109(6):2551-651.
129. Wang X, Liu L, Luo Y, Zhao H. Bioconjugation of Biotin to the Interfaces of Polymeric Micelles via In Situ Click Chemistry. Langmuir. 2008;25(2):744-50.
130. Dhanikula RS, Hildgen P. Synthesis and Evaluation of Novel Dendrimers with a Hydrophilic Interior as Nanocarriers for Drug Delivery. Bioconjugate Chemistry. 2005;17(1):29-41.
131. Anderson GW, Zimmerman JE, Callahan FM. N-Hydroxysuccinimide Esters in Peptide Synthesis. Journal of the American Chemical Society. 1963;85(19):3039-.

132. Pinyou P, Ruff A, Pöller S, Barwe S, Nebel M, Alburquerque NG, et al. Thermoresponsive amperometric glucose biosensor. Biointerphases. 2016;11(1):011001.
133. Matthews BW, Remington SJ. The Three Dimensional Structure of the Lysozyme from Bacteriophage T4. Proceedings of the National Academy of Sciences. 1974;71(10):4178-82.
134. Müller JJ, Barbirz S, Heinle K, Freiberg A, Seckler R, Heinemann U. An Intersubunit Active Site between Supercoiled Parallel β Helices in the Trimeric Tailspike Endorhamnosidase of Shigella flexneri Phage Sf6. Structure. 2008;16(5):766-75.
135. Tang K, Seckler R. Autonomer phagenbasierter Salmonellenbiosensor. Google Patents; 2015.
136. Kerstin Tang RS, inventorAutonomous phage based Salmonellenbiosensor. Germany2014.
137. Inal S, Kolsch JD, Chiappisi L, Janietz D, Gradzielski M, Laschewsky A, et al. Structure-related differences in the temperature-regulated fluorescence response of LCST type polymers. Journal of Materials Chemistry C. 2013;1(40):6603-12.
138. Goodyear C, inventorImprovement in India Rubber Fabrics. USA patent US 3633. 1844 Jun 15, 1844.
139. Posner T. Beiträge zur Kenntniss der ungesättigten Verbindungen. II. Ueber die Addition von Mercaptanen an ungesättigte Kohlenwasserstoffe. Berichte der deutschen chemischen Gesellschaft. 1905;38(1):646-57.
140. M.S. Kharasch JR, F.R.Mayo. Chem Ind (London). 1938;57:752.
141. Kasprzak SE, Martin B, Raj T, Gall K. Synthesis and thermomechanical behavior of (qua)ternary thiol-ene(/acrylate) copolymers. Polymer. 2009;50(23):5549-58.
142. Ipatieff VN, Friedman BS. Reaction of Thiol Compounds with Aliphatic Olefins. Journal of the American Chemical Society. 1939;61(1):71-4.
143. Griesbaum K. Problems and Possibilities of the Free-Radical Addition of Thiols to Unsaturated Compounds. Angewandte Chemie International Edition in English. 1970;9(4):273-87.
144. ten Brummelhuis N, Diehl C, Schlaad H. Thiol−Ene Modification of 1,2-Polybutadiene Using UV Light or Sunlight. Macromolecules. 2008;41(24):9946-7.
145. Morgan CR, Magnotta F, Ketley AD. Thiol/ene photocurable polymers. Journal of Polymer Science: Polymer Chemistry Edition. 1977;15(3):627-45.
146. Lowe AB. Thiol-ene "click" reactions and recent applications in polymer and materials synthesis: a first update. Polymer Chemistry. 2014;5(17):4820-70.
147. Li Q, Zhou H, Hoyle CE. The effect of thiol and ene structures on thiol–ene networks: Photopolymerization, physical, mechanical and optical properties. Polymer. 2009;50(10):2237-45.
148. Dondoni A. Die Entwicklung der Thiol-En-Kupplung als Klick-Prozess für die Materialwissenschaften und die bioorganische Chemie. Angewandte Chemie. 2008;120(47):9133-5.
149. Skinner EK, Whiffin FM, Price GJ. Room temperature sonochemical initiation of thiol-ene reactions. Chemical Communications. 2012;48(54):6800-2.
150. Roper TM, Guymon CA, Jönsson ES, Hoyle CE. Influence of the alkene structure on the mechanism and kinetics of thiol–alkene photopolymerizations with real-time infrared spectroscopy. Journal of Polymer Science Part A: Polymer Chemistry. 2004;42(24):6283-98.
151. Jacobine AF. In Radiation Curing in Polymer Science and Technology III. London: Elsevier; 1993.
152. Cramer NBB, C. N. Investigation into the kinetics of thiol-ene and thiol-acrylate photopolymerizations using real-time FTIR. Polymer Preprints (American Chemical Society, Division of Polymer Chemistry). 2001;42(2):699.
153. Roper TM, Kwee T, Lee TY, Guymon CA, Hoyle CE. Photopolymerization of pigmented thiol–ene systems. Polymer. 2004;45(9):2921-9.
154. Chiou B-S, Khan SA. Real-Time FTIR and in Situ Rheological Studies on the UV Curing Kinetics of Thiol-ene Polymers. Macromolecules. 1997;30(23):7322-8.

155. Jacobine AF, Glaser DM, Grabek PJ, Mancini D, Masterson M, Nakos ST, et al. Photocrosslinked norbornene–thiol copolymers: Synthesis, mechanical properties, and cure studies. Journal of Applied Polymer Science. 1992;45(3):471-85.
156. Claisse JA, Davies DI. The addition of thiols to 5,6-dimethylenenorborn-2-ene, and its reactivity towards thiol addition relative to the reactivity of other bridged polycyclic olefins. Journal of the Chemical Society C: Organic. 1966(0):1045-50.
157. Stock LM. The origin of the inductive effect. Journal of Chemical Education. 1972;49(6):400.
158. Cole MC. Photopolymerizationof Vinyl Donor/Vinyl Acceptor Systems and Thiol-Ene Systems [PhD Thesis]. University of Southern

Mississippi2002.
159. Patai S. The chemistry of the thiol group: Wiley; 1974.
160. Inoue S, Kumagai T, Tamezawa H, Aota H, Matsumoto A, Yokoyama K, et al. Predominant methyl radical initiation preceded by [beta]-scission of alkoxy radicals in allyl polymerization with organic peroxide initiators at elevated temperatures. Polym J. 2010;42(9):716-21.
161. Jonas AM, Glinel K, Oren R, Nysten B, Huck WTS. Thermo-Responsive Polymer Brushes with Tunable Collapse Temperatures in the Physiological Range. Macromolecules. 2007;40(13):4403-5.
162. Vollhardt KPC, Schore NE. Organische chemie: John Wiley & Sons; 2011.
163. Chan JW, Hoyle CE, Lowe AB. Sequential Phosphine-Catalyzed, Nucleophilic Thiol− Ene/Radical-Mediated Thiol− Yne Reactions and the Facile Orthogonal Synthesis of Polyfunctional Materials. Journal of the American Chemical Society. 2009;131(16):5751-3.
164. Fairbanks BD, Sims EA, Anseth KS, Bowman CN. Reaction Rates and Mechanisms for Radical, Photoinitated Addition of Thiols to Alkynes, and Implications for Thiol− Yne Photopolymerizations and Click Reactions. Macromolecules. 2010;43(9):4113-9.
165. Hoogenboom R. Thiol–Yne Chemistry: A Powerful Tool for Creating Highly Functional Materials. Angewandte Chemie International Edition. 2010;49(20):3415-7.
166. Hensarling RM, Doughty VA, Chan JW, Patton DL. “Clicking” Polymer Brushes with Thiol-yne Chemistry: Indoors and Out. Journal of the American Chemical Society. 2009;131(41):14673-5.
167. Naik SS, Chan JW, Comer C, Hoyle CE, Savin DA. Thiol–yne ‘click’chemistry as a route to functional lipid mimetics. Polymer Chemistry. 2011;2(2):303-5.
168. Huang Y, Zeng Y, Yang J, Zeng Z, Zhu F, Chen X. Facile functionalization of polypeptides by thiol-yne photochemistry for biomimetic materials synthesis. Chemical communications. 2011;47(26):7509-11.
169. Konkolewicz D, Poon CK, Gray-Weale A, Perrier S. Hyperbranched alternating block copolymers using thiol–yne chemistry: materials with tuneable properties. Chemical Communications. 2011;47(1):239-41.
170. Massi A, Nanni D. Thiol–yne coupling: revisiting old concepts as a breakthrough for up-to-date applications. Organic & biomolecular chemistry. 2012;10(19):3791-807.
171. Huisgen R. Proceedings of the Chemical Society. October 1961. Proceedings of the Chemical Society. 1961(October):357-96.
172. Himo F, Lovell T, Hilgraf R, Rostovtsev VV, Noodleman L, Sharpless KB, et al. Copper(I)-Catalyzed Synthesis of Azoles. DFT Study Predicts Unprecedented Reactivity and Intermediates. Journal of the American Chemical Society. 2005;127(1):210-6.
173. Lutz J-Fo, BÃ¶rner HG, Weichenhan K. Combining ATRP and â€œClickâ€• Chemistry:â€‰ a Promising Platform toward Functional Biocompatible Polymers and Polymer Bioconjugates. Macromolecules. 2006;39(19):6376-83.
174. Yang SK, Weck M. Modular Covalent Multifunctionalization of Copolymers. Macromolecules. 2007;41(2):346-51.
175. Kakwere H, Perrier Sb. Orthogonal â€œRelayâ€• Reactions for Designing Functionalized Soft Nanoparticles. Journal of the American Chemical Society. 2009;131(5):1889-95.

176. Zhang J, Wang X, Wu D, Liu L, Zhao H. Bioconjugated Janus Particles Prepared by in Situ Click Chemistry. Chemistry of Materials. 2009;21(17):4012-8.
177. Wang K, Bi X, Xing S, Liao P, Fang Z, Meng X, et al. Cu 2 O acting as a robust catalyst in CuAAC reactions: water is the required medium. Green Chemistry. 2011;13(3):562-5.
178. Liang L, Astruc D. The copper (I)-catalyzed alkyne-azide cycloaddition (CuAAC)“click” reaction and its applications. An overview. Coordination Chemistry Reviews. 2011;255(23):2933-45.

10. List of Publications

10.1. Publications

PEG Hydrogels – Versatile Materials for Biomedical Applications. E. Wischerhoff, A. Laschewsky, J. Buller, S. Dippel, D. Stöbener,Proceedings of 9. ThGOT Thementage Grenz- und Oberflächentechnik & 9. Thüringer Biomaterialkolloquium, 3-5.Sept. 2013, Zeulenroda (Germany).

10.2. Poster:

Towards Bio-responsive Hydrogels.A. Laschewsky*, J. Buller, S. Dippel, J. Kölsch, M. Sütterlin, Ch. Wieland, J. Buchs, D. Janietz, E. Wischerhoff,Potsdam Days on Bioanalysis 2011, 9-10.11.2011, Potsdam (Germany)

Responsive Polymer Hydrogels and their Modulation by Molecular Recognition J. Buller, S. Dippel, A. Laschewsky, M. Sütterlin, M. Päch, E. Wischerhoff, Makromolekulares Kolloquium Freiburg, 23-25.02.2012, Freiburg (Germany)

Bioconjugable Monomers for Smart Hydrogel Systems Aimed at Bioanalytics. S. Dippel, R. Bernin, J. Buller, M. Sütterlin, E. Wischerhoff, A. Laschewsky,27.Tag der Chemie Berlin-Brandenburg 2012, 28.06.2012, TU Berlin, Berlin-Charlottenburg

New water-soluble polyacrylates bearing azobenzene side chains: Combining photo- with thermo-sensitive behaviour .A. Miasnikova, A. Benítez-Montoya, S.Dippel, A. Laschewsky, M. Päch,Polydays 2012: Polymers and Light, 30.09-02.10.2012, Berlin (Germany)

Bioconjugable Monomers for Smart Hydrogel Systems Aimed at Bioanalytics. S. Dippel, R. Bernin, J. Buller, M. Sütterlin, E. Wischerhoff, A. Laschewsky,Potsdam Days on Bioanalysis 2012, 08.11.2012, Potsdam-Golm (Germany)

Synthesis of block, star and star block copolymers by RAFT polymerization: New pathways to associative thickeners .C. Herfurth, S. Dippel, A. Miasnikova, C. Wieland, A. Laschewsky,Makromolekulares Kolloquium Freiburg, 21-23.02.2013, Freiburg (Germany)

From Monomers to Hydrogels – Smart, Bioconjugable Systems for Bioanalytics .S. Dippel, J. Buller, N. Sickert, E. Wischerhoff, A. Laschewsky,28. Tag der Chemie Berlin-Brandenburg 2013, 27.06.2013 (Potsdam-Golm)

From Monomer Synthesis to Smart Bioconjugable Hydrogels .S. Dippel, J. Buller, J.-Ph. Couturier, E. Wischerhoff, A. Laschewsky,5th Potsdam Days on Bioanalysis 2013, 07-08.11.2013, Potsdam-Golm (Germany)

Appendix

A1. ^{1}H-NMR Spectra

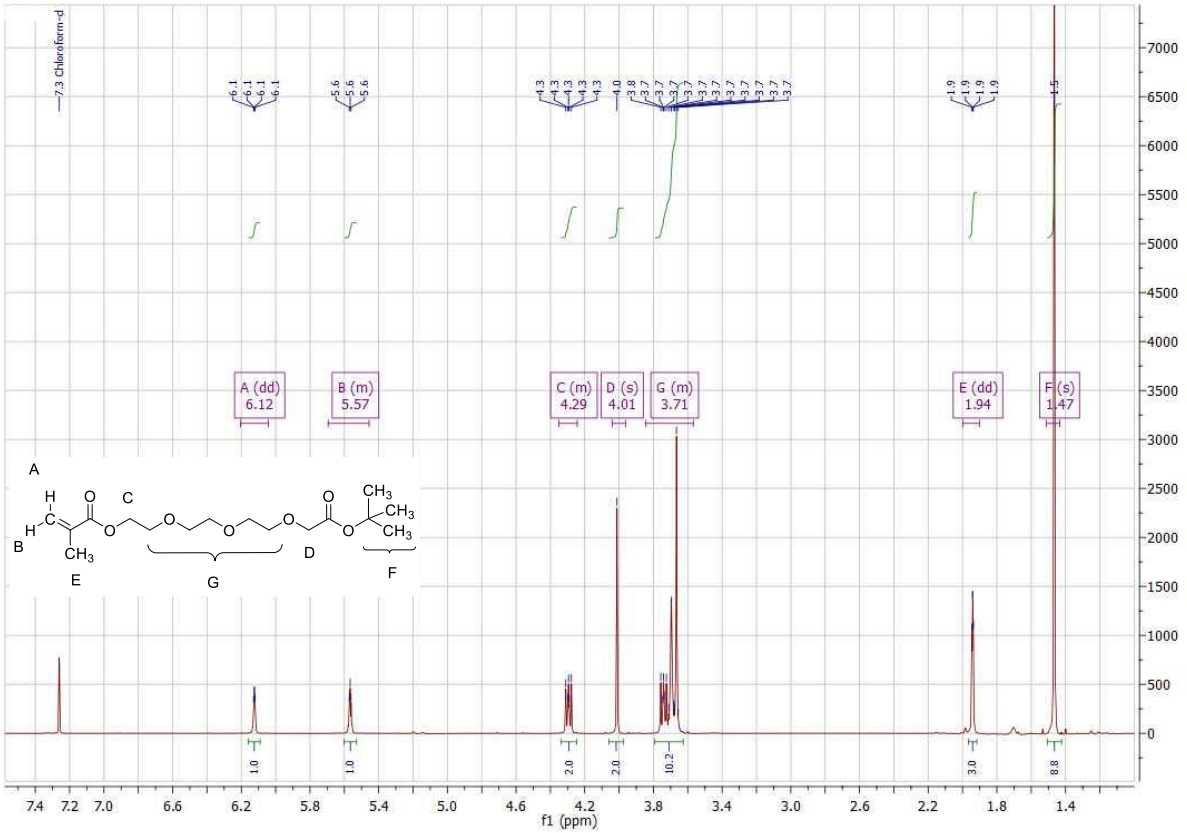

Figure 39: *^{1}H-NMR Spectra of monomer* ***2***

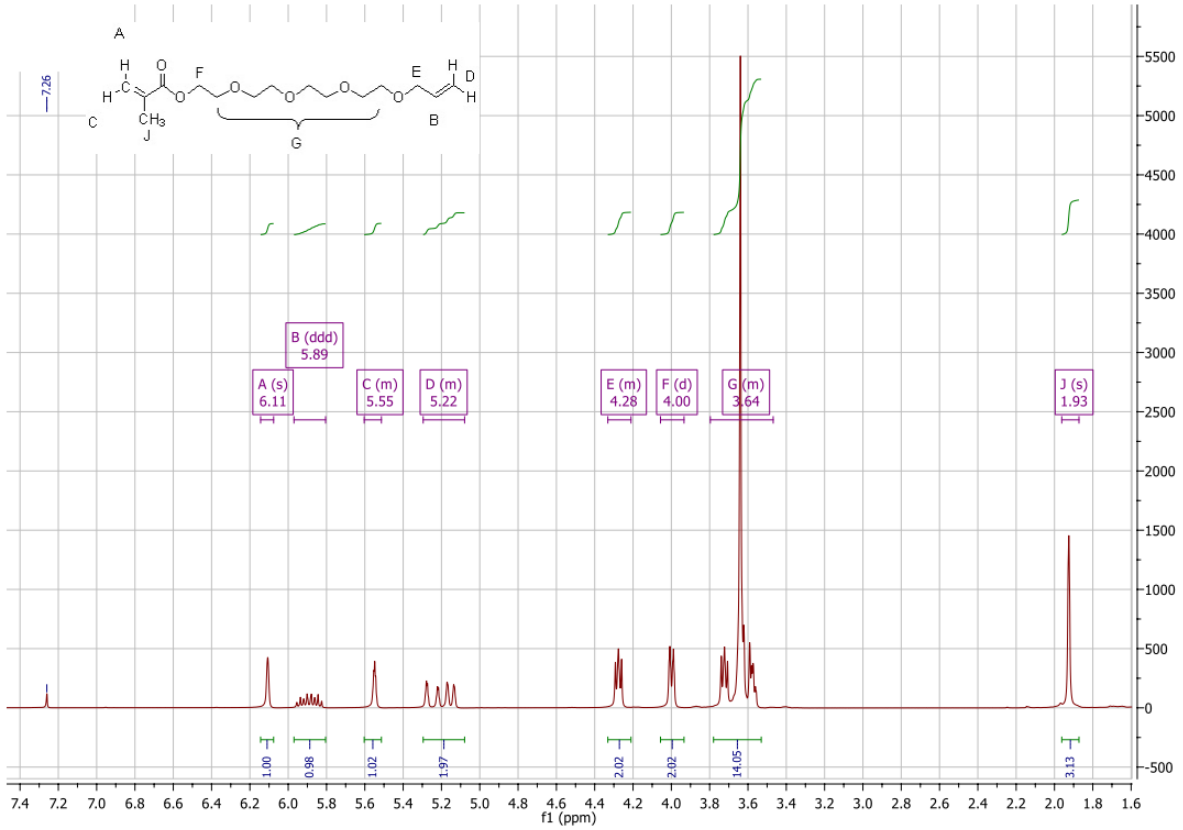

Figure 40: *^{1}H-NMR spectra of monomer* ***4***

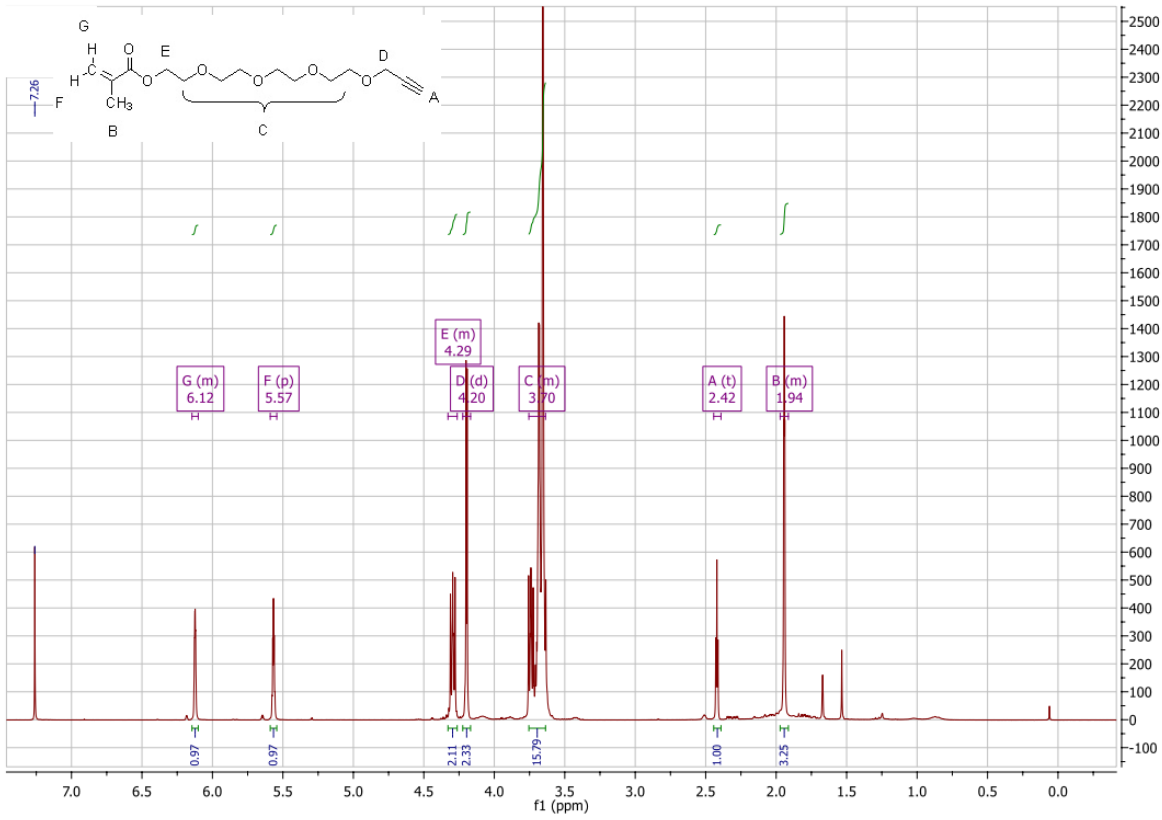

Figure 41*: 1H-NMR Spectra of monomer* ***6***

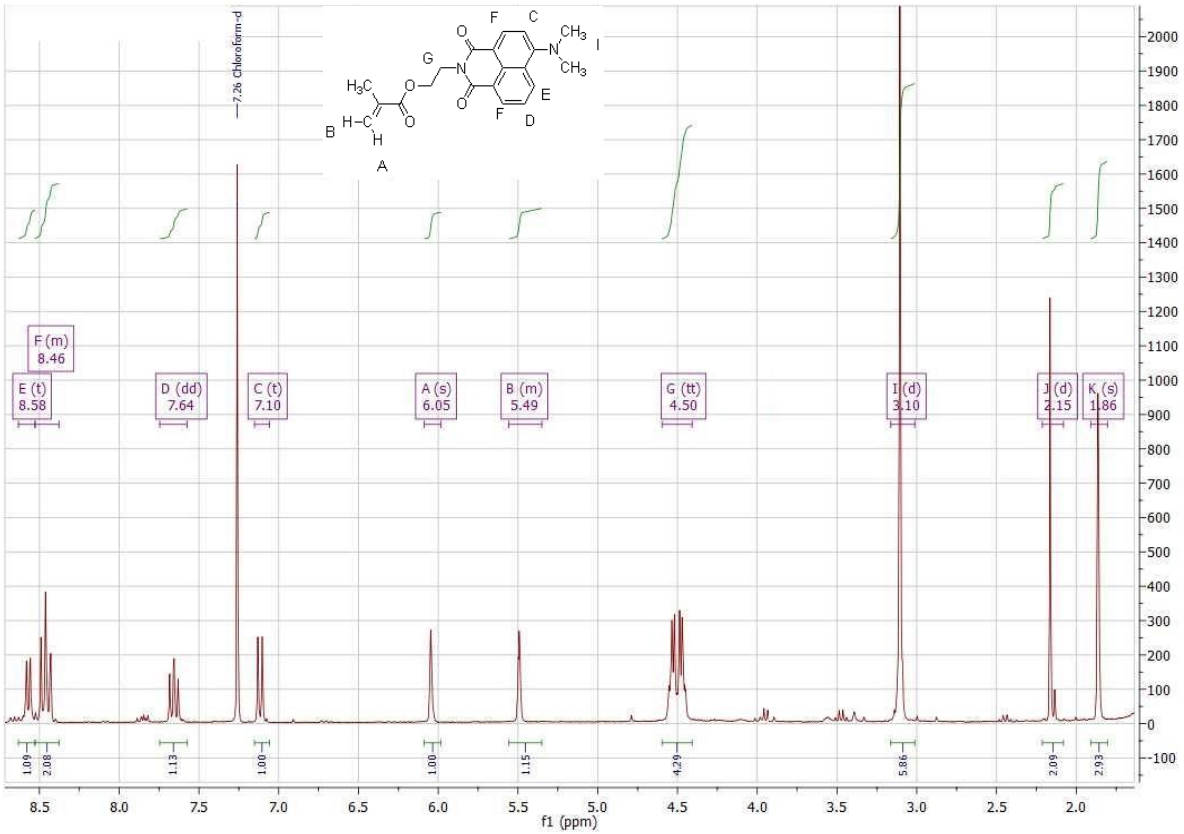

Figure 42**: 1H-NMR Spectra of monomer **8

A2. List of tables

A3.List of Figures